




Review

Recent Advances in Chemical Sensors for Soil Analysis: A Review

Marina Nadporozhskaya ¹, Ninel Kovsh ¹, Roberto Paolesse ² and Larisa Lvova ^{2,*}

¹ Faculty of Biology, St. Petersburg State University, 198504 St. Petersburg, Russia; m.nadporozhskaya@spbu.ru (M.N.); Spbu@spbu.ru (N.K.)

² Department of Chemical Science and Technologies, University “Tor Vergata”, 00133 Rome, Italy; roberto.paolesse@uniroma2.it

* Correspondence: Larisa.Lvova@uniroma2.it

Abstract: The continuously rising interest in chemical sensors’ applications in environmental monitoring, for soil analysis in particular, is owed to the sufficient sensitivity and selectivity of these analytical devices, their low costs, their simple measurement setups, and the possibility to perform online and in-field analyses with them. In this review the recent advances in chemical sensors for soil analysis are summarized. The working principles of chemical sensors involved in soil analysis; their benefits and drawbacks; and select applications of both the single selective sensors and multisensor systems for assessments of main plant nutrition components, pollutants, and other important soil parameters (pH, moisture content, salinity, exhaled gases, etc.) of the past two decades with a focus on the last 5 years (from 2017 to 2021) are overviewed.

Keywords: chemical sensors; soil main nutrients; macro- and microelements; soil moisture; salinity; pH; pollutants assessment; multisensor systems for soil analysis



Citation: Nadporozhskaya, M.; Kovsh, N.; Paolesse, R.; Lvova, L. Recent Advances in Chemical Sensors for Soil Analysis: A Review. *Chemosensors* **2022**, *10*, 35. <https://doi.org/10.3390/chemosensors10010035>

Academic Editor: Maria Cuartero

Received: 25 November 2021

Accepted: 9 January 2022

Published: 16 January 2022

Publisher’s Note: MDPI stays neutral with regard to jurisdictional claims in published maps and institutional affiliations.



Copyright: © 2022 by the authors. Licensee MDPI, Basel, Switzerland. This article is an open access article distributed under the terms and conditions of the Creative Commons Attribution (CC BY) license (<https://creativecommons.org/licenses/by/4.0/>).

1. Introduction

1.1. Soil Definition, Sustainable Management of Soils

Soil, together with the atmosphere and water, represents one of the most significant components of the Earth [1]. A definition of soil mostly satisfying the goals of environmental research for nature conservation is as follows: soil is the complex, three-phase, multifunctional open system formed on the surface of Earth’s crust over time due to the interactions of parent mineral materials and organisms, sometimes under anthropogenic influences [2].

The peculiarities of soil are its spatial and temporal heterogeneity, its multiplicity, and the sometimes multidirectional actions of soil-forming factors. The spatial variability of soils is caused by the heterogeneity of parent geological rocks, vegetation, relief, fauna, and human activities. Some properties retained by soils over long periods are called “soil memory.” Soil properties that change rapidly over a period of hours or days have been called “soil moments” [3]. Natural soils represent the most essential element of the Earth’s biosphere, but being constantly modified by anthropogenic activities, they can be completely transformed and retain their new properties (not always suitable for ecosystem stability) for a long time [4]. At this point, soils are considered non-renewable natural resources (within practical periods of time).

The 1972 European Soil Charter recognized that any biological, physical, or chemical degradation of soil must be recognized as a major environmental hazard [5]. The pedosphere, unlike the atmosphere and hydrosphere, is generally a more conservative form. Soils, as non-renewable resources, must be managed to maintain their ecological functions and the specific characteristics inherent in their different types. Since the beginning of the 20th century, the accelerating socio-economic development of society has impacted larger and larger areas. Pollutants persist in soil much longer than in air and water, and their impacts in soil can be undetectable for long periods of time. Soils accumulate pollutants over a

long period of time and can degrade after exceeding critical loads. Industrial development, urbanization, increased landfill and mining, and unsustainable agriculture have caused changes in natural ecosystems. Soils are increasingly being disturbed by extensive farming, land clearing, erosion, salinization, compaction, direct pollution or atmospheric deposition, compaction—which can result in dehumification and loss of biodiversity—and loss or inadequate performance of some ecological functions. Hampering soil's functions reduces the quality of soil for ecosystems and reduces its ability to support life. In addition, in the case of urban soils, soil quality and its impact on human health are very significant. There is, hence, no doubt that monitoring soil quality is essential not only for optimal management of the economy, but also for planning measures to protect, reclaim, and restore ecosystems.

Soil quality is the ability of soil to provide nutrients to plants, maintain and improve water and air within the soil, and support human needs [6]. For the primary ecological control of damaging influences and soil quality assessment, the following properties were selected: the soil structure and pH, amount of mineral fraction less than 0.01 mm, mineralogical composition of clay fraction, total content, and quality of Soil Organic Matter (SOM). Based on these parameters, estimated with standard procedures for soil analysis, the environmental assessment of soil vulnerability to the main damaging factors can be carried out as a first approximation [7].

Other common indicators used to assess soil composition include texture, electrical conductivity, bulk density and infiltration capacity, water retention, temperature, and soil respiration [8,9]. For deeper estimation of soil quality, the main components to monitor are soil organic matter (SOM) amount and composition, humic substances fractioning, main nutrients (C, N, P, K, Ca) and microelements (transition metals and other minor elements), physical–chemical parameters (pH, Ox–Red potential, porosity, humidity, etc.), and pollution degree. Evidently, the soil quality is not limited only to the degree of soil pollution, but has much more broad definition: “The capacity of a soil to function within ecosystem and land-use boundaries to sustain biological productivity, maintain environmental quality, and promote plant and animal health”[6]—and hence, constant soil quality monitoring is very important [10].

Among the standard methods of soil analysis are the classical wet chemistry methods, and various new instrumental methods such as molecular emission spectroscopy, atomic absorption spectrometry (AAS), nuclear magnetic resonance (NMR) spectroscopy, high performance liquid chromatography (HPLC), and gas chromatography combined with mass spectrometry (GC-MS). Unfortunately, these methods are often expensive and slow due to the extraction and pretreatment processes, and require specific equipment and qualified personnel. Hence, new, effective, low-cost, rapid, and nondestructive methods of soil analysis are necessary. These new analytical approaches must be fast, non-expensive, and suitable for mass assaying. One way to monitor soil quality is through sensors: physical, biological (including bioassays), and chemical. In the last two decades, these devices have attracted a lot of attention from scientists due to their ease of use, relatively low costs, and sufficient selectivity. Moreover, sensors can monitor soil's chemical content in real time and in situ with no or minimal sample pretreatment, measure several analytes simultaneously, and provide results in real time, which is especially in demand for precision farming applications [11]. The main sensor types involved in soil analysis are listed in the next section.

1.2. Sensors for Soil Analysis

IUPAC defines a chemical sensor as, “A device that transforms chemical information, ranging from the concentration of a specific sample component to total composition analysis, into an analytically useful signal,” a physical sensor as, “A device that provides information about a physical property of the system,” and classifies sensors into physical, chemical, and biosensors [12]. In soil analysis, the last two types of sensors, chemical and biosensors, are the most employed.

Chemical sensors, used for soil chemical monitoring, can be divided by their signal transmission mechanisms into electrochemical (including potentiometric, voltametric, conductimetric, and impedimetric), electromagnetic (optical, measuring color, luminescence, fluorescence, phosphorescence, etc.), and gravimetric (mass-sensitive piezoelectric devices) [13]. The main classes of electrochemical sensors involved in soils analysis are potentiometric (static measurement of voltage at zero current), voltametric (dynamic measurement of current upon applied voltage), and conductimetric sensors [12,14–16]. The use of electrochemical sensing systems to selectively determine one or more soil components to assess soil quality was reported recently by Ali et al. [17]. Some concrete examples, their associated challenges, possible alternatives, and development prospects for electrochemical sensors for soil analysis are discussed therein. For optical sensors, the variations of light properties upon interaction with analyte is considered [18,19]. The most widely used techniques employed in optical chemical sensors for soil analysis are absorption (and visible color change), fluorescence, and luminescence. Sensors based on other spectroscopies and optical parameters, such as refractive index and reflectivity, have also been developed. Optical sensors with bulk sensing membranes (often solvent polymeric membranes) are called optodes [15,16]. In the recent review by Fukuhara, deep insights on the mechanistic behavior of colorimetric and fluorimetric chemosensors are provided and illustrated with 138 works in the field of supramolecular analytical chemistry [20]. A review on proximal active optical sensors' (AOS) application to agricultural sensing was published by Holland, Lamb, and Schepers in [21]. Two-dimensional (2D) planar optodes (POs), employed for biogeochemical analysis of heterogeneous samples such as sediments and soils, and at the sediment-water interfaces, are described in [22]. The principles, configurations, and applications of modern optical chemical and biosensors, and sensor arrays for different fields, including environmental sampling and soil research, have been reported previously [18,23–25]. Mass-sensitive (gravimetric) sensors “transform the mass change at a specially modified surface into a change of a property of the support material” [12] and are based on acoustic wave devices vibrating at a certain frequency (piezoelectric effect). The piezoelectric substrate often is modified with a chemically absorbent coating, which by itself, and upon the accumulation of the analyte in its surface, causes a mass change directly proportional to the transducer resonant frequency variation according to the Sauerbrey law [26]. The bulk acoustic wave (BAW) and surface acoustic wave (SAW) sensors and microcantilevers devices are the most used in environmental analysis and foodstuffs analysis [27]. Biosensors employ some biochemically-mediated recognition, which is detected by an associated, analytically useful signal. Through bioassays, the effects of the analyzed compound (either positive or negative) on select living organisms' (cells, microorganisms, animals, etc.) vitality is studied [28]. Even in the face of serious ethical problems (especially in a case of bioassays), and/or low stability, plus the necessity of low temperatures for testing probe preservation prior to use (biosensors), both bioassays and biosensors have been widely employed for soil bioassessment analysis [29].

In the present paper, the works on sensory applications for analyses of primary nutrients, microelements, pollutants, and different physico-chemical parameters of soils performed in the past two decades, with particular attention on the last 5 years, are overviewed. For the convenience of our readers, we have divided the review into several sections, each of which is devoted to the analysis of a specific soil analyte or property. Additionally, the multisensory analysis applications, and other techniques, including bioassays, image processing, and some non-trivial solutions for soil quality assessment, are provided.

1.3. Soil Sampling and Pretreatment Procedures Prior to Analysis

For analysis, soils are normally collected from the selected site from one or more layers or horizons (most often from the uppermost part, which is of the most interest for agriculture and soil science investigations) with a knife or a spatula from the pits, or with a soil drill. When collecting undisturbed systems, the sampler requires an area and the depth

to be specified. Collected soil samples are placed in clean plastic buckets or bags, keeping samples taken from different depths and specific areas separate from each other for further laboratory analysis [30]. The large roots and pebbles (>2 mm) must be removed from soil by hand; the samples then are dried at a temperature not exceeding 40 °C, and if necessary, are crushed immediately before the analysis [31]. On-site soil samples are generally collected by the “envelope method”—diagonally or in any other way—in such a manner that each sample represents a part of the soil typical for genetic horizons or layers of a given soil type. The number of spot samples is determined by legislation [30,31]. The mixed control sample is then obtained by mixing several samples taken from the same sample site. For chemical analysis, a combined sample is made up of at least five-point samples taken from one sample site. The mass of the combined sample must be at least 1 kg. It is important to stress that there is not one correct method of soil sampling. Since the agrochemical properties of soil vary greatly even in a very small area, in order to determine the exact nutrient content of a field, detailed soil analysis of a large selection of samples collected with high density is recommended. This procedure requires a lot of effort in the sampling step alone, which is then followed with time-consuming and costly laboratory analysis. It is clear why precision agriculture and sensors’ applications to soil quality assessment have become attractive: they are cost-effective and time-preserving compared to the standard soil analysis methods.

Several considerations related to the specifics of sensor applications to soil analysis should be considered all the same. Normally, the chemical sensors are used for the analysis of homogeneous, mainly liquid (less often gaseous) samples. While analyzing soils, the investigator deals with the heterogeneous objects containing mineral particles, inclusions (rocks, clay, and sand) of different sizes, entrapped gases, and various liquids [9,32]. Additionally, a soil sample can be characterized by the presence of fibrous debris, organic matter, and living organisms; and by having different moisture levels, friability, temperatures, etc. Soil’s profile, and as a consequence its properties, vary both across the surface of the land from which it is collected and also with depth. These variations are caused by direct contact with the biosphere, atmosphere, and groundwater. Consequently, chemical sensors meet several application problems concerned with the states of samples and particular pre-treatment requirements. Solid soil samples first need to be diminished to small and uniform pieces, treated with specific reagents, or transformed in some other way into the appropriate phase state in order to be properly measured, and physically brought into close contact with sensitive sensor materials. For this, cold samples must be heated to the sensor’s operation temperature, hot ones should be cooled, heterogeneous—homogenized, etc. Additionally, since most types of chemical sensors operate mainly in a liquid phase (and even more often, in aqueous media), soil sample wetting, dilution, and/or extraction with appropriate and “sensor-friendly” eluents or solvents is essential for successful chemical sensor-based analysis.

2. Sensors for Soil Nutrient Analysis

2.1. Soil Nutrients: Primary, Secondary, and Microelements

The main constituents of SOM playing a fundamental role in balanced soil system formation, besides carbon, are nitrogen, phosphorus, and potassium (N, P, K). All these macronutrients are essential for soil stability and fertility, and play important roles in healthy plant growth. The soil’s fertility is its ability to produce large and high-quality yields of agricultural plants over a long period of time when optimal agronomic practices are applied. A distinction is made between actual (for a given growing season) and potential (long-term realized, total) fertility. Actual soil fertility is part of potential fertility. Potential fertility is characterized by such parameters as: stocks of nutrients for plants and their mobile forms, optimal (both for plant growth and mobilization of nutrients) aeration, and moisture and temperature regimes [33]. Carbon is the basis of the organic compounds that form plants, and the main element in humic substances in soil, humates, and fulvates. It is responsible for potential and actual soil fertility. The humic substances content of

soils varies from 0 to almost 10% [34]. Evaluations of the total amounts of organic carbon in soils and organic fertilizers is important in agricultural chemistry, since such values can represent the potential fertility of a soil, and often serve as measures of fertilizers' effectiveness. Nitrogen is fundamental in chlorophyll synthesis and is an essential element of enzymatic proteins that catalyze and regulate the plant growth processes. Most soil nitrogen is preserved in organic compounds in SOM. The content of mineral forms of nitrogen available to plants usually does not exceed 1–2% of the total nitrogen content in the soil. The inorganic forms of soil N are nitrite (NO_2^-), nitrate (NO_3^-), and ammonia (NH_4^+), with nitrate being the most stable and form available to plants. Phosphorus plays an important role in stimulating root growth. Plants absorb free phosphoric acid and its water-soluble mono- and bis-substituted salts at pH 6.0–7.0. These forms are the most available forms to plants, alongside some organic phosphorus compounds, such as sugar phosphates and phytin. Plants also absorb sulfates and sulfur-containing amino acids from the soil in very small amounts. The amount of potassium needed for plant growth is equivalent to or greater than the amount of nitrogen needed. Potassium is absorbed by plants as a cation, and regulates the water uptake and CO_2 exchange. It is important in production and transport of sugars, and in the enzymatic processes that ensure photosynthesis [35]. Overall, 17 soil nutrients have been established as essential for plant growth [36]. They are listed in Figure 1 in the forms taken up by the plants [37].

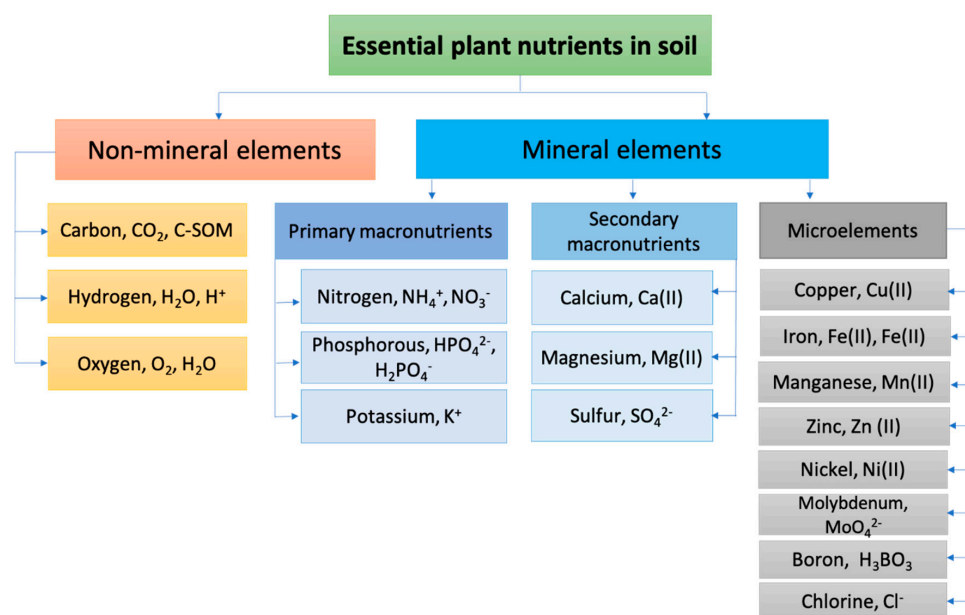


Figure 1. Schematic presentation of soil essential nutrients required for plant growth.

Mineral nutrition is the basis of plant growth and development. According to their contents in plant tissues, chemical elements are divided into macro- (content more than 0.01%: N, P, S, K, Mg, Ca) and microelements (content less than 0.01%: Fe, Mn, Zn, Cu, B, Mo, Cl and others). Macronutrients and microelements are the chemical elements that a plant needs that cannot be replaced by any others. Elements of mineral nutrition are involved in the synthesis of molecules, cells, and plant tissues, and in the formation of enzymatic, hormonal, and genetic materials. Deficiencies in minerals cause stunted formation of vegetative and generative organs, and lower resistance to plant diseases. The real-time monitoring of these nutrients in soils provides useful information on actual soil conditions, permits one to make conclusions on the optimal fertilizing of agricultural crops, and helps to avoid runoff of nutrients excess into surface and groundwater and causing other environmental damage [1,11,35–37]. Currently, the standard laboratory methods are intensively employed for soil nutrient analysis, despite the several drawbacks, such as slow analysis, costly equipment, the need for qualified personnel, and the necessity of

sample pretreatment. Sensors seem to be effective alternatives and/or additional support to the standard instrumental techniques and wet chemistry methods, thanks to their sufficient sensitivity, fast response times, and low costs. In fact, over the last decade the research interest in the sensory analysis of soil nutrients, and in direct in-field soil analysis, has grown significantly, and plenty of research articles and comprehensive reviews in this field have been published. Thus, the chemical, electrical, and optical sensing technologies for NPK analysis in agricultural soils were summarized in [38]. A review on electrochemical sensors and ion-sensitive field effect transistors for rapid in-situ soil analysis is provided in [39]. An update on different sensing methodologies in agriculture for soil moisture and nutrient monitoring was recently published by Kashyap and Kumar [37]. Chemical sensors with optical transduction using two-dimensional (2D) imaging techniques employed in planar optodes (POs) used for biogeochemical analysis of heterogeneous samples, such as sediments and soils, and at the sediment–water interface, are overviewed in [22]. The principles, configurations, and devices used for POs systems are discussed, and the applications of the assessment of O₂, CO₂, pH, temperature, NH₄⁺ ions, and metals ions in sediments and soils are provided. The review of Kim et al. [40] discusses the significance of recent trends in nanomaterial-based sensors available for the sustainable management of agricultural soils; and the roles of nanotechnology in detection and protection against plant pathogens, and in food quality and safety. Additionally, the applications of gas sensors based on membrane diffusion for environmental monitoring [41], the use of electrochemical sensors for soil quality assessments [17], and the applications of piezoelectric sensors for environmental and foodstuff samples analysis [27] have been recently overviewed.

Our analysis of the past 20 years of publications shows that chemical sensors are heavily employed for assessments of ionic forms of individual soil components, or their total contents—total N, P, etc.; for the indirect determination of soil components, such as, total C or humic substances content; and for assessments of soil parameters such as pH, salinity, and soil moisture, which often directly influence the forms and amounts of the main nutrients present in soil. Below we briefly summarize the most outstanding previously reported works on soil sensory analysis and overview the progress in the field of chemical sensors for soil nutrients during 2017–2021. The limitations of sensory technology, especially for real-time soil sensing are also discussed, and the solutions to overcome the limitations by means of multisensor approach and intelligent sensory system architecture are considered.

2.2. *Carbone and Soil Organic Matter*

The quality and quantity of soil organic matter and soil organic carbon are supposed to be the major indicators of soil fertility and nutrient contents. SOM is a complex system resulting in the transformation of plant and animal residues. The transformation consists of two opposite processes, mineralization and humification, which are preceded by different stages of dead material decomposition. According to its resistance to decomposition and mineralization, SOM is divided into labile and stable parts. The labile part is responsible for the actual fertility, and the stable part is responsible for the potential fertility.

Mineralization produces mineral salts, including those available for plants, and CO₂ and H₂O. Decomposition gives sugars, organic acids, hemicellulose, lignin, fats, waxes, and other individual groups of organic compounds. Humification produces the soil-specific organic compounds named humic substances, or fulvic and humic acids, and humin [36,42]. Humic substances are dark-colored, nitrogen-containing, high-molecular-weight compounds that are acidic [43]. The “humic substances” paradigm has been criticized in recent years due to the artificial synthesis of humic acids in alkaline extraction [44]. Some soil scientists have come to a compromise on the probable coexistence of specific humic macromolecules and supramolecular compounds, in which smaller molecules are not bound by covalent bonds [45,46]. SOM improves the physical, chemical, and biological properties of the soil; optimizes the soil structure; and balances the water–air and temperature regimes. At present, the problem of organic matter is becoming more acute. Soils are being dehu-

mified due to irrational use of forest and agricultural lands. Rational farming requires a long-term forecast of the effectiveness of applied mineral and organic fertilizers [1,9–11,43].

General methods for organic compound assessments are based on their oxidation to CO_2 and H_2O either by burning a sample of soil at temperatures of 650–750 °C (also known as ignition), or by oxidation with solutions of strong oxidants, sulfuric acid, and potassium dichromate (so-called oxidative wet chemistry), according to Anne, Walkley-Black, and Tyurin methods [33]. Both analytical approaches have several drawbacks. The ignition method measures the loss of inorganic carbon in the total. The oxidative wet chemistry technique overestimates the carbon SOM amount for soils with high contents of reduced compounds (waterlogged soils, forest litter) or with chloride salinization.

The new sensory approaches recently developed for SOM and soil carbon estimation are based on mass-sensitive devices [47] and use metal oxide semiconductor (MOS) gas sensors [48]. Thus, a method for total soil carbonates estimation by means of a ZnO-based microcantilever was previously reported by Plata et al. [47]. The method is based on the selective excretion of CO_2 from soil samples in a closed system and the measuring of the gas pressure on the micro-sensor. The analysis was reliable in the 3–75 mg range, with a relative standard deviation (RSD) of 1.7% and a low detection limit of 0.91 mg. The method was applied to the analysis of different soil samples. The results were in agreement with those of CaCO_3 content measured by the standard Bernard's calcimeter method.

Recently, Zhu et al. reported an artificial olfactory system based on 10 identical gas sensors (IDT SGAS707 type polymer-MOx composite material gas sensors from Integrated Device Technology Inc., San Jose, CA, USA) operating at different temperatures for soil organic matter (SOM) determination through the detection of VOCs in emitted soil gas, with the aim of amending the optimized fertilization of cultivated soils [48]. See Figure 2.

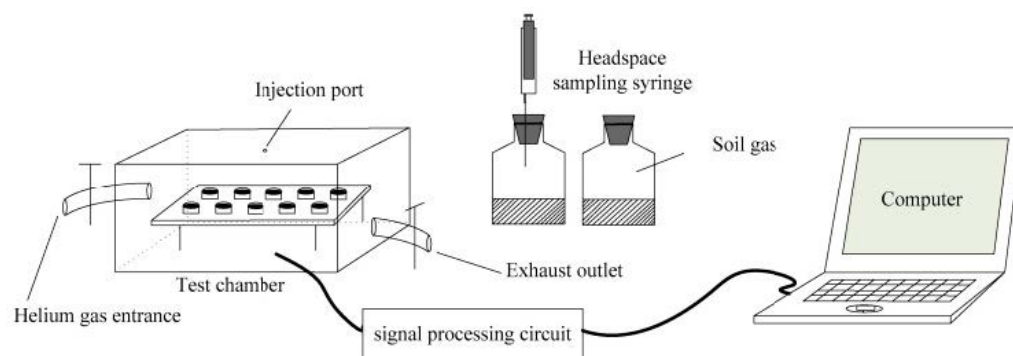


Figure 2. Artificial olfactory measurement system SOM setup. Reprinted from [48].

The assumption of a closer relationship among the gas compositions of soil air under anaerobic soil regimes than those of soil under aerobic conditions is the basis of the method. The system was tested on 102 soil samples collected in Jilin Province, in the northeast region of China. Soil types included dark brown soil, chernozem, planosol, herbal soil, and black soil, on which corn, soybeans, and wheat were mainly grown. The system output was treated as a “fingerprint” of a total gas sample. Four features (maximum value, mean differential coefficient value, response area value, and the transient value at the 20th second) extracted from the response curve of each sensor were used to build the SOM prediction models based on back-propagation neural network (BPNN), support vector regression (SVR), and partial least squares regression (PLSR) in order to correlate the array response with a standard SOM content examination method based on the oxidation of organic carbon in soil with a potassium dichromate solution at a high temperature and further titration of the remainder with ferrous sulphate. The SVR model has shown the best predictions of SOM, thereby demonstrating the feasibility of developing an artificial olfaction system to detect SOM content. The proposed method, anyway, can be characterized as a pilot and requiring verification. The work noted anomalous soil samples that did not satisfy the general calculated pattern of the ratio of measured to predicted SOM values (predicted by

the new method). The results also depend on compliance with the measurement conditions (soil moisture, anaerobic residence time, and temperature).

2.3. Total and Mineral Nitrogen

Nitrogen is a key nutrient source in agriculture, since it plays an important role in living organisms, being one of the fundamental components of proteins and nucleoproteins. In soils, nitrogen naturally appears in inorganic forms such as ammonia, nitrite, and nitrate via fixation of atmospheric nitrogen gas, and from decomposition of various wastes generated by the deaths of living things by the denitrification bacteria in the soil [49]. Another source of nitrogen in soils is fertilizers, used in order to enhance crop yields [11]. Excessive fertilizer use seriously affects soil quality and leads to excessive nitrogen in the soil. The precise and selective determination of total nitrogen and its inorganic ionic forms in soil is an important analytical task, sufficiently afforded by the application of chemical sensors. Nitrogen assessment using chemical sensors has been explored for several decades.

Plenty of electrochemical sensors, such as potentiometric ion-selective electrodes (ISEs), and ion-selective field-effect transistors (ISFETs); impedimetric sensors with solvent polymeric membranes; and optical sensors, have been developed for nitrogen's ionic forms in soils [37]. Artigas et al. developed a screen-printed sensing probe based on a graphite–epoxy composite, incorporating three thick-film nitrate-selective sensors each at a different depth, and a copper reference electrode for the in-field automated monitoring of fertilizing [50]. The device was employed for the analysis of nitrate content in soil extracts. The results correlated well with those of the standard Kjeldahl method. Air-gap sensors using a pH electrode and a nitrate-ion-selective electrode for the detection of nitrogen oxides and nitrite in water extracts of soils were reported in [51]. The nitrite amounts determined with the developed sensors were well correlated with the amounts determined by the standard Griess method. Adamchuk et al. performed N-NO_3^- assessments with a nitrate-selective electrode, simulating in-field soil analysis in laboratory conditions [52,53].

ISFETs sensors in combination with flow-injection analysis were employed for NO_3^- concentration assessment in extracts of 14 Illinois surface soils [54]. A nitrate extraction system was developed in [55], and in combination with ISFET technology was used for a rapid on-the-go soil nitrate mapping. Gieling et al. have developed a fertigation strategy for precise dosage of liquid fertilizing agents in horticultural greenhouses [56]. ISFET and ISE sensors were employed to measure nitrate, potassium, ammonia, and calcium in a nutrient supply and a drain in a greenhouse housing a real crop. Changes in nutrient concentrations in inflow and outflow provided information about the uptake of ions by plants and provided feedback about the nutrient needs of plants to be met. Selected applications of polymeric materials for nitrite assessment in nature, with particular attention on sensing materials' compositions and performances, are overviewed by Yenil and Yemiş in [57].

Recently, a flexible, solid-state ISE using inkjet-printing technology for in-field nitrate detection was reported by Jiang et al. in [58]. The classical PVC-based nitrate-selective membranes were doped with tetra-n-octylammonium bromide (TOA-bromide) and plasticized with di-n-butyl phthalate plasticizer and had different thicknesses while deposited on ISE (25, 50, and 140 μm). Fast conditioning for thinner membranes and better stability for thicker membranes were found, and this information can be useful for practical applications. The developed ISE had a linear sensitivity within the nitrate range 0.0001 to 0.1 M and a high accuracy of ~95% for nitrate detection in 3:5 w/w soil/water mixtures. Other solid-state, portable sensors for selective determination for potassium and nitrate ions using a tetrathiafulvalene-tetracyanoquinodimethane (TTF-TCNQ) solid contact layer for improved potential stability were developed in [59].

Laser induced graphene (LIG) electrodes fabricated on polyimide/Epson printer paper and functionalized with PVC-based membranes doped with tridodecylmethylammonium nitrate (TDMANO₃) and nonactin ionophores for nitrite and ammonia ion assessments, respectively, were reported in [60]. The the DL of ISEs were 28.2 and 20.6 μM for NH_4^+ and

NO_3^- , respectively. The nitrite-doped polypyrrole (PPy- NO_3) with a nanohybrid composite mediate layer of electrochemically reduced GO and Au nanoparticles was employed for an all-solid-state nitrate ion-selective electrode for in-situ soil nutrient monitoring in [61]. The sensor had a DL of $6.3 \mu\text{M}$ and an over two-month lifetime. The recoveries of nitrate and ammonia in spiked soil slurry were not lower than 95%. A patterned Au working electrode coated with a nanocomposite of poly(3-octyl-thiophene) and molybdenum disulfide (POT-MoS₂) coated over with TDMANO₃-based solvent polymeric membrane was reported in [62]. The presence of a hydrophobic redox POT-MoS₂ layer provided the enhanced ion-to-electron transfer on the electrode surface, thereby improving sensor's characteristics; see Figure 3. The sensor was calibrated with both standard and extracted soil solutions, exhibiting a dynamic response range relevant for agricultural applications (1–1500 ppm), a Nernstian sensitivity with a slope of 64 mV/pNO₃, and an almost one-month lifetime during continuous monitoring of nitrate in a soil slurry. The same research group previously developed a microfluidic impedimetric nitrate sensor using a composite of graphene oxide (GO) nanosheets and poly(3,4-ethylenedioxythiophene) nanofibers, PEDOT-NFs-GO, as an effective matrix for immobilization of nitrate reductase enzyme. Its sensitivity is $61.15 \Omega/(\text{mg/L})/\text{cm}^2$ in a concentration range of 0.44–442 mg/L for nitrate ions in agricultural soils with a DL of 0.135 mg/L [63]. Other works on the development of electrochemical sensors for soil macronutrient assessments, with a focus on N-nitrite analysis, are summarized in a previous review by the same authors [17].

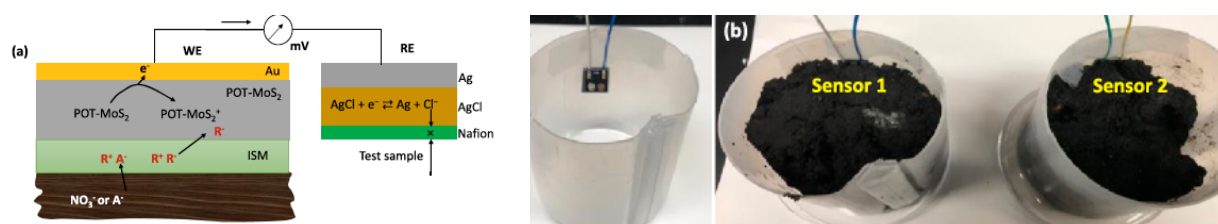


Figure 3. Schematic representation of an NO_3^- -SM/POT-MoS₂/Au sensor versus a Nafion-coated Ag/AgCl reference electrode (a). A photograph of the developed sensor and its application in long-period soil slurries analysis (b). Reprinted with permission from [62].

Applications of nitrate reductase (NR) for the development of nitrate-selective biosensors for soil analysis have been reported previously in several other, but not numerous, studies. Among them is an FET-based enzymatic sensor based on nitrate reductase (NR) and modified with a bipyridinium derivative and sodium dithionite, used as an electron transfer mediator and as an enzyme electron donor in the solution, respectively [64]. Vakilian and Massah reported a cyclic voltammetry (CV) nitrate biosensor based on a GC electrode modified with an anthraquinone-2-sulfonate (AQ) mediator of NR and covered with a perm-selective dialysis membrane to avoid enzyme loss during the analysis [65], and a portable nitrate biosensing device using a bi-modal approach combining electrochemical and spectroscopy-based measurement [66]. Alternatively to NR, ionic-liquids, ILs, have been also studied for nitrite-selective sensors. The unique properties of ILs, such as high viscosity and low volatility, and even more so their large electrochemical window and high conductivity, make them very promising for electrochemical sensors. Thus, in the work of the Radu group, a comparison between the traditional, portable colorimetric techniques, and graphite pencil-drawn electrodes prepared with phosphonium-based ILs or poly(methyl methacrylate)/poly(decyl methacrylate) (MMA-DMA) copolymer-based membranes (as alternatives to common PVC-membranes) doped with an anion-exchanger (ionophore-free, for NO_3^- assessment) and nonactin ionophore, for ammonia ion detection) in soils was reported [67]. IL-based membranes showed good suitability for NO_3^- -ISE with a DL of 5.5×10^{-7} M. An application of MMSA-DMA copolymer-based membranes showed suitability for both ion analyses and were employed for assessments of nitrate and ammonia-ions in 8 water and 15 soil samples. A comparison of results using the ISEs

and a colorimetric assay showed excellent correlations: Pearson's correlation coefficients R of 0.97 and 0.99 for NO_3^- and NH_4^+ , respectively. Cu nanoparticles, with reduced graphene oxide and carbon nanotubes as mediators for the electro-reduction of nitrate to ammonium ion on copper-based electrodes (coated wire electrodes), have also been employed for simultaneous detection of nitrite and nitrate in [68]. An application of square wave voltammetry has permitted analyte detection in a range from 0.1 to 75 μM .

Besides the many benefits, using electrochemical sensors for in situ and online measurements of total nitrogen (TN) and mineral N in soils has drawbacks. Several of them are discussed in [69]. A state-of-the-art review of the proximal sensing of soil nitrogen based on alternative methods based on visible and near-infrared spectroscopy (vis-NIRS) and mid-infrared spectroscopy (MIRS) is provided. These overcome the drawbacks of electrochemical techniques. Thus, in [70] the innovative, portable mid-infrared chemical sensor system for quantifying gaseous N_2O via coupling a substrate-integrated hollow waveguide (iHWG), simultaneously serving as highly miniaturized mid-infrared photon conduit and gas cell to a custom-made preconcentrator, was developed. The N_2O was collected on a solid sorbent material placed in the preconcentrator, and after being released by thermal desorption was detected with an iHWG-MIR sensor utilizing a compact Fourier transform infrared (FTIR) spectrometer with a DL of 5 ppbv. The tool for visualizing NH_3 emission and the local O_2 and pH microenvironment of soil upon manure using optical sensors, namely, the two dimensional (2D) optode, was reported by Merl and Koren [71]; see Figure 4. The developed NH_3 optode had a limit of detection of 2.11 ppm and a large working range (0–1800 ppm), and its suitability for studying NH_3 volatilization from soil was demonstrated.

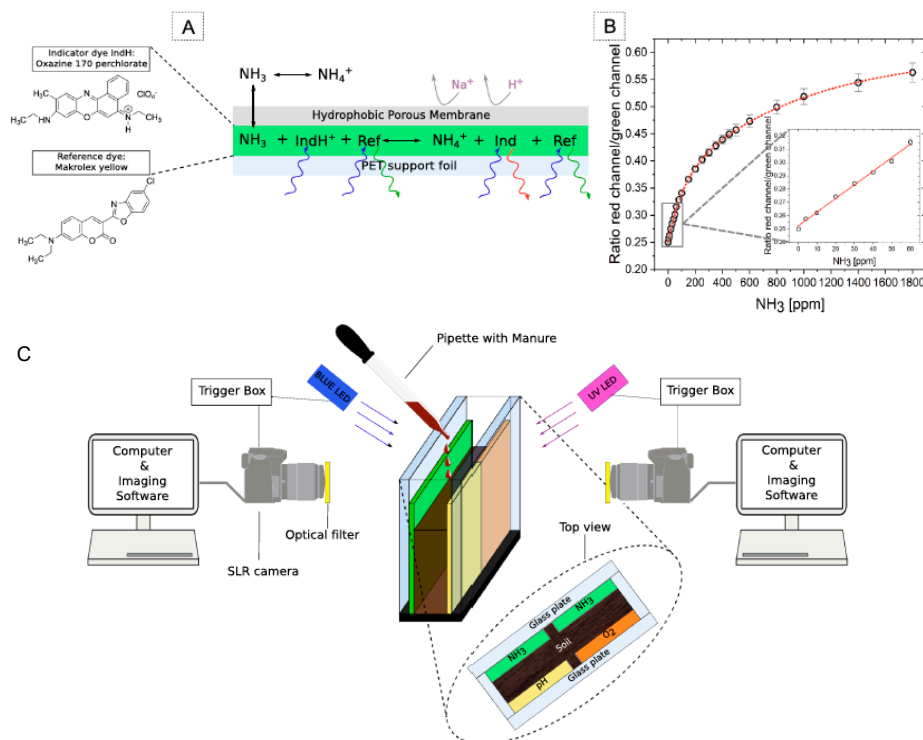


Figure 4. (A) The schematic of planar NH_3 optode composition and response: the interaction with ammonia that leads to changed emission of the indicator dye. (B) Calibration curve of the optode represented as concentration of NH_3 versus image intensity in red over the green channel. (C) The 2D planar optode experimental setup: soil was placed between two transparent glass plates that were 4 mm apart. Optodes (one O_2 , one pH and two NH_3) were attached to the insides. Two single-lens reflex cameras and blue and UV LEDs were positioned on the respective sides for simultaneous imaging of the three parameters. Manure was applied to the soil surface from the top using a pipette. Reported with permission from [71].

Another sensor for in-situ monitoring of ammonia volatilization from soils through gas phase ammonia detection based on a gas-permeable membrane-based conductivity probe (GPMCP) was reported in [72]. The abilities to monitor agricultural ammonia fertilizer's utilization efficiency and conclude on a labile N content in agricultural soils (two rice fields were monitored) were shown with the developed GPMCPs.

2.4. Total Phosphorous and Phosphates

Phosphorous (P) is the second most limiting macronutrient after nitrogen; it is especially important for agricultural applications and crop production, and is often supplemented in soil with external fertilizer. Most phosphorus compounds in the soil are insoluble and practically are not leached out of it. The poor solubility of phosphorus-containing mineral and organic compounds is the main reason for the low availability of soil phosphates and fertilizers to plants. Therefore, one of the most and important tasks of agrochemistry is the development of methods to increase the availability of soil phosphates to plants, and to monitor the amount of plant-available P. Chemical sensors are especially convenient for this last task. The content of P (total) in different soils (% of dry weight) varies in a fairly wide range: e.g., in soddy-podzolic soils, 0.05–0.15; grey forest, 0.10–0.20; and chernozems, 0.15–0.30. However, the gross phosphorus content in the soil cannot serve as a strict indicator of its plant availability. Only water-soluble dihydrogen phosphates H_2PO_4^- are readily available to plants, and to a lesser degree, hydrophosphates, HPO_4^{2-} , the concentration of which in soil is insignificant, since they gradually turn into poorly soluble phosphates [35,42,43].

The solubility of phosphates depends on the pH of the soil: below pH 7, H_2PO_4^- is prevalent, and therefore, the majority of potentiometric ISEs have been developed for detection of this ion in soils, even if the development of highly selective potentiometric sensors for detection of the hydrophilic phosphates is a rather challenging task. Novel ionophores and sensing ligands, permitting selective binding of H_2PO_4^- and HPO_4^{2-} ions, should be employed inside sensing membranes in order to replace the classical anion-exchangers having the lowest selectivity to these hydrophilic ions according to the Hoffmeister selectivity sequence determined by the free energy of ion solvation.

Previously, several macrocyclic organometallic ionophores were reported for phosphate sensing with ISEs. Thus, a group created a bis(tribenzyltin) oxide ionophore-doped PVC-based membrane for HPO_4^{2-} detection in soils [73]. The sensor has shown a close to Nernstian response in a hydrophosphate concentration range of 5×10^{-6} to 0.1 M. An orthophosphate-selective chemical sensor within a PVC-based membrane was developed and used for assessment of soil phosphorous in [74]. The amount of P estimated with the PO_4^{3-} -ISE was in good agreement with the amount found by the standard spectroscopy method, indicating potential applicability of the developed sensing probe for soil nutrient monitoring and rational soil fertigation assessments. The Cu-phthalocyanines were also reported as hydrophosphate-selective ionophores [75,76]. Thus, in [75] a copper monoaminophthalocyanine (CuMAPc) covalently attached to poly(n-butyl acrylate) (PnBA) was bound to a gold electrode pre-coated with the PEDOT poly(3,4-ethylenedioxythiophene), which was used as an ion-to-electron transducer. The ISE showed sufficient selectivity and a wide linear detection range of 4×10^{-9} to 0.01 M and was applied for FIA of environmental waters. In [76] a capacitive sensor based on the Cu-C,C,C,C-tetra-carboxylic phthalocyanineacrylate polymer adduct (Cu(II)TCPc-PAA) immobilized on Al-Cu/Si-p/SiO₂/Si₃N₄ substrate was developed for phosphate ion detection at low concentrations (10^{-10} – 10^{-5} M range with a slope of 27.7 mV/pHPO₄²⁻).

Metal electrodes, electrodes based on metal compounds, QDs (quantum dots), and enzyme-employing biosensors have also been reported for phosphate assessment in soils. Among them are Co electrode applications based on the conversion of surface cobalt oxide (CoO) to cobalt phosphate $\text{Co}_3(\text{PO}_4)_2$, tested by CV in ammonium lactate-acetic acid soil extracts for H_2PO_4^- detection [77]; and applications based on the transformation of $\text{Co}(\text{H}_2\text{PO}_4)_2$ to CoO and/or $\text{Co}(\text{OH})_2$ on cobalt wire electrodes [78]. A disposable

on-chip micro-sensor with planar cobalt (Co) microelectrodes and an Ag/AgCl reference for phosphate detection in soil extracts was reported by Zou et al. [79]. The sensor had a response range of 0.31–310 ppm phosphate-P, and permitted them to analyze both inorganic and organic phosphate compounds (KH_2PO_4 , adenosine 5'-triphosphate (ATP) and adenosine 5'-diphosphates (ADP), respectively) in soils.

In [80], a pencil graphite electrode electrochemically modified with molybdenum blue (Mo blue) and coated with PVC film was used in the detection of PO_4^{3-} ions based on a two-step phosphate reduction by differential pulse voltammetry (DPV) in acidic conditions. Cinti et al. have described a similar procedure performed on a reagent-less, paper-based screen-printed electrode [81]. The method nevertheless required the incorporation of external reactants, such as 0.1 M molybdate ions, 0.1 M KCl supporting electrolyte, and relatively concentrated 0.1 M sulfuric acid for the formation of phosphomolybdic complex in the presence of phosphate ions, to be detected further on the paper WE. The formation of silver phosphate, Ag_3PO_4 , was monitored for phosphate ion detection, with the nozzle-jet-printed, silver/reduced, graphene oxide (Ag/rGO) composite-based ISFET sensor reported in [82]. In [83] a nickel oxide/oxyhydroxide-modified printed carbon electrode was employed for chrono-potentiometric assessment of nickel phosphate (NiPO_4) produced as a result of first Ni(II)O oxidation to Ni(III)OOH in alkaline media. As a result of further Ni(III)OOH interaction with H_2PO_4^- , it was possible to detect the latter by means of indirect procedure.

Cadmium telluride (CdTe) QDs capped with synthesized thioglycolic acid (TGA) and initially quenched by the presence of Eu^{3+} ions in solution were used in a “turn-on” fluorescence sensor (excited at 365 nm) based on the photoinduced electron transfer (PET) effect for inorganic phosphate detection in an aqueous solution [84]. In [85], a ZnO nanorod array grown directly on seeded SiO_2/Si substrate in the gate region of a field-effect transistor (FET) and functionalized with pyruvate oxidase (PyO) were employed for phosphate detection in linear range of 0.1 μM to 7.0 mM. Other phosphate biosensors used pyruvate oxidase and a cobalt phthalocyanine screen-printed carbon electrode (CoPC-SPCE) for amperometric phosphate biosensing [86]; or two-enzymes, such as purine nucleoside phosphorylase (PNP) and xanthine oxidase (XOx), to detect phosphates after the several steps cascade oxidation to uric acid [87]. Molecularly Imprinted Polymers, MIPs, obtained from methacrylic acid (MAA) and N-allylthiourea monomers, templated with diphenyl phosphate, triethyl phosphate, and trimethyl phosphate, and deposited on an interdigital capacitive transducer, were reported for phosphate detection in a hydroponic system [88].

Optical methods have been employed previously for P assessment in soils by Bogreki and Lee [89]. The 345 sandy soil samples were collected from the Okeechobee Lake drainage basin. In these samples, the total P concentration varied in a wide range, from a few mg/kg to 2709 mg/kg. The modified spectra of soils were obtained by removing the nutrients, organic matter, and moisture contents of each soil sample and measuring using diffuse reflectance spectroscopy in the ultraviolet (UV), visible (VIS), and near-infrared (NIR) regions. Obtained in this way, soil spectral signatures were used to predict P concentrations by means of partial least squares regression, PLS, and provided the possibility to identify soil samples with very high P concentrations using soil signatures. Constituent spectra in the UV, VIS, and NIR regions with a root mean square error of prediction (RMSEP) from 172 to 222 mg/kg were demonstrated. Recently, a smartphone assisted optical sensor application for phosphates in environmental soils was reported by Sarwar et al. [90]. The paper-based fluorescent sensor was developed using the fluorophore N-[2-(1-maleimidyl)ethyl]-7-(diethylamino)-coumarin-3-carboxamide (MDCC), which when bound to a bacterial phosphate binding protein generates a fluorescent optical signal proportional to the concentration of phosphate. The sensor exhibited a linear detection range of 1.1 to 64 ppb.

2.5. Potassium Detection in Soils

Potassium is the third critical nutrient for crop production, and even if it is present in the soil in large quantities, the potassium pool available to plants is small [91], so potash fertilizer is necessary. Therefore, controlling the potassium content in the soil is extremely important. Electrochemical and optical sensors have been developed previously for potassium assessments in soils. The valinomycin-based ISE was used previously for determination of assimilated potassium in Egner-Rhiem soil extracts in [92]. The results of K assessment in soil extracts obtained with potentiometry and the flame photometry reference method were well correlated ($R^2 = 0.84$). An in-soil potentiometric potassium sensor system based on ion-selective PVC membranes deposited over graphite-epoxy solid inner contacts and incorporated in PVC tubes at three depths: 5, 20, and 50 cm, thereby permitting the monitoring of the potassium profile in different soil horizons, was reported in [93]. A linear relationship between in-field potassium contents found with the developed sensor system and with flame photometry ($R^2 = 0.992$ and $R^2 = 0.995$, for depths of 5 and 20 cm), was obtained. In [94] the ISEs were applied for simultaneous K and N analysis of Missouri and Illinois soil samples. Due to the large differences in K concentrations measured with ISE and determined by standard methods (below 50% of the real value), the use of a calibration factor was proposed in order to obtain actual nutrient concentrations. The same soil macronutrient sensing system was employed recently for the analysis of 36 soils collected from a single site, and the ability to estimate variations in $\text{NO}_3\text{-N}$, P, and K within a single test site was demonstrated [95]. An array of ISEs fabricated with new membranes and a cobalt rod, in conjunction with the previously developed normalization methods and calibration models, accurately estimated $\text{NO}_3\text{-N}$, P, and K in solution without the need to recalibrate the ISE system through standard laboratory analysis of soil samples from the new test site. A reduced GO was proposed as an ion-to-electron transducer for a screen printed valinomycin-based potassium ISE in [96]. The membrane cocktail was drop-casted on to the surface of an rGO/Au electrode. The sensor had improved potential stability through the inhibition of thin water layer formation on the electrode's surface. A plasticizer-free, butyl acrylate, potassium-selective membrane doped with valinomycin ionophore and a TpCIPBK (potassium tetra-p-chlorophenylborate) lipophilic cation-exchanger was used in a screen-printed handheld device deployed for detecting K in soil (extracted using strontium chloride) [97]. The analysis results were in a good agreement with ICP-atomic emission spectroscopy. The group of Bobacka reported the application of electrosynthesized polypyrrole/zeolite composites as a solid contact for an potassium ion-selective electrode with an enhanced detection limit ($6.3 \mu\text{M}$) [98]. One of the few examples of non-valinomycin-based selective membranes was recently reported in [99]. The authors prepared a potassium-selective ISFET device using potassium-ionophore-III incorporated into parylene encapsulated graphene FET. The ability to sense potassium ions down to 1 nM was shown, and its use with biological samples was demonstrated. Some examples of optical sensors for potassium assessment in biological samples (with possible application in soils) have been also published recently. Naderi et al. prepared an aptasensor based on the interaction of gold nano-particles (AuNPs) and a cationic dye for naked-eye K detection [100]. A selective fluorophore probe composed of 2-dicyanomethylene-3-cyano-4,5,5-trimethyl-2,5-dihydrofuran (TCF) as the chromophore and phenylazacrown-6-lariat ether (ACLE) as the K-ion recognition unit was prepared and used for colorimetric, fluorescent, and photoacoustic detection of potassium in a wide linear detection range, from 5 to 200 mM [101].

2.6. pH, Soil Salinity, and Other Macroelements

The soil pH is another key parameter responsible for macro- and microelement bioavailability, transport processes, and multiple biogeochemical factors—including C, N, P, and S cycling, metal availability, and soil fertility [102]. Typically soil pH ranges between 5.5 and 8. Shifting pH values outside of this range can lead to degradation of soil structure, changes in plant-available trace elements, and inhibition of soil microbial activity. Classical

glass membraned pH-selective electrodes are widely used for routine laboratory analysis of soils (mainly in aqueous or saline extracts) [43]. As noted, standard soil analysis methods require sampling and collection procedures; in addition, the final laboratory procedure (even if this measurement is often made with a standard glass pH electrode) is limited by the personnel and costs of laboratory analysis. Automating pH measurements can help solve this issue. In order to lower the cost of such work and create a field map of pH distribution, Staggenborg et al. measured the pH of Kansas soils directly in the field using a mobile device with an incorporated pH sensor [103]. In the study of Silva and Molin, the manual and automated methods of an ion-selective sensor in determining soil pH were compared [104], with the better results being provided by the manual operation. The in-field application of pH-ISEs is somewhat difficult and does not always meet the requirements of precision agriculture [105]. Therefore, more and more sensitive materials and analytical procedures are being developed to estimate soil pH using sensors.

Different types of chemical sensors have been used to estimate soil pH: electrochemical ISEs [52,53,105] and ISFETs [106,107], and colorimetric optodes, including planar optodes (POs) [22]. For instance, an analytical platform combining temperature and moisture sensors, together with all-solid-state pH and Ca-ISEs, was used for precision agriculture soil analysis in [108]. The pH and Ca contents estimated with the developed system correlated well with the standard soil analysis methodologies (pH glass electrode used for soil extracts with 0.05 M CaCl₂, and Ca extraction in an ion-exchange resin with flame atomic absorption spectrometry detection, respectively). Additionally, the possibility to correct the measured Ca²⁺-ions concentrations at different soil depths, and the possibility to estimate the soil's buffering capacity based upon the relative soil moisture variation, were shown through a multiple linear regression model.

A fiber-optic sensor based on a stainless-steel guideline equipped with an optical sensing tip modified with sensing material composed of resin beads coated with a phenol red pH indicator for soil pH assessment at different depths was reported in [109]. The sensor was adapted for measurements at high pressures up to 17 bar, and was used to analyze the pH levels of groundwater. Nowadays, after the application of fiber-optic sensors, the next generation pH optical sensors employ 2D imaging in planar optodes. Indeed, in [110], Hofer et al. developed a method for direct pH imaging using PO prepared with ultra-thin (<100 μm) polyurethane-based gels, incorporating anion and cation binding materials and the fluorescent pH indicator DCIFODA (2',7'-dichloro-5(6)-N-octadecyl-carboxamidofluorescein). The dynamic range for PO-based pH mapping was between pH 5.5 and 7.5 with a t₉₀ response time of about 1h. The case-study in the *Salix Smithiana* rhizosphere (the soil zone around the plant roots) demonstrated the gel's suitability for multi-analyte solute imaging, and for pH gradient mapping and concurrent metal solubility pattern generation.

In [111], a conductometric microsensor modified with a polyaniline doped with dodecylbenzene sulfonic acid (PANI-DBSA) and an SU-8 (an epoxy resin) nanocomposite film to measure changes in soil pH is reported. The nanocomposite was spin coated on Au-IDE patterned on Si/SiO₂, and exhibited an excellent response towards changes in pH in three different conditions, namely, standard buffer solutions with pHs ranging from 2 to 10, in red and bentonite soils (pH varied with soil moisture content), and pHs in different concentrations of a calcium chloride (CaCl₂) solution. The sensitivities of 41 and 52 μS/pH (CaCl₂) for red and bentonite soil samples were achieved with response and recovery times of 10 and 30 s, respectively, indicating the potential applicability of the PANI/SU-8 composite microsensor to measuring variations in soil pH important for precision agriculture applications. Chang et al. proposed a new method utilizing a fluorocarbon thin film via fluorine termination and boron-doped diamond (BDD) solution-gate field effect transistors (SGFETs) for pH sensing with potential agriculture applications [112]. The developed device demonstrated high pH sensitivities of 67.4 and 34.9 mV/pH in acid and alkaline pH regions, respectively. Together with NH₃ visualizing PO optodes, the pH and O₂ optodes were used for the soil microenvironment monitoring of manure in [17].

Soil salinity is an extremely important soil quality parameter, especially in arid regions, where it may increase significantly and damage plants. The soil salinity is estimated by measuring of electrical conductivity of soil extracts. While estimating the soil salinity, the nature and the composition of soluble salts; and the temperature, moisture, and texture of the soil must be considered, since all these parameters influence the measured electric conductivity. Hence, the development of new analytical procedures for soil salinity evaluation is needed. Additionally, being the dynamic parameter that characterizes the “soil moment”, the soil salinity should be measured quickly, and should consider all the above-listed influencing factors [3].

Sensors, through permitting fast and in-field analysis, well meet the soil salinity estimation requirements, and some sensory applications have been reported previously. For instance, the frequency-domain reflectometry (FDR) sensor was designed for soil salinity assessments of sandy soils characterized by soil moisture and bulk electrical conductivity varying in a wide range [113]. A soil salinity index is estimated from dielectric permittivity spectra acquired in the 10–500 MHz, frequency range and is derived from the bulk electrical conductivity value. For five tested soil samples, the linear relationship between bulk electrical conductivity and dielectric permittivity was established. The developed FDR procedure of soil salinity index estimation was further extended to the in-field analysis of loam and clayey soils. In [114], the commercially available FDR and capacitance-conductance (CC) sensors were used to estimate the dielectric permittivity and electrical conductivity of bulk soil. On the basis of these values, a combined equation was obtained to estimate the pore-water electrical conductivity, which is closely related to the salinity of a soil in contact with plant roots. Recently, in [115] the new time-varying dynamic linear model for estimating sandy soil pore water electrical conductivity from FDR records for ecological and hydrological applications was proposed.

Detection of water-soluble forms of calcium and magnesium in soils and fertilizers have been also reported previously. Thus, ISEs and ISFETs with photocurable sensing membranes based on aliphatic diacrylated polyurethane for evaluation of Ca^{2+} activity in water samples extracted from agricultural soils were reported in [116]. They have demonstrated long lifetimes (>8 month) and close to Nernstian (26–27 mV/dec) responses in a concentration range from 5×10^{-6} mol/L to 8×10^{-2} mol/L. Such a sensor was employed for Ca^{2+} assessment in agricultural soils extracts. The results well correlated with standard methods' estimates. In recent work by our group, the assessment of Mg^{2+} concentrations in fertilizers was performed with novel all-solid-state optical sensors based on phenyl-substituted diaza-18-crown-6 8-hydroxyquinoline (DCHQ-Ph) [117]. The improved Mg-selectivity of optodes in comparison to the highly influencing Ca ions was demonstrated, indicating the sensor's utility for assessments of magnesium in environmental samples, and soils in particular, with high concentrations of calcium ions.

2.7. Soil Moisture

Soil moisture is an important hydroecological parameter, determining to a high degree the rates of many soil processes, for instance, biota growth and diversity, the accumulation and removal of organic and inorganic compounds, and substances' transformations (oxidation, dissolution, precipitation, etc.). The natural soil moisture balance is determined by several parameters. Among them, the most influential are the climate, the landscape, the vegetation, and anthropogenic activities. The importance of soil moisture monitoring is evident not only to achieve efficiency and sustainability in agriculture, but also for landscape moisture statistic monitoring and long-term global soil moisture mapping. The soil moisture sensing methodologies include laboratory (mainly gravimetric) methods, in-situ moisture sensing methods, and remote and proximal in-field applications [37]. Soil moisture is estimated as the gravimetric water content, $W:W(\%) = 100(V_w/V_s)$, where V_w is the total mass of water in the soil and V_s is the total mass of all soil components [2]. The water holding capacity, water permeability, and wettability of soil, all depending on both mineral and organic soil composition, significantly influence the soil moisture. Typically, it

varies between 40% and 60%, and depends also on soil porosity and the volumes of liquid and gaseous fractions. The most common and reliable laboratory technique with which to measure the water content in the soils is the thermogravimetric method, but unfortunately it is time consuming, non-repeatable, and suffers from a soil removal requirement (the sample must be physically sampled and removed from the collection site). Indirect methods of soil moisture assessment are based on measurements of electrical conductivity, thermal conductivity, or absorption of radiation. Among them, time domain reflectometry (TDR) and electromagnetic impedance measurements can be distinguished. While measuring the moisture content, one should consider the special dynamism of its values, its relationships with the temperatures of air and soil, the amount of rainfall, an uneven distribution over the surface of the soil, and the soil profile. Often, traditional laboratory methods are not sufficient to obtain accurate data on landscape soil moisture, and applications of the new methods based on measurements of undisturbed samples in the field are required.

Several soil moisture sensing technologies have been developed previously, and among them, sensors have become widely applied. A very comprehensive overview of the latest works reported on the different soil moisture sensing methodologies is reported in [37]. In [118], using carbon-based materials for humidity sensing, including soil water content determination for agricultural applications, is discussed. A survey of 77 recent studies dealing with carbonaceous materials used as capacitive and resistive humidity sensors is provided.

Among the soil moisture sensors, capacitive sensors are the most exploited. Thus, a soil profile moisture sensor based on a high frequency capacitor was designed in [119]. A good correlation between traditional gravimetric method results and the sensor response was obtained: an RSD less than 4.7% and a correlation coefficient of 0.967. The design and fabrication of a self-powered and autonomous fringing field capacitive sensor based on a porous ceramic to measure soil water content is reported in [120]. The sensor's capacitance was measured in a laboratory prototype and increased up to 5% when the volumetric water content of the porous ceramic changed from 3 to 36%, resulting in a sensitivity of $S = 15.5$ pF per unit change. System functioning under the complete irrigation cycle was investigated. The potential use of graphene quantum dots, GQDs, as soil moisture sensors was explored in [121]. The micro-sensor with GQDs as the sensing material was used to perform soil moisture measurements of two different soils. It was shown that upon soil water content variation from 0 to 32%, the sensor resistance changed by 99% and 97% for the red soil (silt loam) and black soil (clayey), respectively. The sensor's response time was around 180 s for both analyzed soils. Patil et al. investigated polyvinyl alcohol (PVA)-modified zinc oxide nanowires (ZnONW)-based microsensors to measure relative humidity and gravimetric soil moisture contents for agriculture applications [122]. The ZnO NW were hydrothermally grown on the inter digitated electrodes (IDEs) patterned on Si/SiO₂ substrate, and further functionalized by drop-casting a PVA solution. The microsensors were exposed to different levels of relative humidity (% RH) ranging from 40 to 90%, and various moisture contents of bentonite and red soils, demonstrating decreasing resistance with increasing humidity (% RH) and gravimetric soil moisture, with satisfactory sensitivities of 7.5 and 12.2 K Ω /0.1% change in gravimetric water content when exposed to bentonite and red soil samples, respectively, indicating the potential utility of the platform for measurements of humidity and soil moisture contents in agricultural applications. Novel, low-cost, screen-printed (thick-film) conductivity sensors were designed and used for monitoring changes in the soil structure by correlating changes in soil conductivity and water content during cyclic wetting and drying of the soil in [123]. The thick-film conductivity sensor contained four electrodes. It used an alternating polarity square wave current source at a frequency of 1 kHz for the drive signal to the current sourcing electrodes, and measured the resulting potential difference across the voltage sensing electrodes. Sensors were incorporated into laboratory-based soil columns and used together with water-content sensors. Significant differences were found in the relationships between the electrical conductivity and water content (CWC) characteristics of the three soil types:

Leighton Buzzard type E sand, commercial builder's sand, and a sand-silt-Cl Leighton Buzzard type E sand. Some works on soil moisture assessment have been devoted to the problem of a huge amount of data obtained in in-field measurements. In [124] it was shown that the selection of appropriate time series, and wavelet filtering applied to identifying the representative soil sample points and sampling depths through analysis of hourly measured soil moisture, allowed decreasing the number of moisture sensors (to 16 from 28) without a significant loss of information.

2.8. Other Compounds and Sensory Applications

The gases entrapped in or exhaled by soil not only allow for respiration of both plant roots and soil organisms, but can also serve as the indicators of soil quality and pollution, and provide important information on the effectiveness of fertigation and irrigation, for decisions on best treatment practices. Moreover, the control of soil gas emissions (among these gases are CO₂, CH₄, NO and NO₂, NH₃, SO₂, and others) is useful for understanding the role of soil in greenhouse gas accumulation in atmosphere.

Several reports on sensors for soil gas monitoring have been published. A review on gas sensors based on membrane diffusion to achieve real-time and continuous monitoring of important trace gases (e.g., CO₂, SO₂, and NH₃) in the natural environment (water, soil, and air) is presented in [41]. A membrane-based linear gas sensor applied to monitoring and quantifying the carbon dioxide (CO₂) emitted by soil that could originate (escaping) from pipelines, underground storages, etc., was presented in [125]. The sensor has the form of a flexible tube and by the selective permeation of a gas, such as CO₂, H₂, or natural gas (consisting primarily of CH₄), through its tubular membrane, enables the monitoring of the gas's concentration mean measured along its total length [126]. Such an approach can be useful for, e. g., rapid leakage detection with respect to carbon capture and storage (CCS) issues.

Planar optodes have been used to investigate ammonium concentrations, diffusion, and transport in soil after fertilization [71,127,128]. The oxygen consumption and greenhouse gas emissions (mainly CO₂) in soils after were tested after amendment with organic fertilizers [129], and applications of digestate to soil [130] were previously monitored with PO sensors. An application of a SAW sensor functionalized with a polymeric coating (based on α,ω -dihydroxyalkyl lead(II)carboxylate complexes with 1,3-butadiene diepoxide as the co-monomer and 1,3,5-trihydroxybenzene as the reticulating agent) and a geophysical tool—ground penetrating RADAR (GPR)—to register sensor response, was reported to detect H₂S in gas phase in a wireless configuration in soil and in real conditions (weather, temperature, and humidity) in [131]. The utility of the developed device for the land preservation of industrial sites was underlined. Moreover, the applications of gas sensor arrays for soil quality evaluation and contamination monitoring through the analysis of exhaled gases and volatile organic compounds (VOCs) have been reported and are discussed in more detail in the Section 5 of the present review.

Among other sensing technologies, nanomaterial-based sensors have been employed for sustainable management of agricultural soil, for the detection and quantification of various hazardous pollutants, and in applications for other important issues, such as pollutant remediation, nutrient bioavailability, and metallic immobilization. All this is discussed in detail in recent reviews [132,133]. The recent trends and practical applications of nano-enabled sensors to directly measuring soil nutrients, macro- and microelements, pH, and pollutants [134], such as metals, organics (including pesticides and herbicides), inorganic ions, and others, are discussed. The general impacts of nanomaterial applications for soil analysis are represented in Figure 5.

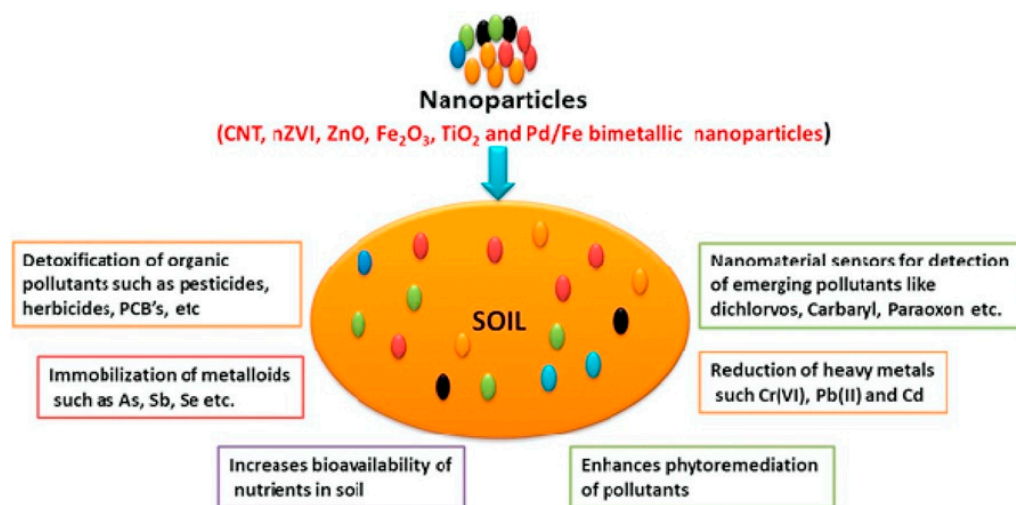


Figure 5. Illustration of the main uses of nanomaterials in soil analysis and remediation. Reprinted with permission from [133].

Additionally, several recently reported examples of different and non-trivial sensing techniques for soil analysis are listed below. In [135], an interesting and useful sensory application for monitoring the changes in soil moisture using fiber Bragg grating (FBG) sensors and water-swelling polymers is reported. The polymer material swells to several times the original volume upon the absorption of water, and the expansion induces measurable tension in the FBG sensor. The scour monitoring system is vertically embedded in soil, and the measured wavelength shifting of a particular sensor is able to indicate that the sensor is no longer covered with soil. The developed device can be useful to estimate the soil humidity, but also can be used for subsea pipeline scour monitoring and other types of chemical sensing by interchanging the polymer with materials sensitive to other measurands, such as oils. A very curious application of sensing technologies, robotics, and wireless sensing networks inside a real-time, farmer-assistive flower-harvesting agricultural robot was recently reported by Bhaskar et al. in [136]. The AGROBOT performs multi-functional operations: It identifies healthy flowers with imaging and machine learning and neural network algorithms for image processing. The robot detects the water content, pH, and fertility of a soil with the incorporated sensor unit comprising a moisture hygrometer and an electrochemical pH and fertility sensor; the passive infrared (PIR) sensor is used for territorial control. The data are saved on AGROBOT's SIM card with real-time owner access. This new device was developed for farm labors, in order to reduce their work and time expenditure.

3. Detection of Soil Microelements and Pollutants

3.1. Contamination by Heavy Metals

The necessity of detecting heavy metals is determined by the importance of these elements and their amounts in balanced soil systems, and due to the growing environmental multi-metal contamination that pose serious threats to public health due to their toxicity and ability to accumulate. While present in ionic forms, metal pollutants alter the properties of the soil, such as the pH, color, porosity, and natural chemistry, and also contaminate water. Absorbed by plants, they enter the food chain, and upon accumulation in animals and humans, bring about serious problems with the central nervous system (CNS); gastrointestinal, kidney, and reproductive system disorders; bone demineralization; and an increased risk of lung cancer [137]. Hence, sensitive and selective sensing methods for detecting heavy metals in trace amounts in soils are greatly required. Several studies on heavy metal detection in soils, mainly performed by chemical sensors with different transduction principles, have been reported, as described below [138–189].

Among the transition and heavy metal contaminants, copper, zinc, iron, cobalt, nickel, cadmium, lead, and mercury are especially controlled in soils, and the last four metals are considered the most toxic; they are the least permissible. In drinking water (WHO): 0.0008 mg/L, 0.001 mg/L, 0.005 mg/L, 0.05 mg/L, and 0.01 mg/L for Ni(II), Hg(II) and Co(II), Cd(II), and Pb(II), respectively [138,139].

3.1.1. Pb(II) and Hg(II) Sensors

Lead ion detection with a LOD of 2–5.8 $\mu\text{g/L}$ was performed with square-wave stripping voltammetry (SWSV) using screen-printed gold electrodes, with wastewaters and soil extracts from polluted sites [140]. Several ion-selective electrodes demonstrating enhanced Pb^{2+} -selectivity were also developed [43,141,142]. In [141] a Pt wire coated with a phenylhydrazone-derivative-carbon composite in a PVC membrane for monitoring of Pb(II) in the environment arising from the contaminated soils and rocks that undergo weathering was proposed. Liquid and solid-contact ISEs were developed and used for assessments of Pb(II) levels of between 30 and 29,100 mg/kg in soil samples from abandoned mining sites, demonstrating good agreement with the reference AAS method [142]. Wilson et al. have tested two PVC-based ISEs doped with bis-thioureas ionophores 1,3-bis(N'-benzoylthioureido)benzene and 1,3-bis(N'-furoylthioureido)benzene for direct potentiometric determination of Pb(II) in soils [143]. The sensors exhibited Nernstian responses and good selectivity for Pb(II) over other metal ions in a wide concentration range (4×10^{-6} to 10^{-2} M) in solutions with pHs of 2.2–6.0.

In [144], Chen and co-authors have reported ion-selective high electron mobility transistors (ISHEMT) based on a classical PVC-based polymeric membrane doped with commercially available lead ionophore IV or mercury ionophore I, which is suitable for the detection of Pb(II) and Hg(II) in environmental samples. Due to its construction, the highly modulated ISHEMT sensors demonstrated enhanced sensitivity (with super-Nernstian responses) and low DL of 10^{-10} M for Pb^{2+} and 10^{-11} M for Hg^{2+} , respectively. The possibility of lowering the DL of lead assessments to picomolar concentrations was demonstrated for mass-sensitive SAW sensors functionalized with polypyrrole (PPy) ionic imprinted polymers, using two chelating agents, L-cysteine (LCys) and acrylic acid (AA), in [145]. The latter sensor demonstrated the lower DL (0.1 pM) and higher selectivity for gravimetric detection of lead in Bousselem River (in Sétif city, Algeria) water samples. The utility of sensors for soil analysis was also discussed. In [146] differential pulse anodic stripping voltammetry analysis (DPASV) was employed for detection of trace heavy metal ions, lead and cadmium in particular, using a glassy carbon electrode modified with a mixture of SWCNTs and inactive *Trichoderma asperellum* fungus biomass, selected from soil contaminated with metals. The biomass cell walls were able to fix metal ions due to a large number of appropriate chemical groups (carboxyl, sulfonate, amine, hydroxyl, carbonyl, imidazole, etc.). The resulting peak currents were linearly related to the concentrations of the metal ions, with DL 10^{-8} and 10^{-7} M for Pb^{2+} and Cd^{2+} , respectively. The sensors were tested with real water samples with recoveries in the range of 95.3–106.5%, suggesting their potential applicability to environmental monitoring, including that of soils.

A fluorescent aptasensor based on a thrombin-binding aptamer (TBA) probe and labeled with the donor carboxyfluorescein (FAM) and 4-([4-(dimethylamino) phenyl]azo)benzoic acid (DABCYL) quencher at its 5' and 3' termini, respectively, was used by Liu et al. for a Pb^{2+} assessment of Montana soil [147]. Two different conformations of aptamer were found upon binding with Pb^{2+} and Hg^{2+} ions, allowing the selective detection of both ions at low concentrations in the 300 pM–5.0 nM range. Later, the G-quadruplex DNAzyme-based Pb(II)-selective fluorescence assay was reported by Li et al. [148]. The assay had a wide linear detection range from 0 to 1000 nM, a DL of 0.4 nM, and was employed for a Pb(II) assessment of water extracts from soils, and the results comparable with those of an ICP/MS-method. The aptamer/reporter conjugates of polythymine(T33)/benzothiazolium-4-quinolinium dimer derivative (TOTO-3) and polyguanine (G33)/terbium ion (Tb^{3+}) conjugates, were used, respectively, for the detection of mercury (II) and lead (II) ions in

soil and pond water samples [149]. The DL for Hg^{2+} and Pb^{2+} ions were 10.0 and 1.0 nM, respectively, and the results correlated well with those of the standard ICP-MS method. In [150] Xiao et al. reported an electrochemical DNAzyme-based biosensor using methylene blue (MB) as a redox active component immobilized onto an Au working electrode (WE) surface through Au-sulphur bonding for Pb^{2+} detection, with a DL of 300 nM and a linear working range from 0.5 to 10 μM . The sensor was used for lead assessments of extracts of soil spiked with lead, illustrating the sensor's applicability. More examples of optical and electrochemical nucleic acid-based biosensors for analysis of lead in real samples, including soils, are given in comprehensive reviews by Liang et al. in [151], Dolati et al. [152], and Khoshbin et al. [153]. The application of nanomaterial-based fluorescent sensors for the detection of lead ions was very recently summarized by Singh et al. [154].

3.1.2. Cd(II) Sensors

Among the transition metals, cadmium is one of the most widespread health-hazardous pollutants due to its wide range of applications in many fields, such as mining, metal smelting, and fuel combustion. Cd(II) is accumulated in soils from vessel and mining plants emissions, polluted sewage sludges, and waste incineration. From soil, cadmium can easily enter the food chain. Therefore, much attention was given previously to Cd^{2+} detection in soils.

Md Noh et al. developed screen-printed carbon electrodes modified with in situ co-deposition of Hg and cysteine, which were sensitive for cadmium(II) detection via stripping chronopotentiometry [155]. Those sensors have shown improved Cd (II) selectivity in the concentration range of 0.4 to 800 $\mu\text{g/L}$ with a DL of 0.4 $\mu\text{g/L}$, and were employed for Cd (II) assessments of wastewater and soils sampled from contaminated sites. The portable Au interdigitated sensors fabricated using xurographic technology were tested for in-situ Cd(II) concentration assessments of soils by Radovanović et al. [156]. The capacitance and impedance changes as functions of frequency were investigated by exposing the sensors to different concentrations of cadmium in agricultural soil samples collected in the Northern Province of Vojvodina, Republic of Serbia. Among the tested pollutants (Cd, Cu, As), the developed sensing platform showed sensitivity to Cd. In [157] a $\text{Bi}_2\text{O}_3/\text{Fe}_2\text{O}_3$ -doped graphene oxide nanocomposite was synthesized for square wave voltammetric detection of toxic cadmium ions in environmental and biological samples. The synthesized composite material, $\text{Bi}_2\text{O}_3/\text{Fe}_2\text{O}_3@\text{GO}$, was found to be selective towards Cd(II) in the presence of other metal ions and biomolecules; the experiments with Cd(II)-spiked soils resulted in recoveries in the 97–99% range.

In recent work by our group, the two fluorescent chromophores obtained from the 2,8-dithia-5-aza-2,6-pyridinophane macrocycle substituted either with 2-(20-hydroxy-30-naphthyl)-4-methylbenzoxazole (HNBO, ligand L1) or 7-(2-ethylamino)-4-methylcoumarin (ligand L2) were tested for the detection of Cd(II) and Zn^{2+} ions in soils [158]. Ligands were incorporated inside PVC membranes, and optical sensors and a sensor array based on the photoassisted technique (PT) for sensing membrane luminescence were developed; see Figure 6. The enhanced selectivity to Cd^{2+} of L1-doped optodes has permitted the detection of this ion in aqueous extracts of tree soil samples with different andrological impacts (see Section 4 for more details). The results were in agreement with the Cd^{2+} contents estimated with the standard AAS method ($[\text{Cd}^{2+}]_{\text{L1}} = 0.511, 0.007, 0.024 \text{ mg/kg}$ vs. $[\text{Cd}^{2+}]_{\text{AAS}} = 0.574, 0.010, 0.030 \text{ mg/kg}$ for airport, garden, and waste dump samples, respectively).

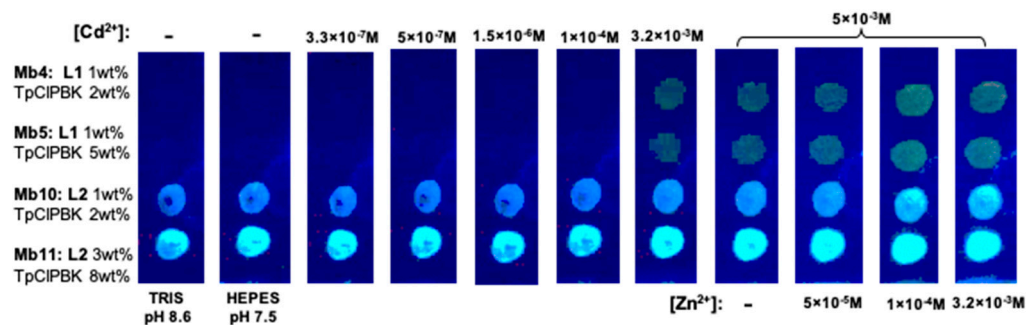


Figure 6. The PT response of L1- and L2-based optodes in binary solutions of Cd^{2+} and Zn^{2+} ions, in 0.01 M HEPES buffer at pH 7.5 and LED illumination at $\lambda_{\text{ex}} = 380$ nm. Reproduced from [158] with permission from the Centre National de la Recherche Scientifique (CNRS) and the Royal Society of Chemistry.

3.1.3. Cu(II) Sensors

Among the transition metals, copper is one of the important essential trace elements, since it is a key constituent of many enzymes [159]. Nevertheless, when present in large quantities, copper is toxic. It may cause gastrointestinal bleeding, intravascular hemolysis, hepatocellular toxicity, and acute renal failure, and hence, levels of copper pollution should be monitored. In soil, copper accumulates due to the electrical and textile industries and from agricultural maintenance, passing then in the ground water and food chain. According to our literature analysis, fluorometric and colorimetric optical sensors remain the most popular devices for copper assessment in environmental samples (mainly waters) over the last decade [160–165]. At the same time, the number of reports on applications of optical chemical sensors in soils or aqueous soil extracts is quite small. In [166] an optical sensor based on a polyaniline (PANi) film modified with denatured antibody immunoglobulin G (IgG) and deposited on the core of an optical fiber was reported. It has excellent selectivity towards Cu(II) ions over several other metal ion interferents. The possibility of applying this sensor in soils was considered. Sutariya et al. employed a calix[4]arene conjugate bearing 1-aminoanthraquinone with an amide linkage for recognition of Cu^{2+} , La^{3+} , and Br^- ions via fluorescence spectroscopy [167]. The sensor demonstrated a DL of 0.19 nM for Cu^{2+} , 0.88 nM for La^{3+} , and 0.15 nM for Br^- in the working concentration range of 5–120 nM for each of the tested ions. Deposited on a paper support, the fluorophore conjugate underwent fluorescence resonance energy transfer with fluorescence quenching in the presence of Cu^{2+} and Br^- ions, or enhancement for La^{3+} . The sensor was used to sense spiked La^{3+} in industrial soil samples, Cu^{2+} in blood serum, and Br^- from industrial wastewater samples using fluorescence titration with good recoveries of 94–99%.

A fluorescent chemosensor based on a dissolvable conjugated polymer, oligo (1-pyreneboronic acid) (OPYBA), obtained by electrosynthesis for highly selective analysis of Cu^{2+} at ultra-trace levels was reported by Zhang et al. [168]. The polymer was first obtained by potentiostatic electropolymerization from monomer in an *can*/tetrabutylammonium tetrafluoroborate solution (vs Ag/AgCl at 1.0 V), de-doped with dilute HCl, and dissolved in THF (5.0×10^{-8} M) for analysis of Cu^{2+} in two linear ranges of 25 pM–88.2 μM and 188–750 μM with an LDL limit of 23 pM. The possibility of detecting Cu^{2+} in cropland soil with recovery of 101.7% and in other environmental and agro-product samples was shown.

Recently, we reported colorimetric sensors based on two novel Zn-tetraphenyl-porphyrin ligands (ZnTPP)—one functionalized with 1,3-bis(2-pyridylimino)isoindoline, ZnTPP-BPI, and another Zn(II)TPP-BPI-crown (ZnPC), functionalized with two dibenzocrown-ether moieties—for cation assessments of soils [169]. The ligands were incorporated inside PVC-based polymeric membranes, which then were tested on paper or glass solid supports. The visibly (naked eye) observed color changes of optode demonstrated the suitability of the ZnPC-based optodes to performing fast monitoring of Cu(II) ions in the concentration range between 6.6×10^{-7} and 2.4×10^{-2} M, with an LDL of 0.03 mg/L, which is lower

than WHO's guideline value of 2 mg/L for natural waters. The results of the optodes' use for aqueous soil extracts were in a good agreement with those of a standard ASS method, suggesting the utility of these sensors for the aims of express environmental monitoring. The developed optical sensors were able to rapidly assess the presence of copper ions above the established borderline concentration of 1×10^{-3} M (high copper levels in soils are hazardous for many species), providing different visual responses for soils contaminated with other metals sampled close to the airport and fuel stations. Additionally, a high copper concentration was detected in a soil sample collected in the "Tor Vergata" University garden (placed in the proximity to the highway).

Several potentiometric Cu-selective ISEs have been also developed. A 1-phenyl-2-(2-hydroxyphenylhydrazo)butane-1,3-dione (H₂L) ionophore-based copper-selective PVC membrane electrode for precise copper analysis in soils polluted by oil was developed by Kopylovich et al. [170]. Singh et al. have exploited benzothiazole-based chelating ionophores, 1,3-bis[2-(1,3-benzothiazol-2-yl)-phenoxy]propane (L1) and 1,2'-bis[2-(1,3-benzothiazol-2-yl)-phenoxy]2-ethoxyethane(L2) [171]; two polydentate Schiff bases, 4-(5-mercapto-1,3,4-thiadiazol-2-ylimino)pentan-2-one (S₁) and (2-(indol-3-yl)vinyl)-1,3,4-thiadiazole-2-thiol (S₂) [172]; and ionophores inside PVS-based solvent polymeric membranes for selective detection of Cu²⁺ ions. Optimization of membrane composition, working conditions, and transducer material (classical inner liquid contact sensors vs. coated graphite electrodes, CGE, and coated pyrolytic graphite electrodes, CPGE) was performed. The developed sensors were used successfully for the potentiometric determination of Cu²⁺ in soils (locations Haridwar and Rishikesh, India), water, and some plants and edible oil samples. Good agreement of the ISEs' responses with AAS results was found.

3.1.4. Detection of Other Trace Metals

A review of different techniques with a primary focus on biosensors for the detection of trace metals and multi-metal sensing in the environment is given in [173]. In [174], a review of the relevant literature on the detection of uranium (highly carcinogenic and biologically toxic) and its compounds (uranyl ions), produced by the nuclear industry, is summarized. Among other recent studies, Van der Horst et al. have reported in [175] a sensor using a glassy carbon electrode coated with bismuth–silver bimetallic nanoparticles, modified with dimethylglyoxime (DMG) as the chelating agent for the stripping voltametric analysis of platinum group metals in soil samples. The differential pulse adsorptive stripping peak current signal was found to be linear, ranging from 0.2 to 1.0 ng/L with LODs of 0.19, 0.20, and 0.22 ng/L for Pd, Pt, and Rh, respectively. The sensor showed good reproducibility, with an RSD of 4.61% for Pd(II), 5.16% for Pt(II), and 5.27% for Rh(III), respectively, indicating the practical utility of the developed approach for the determination of trace amounts of Rh(III), Pt(II), and Pd(II) in roadside dust and soil samples. Additionally, fluorescent sensors for potential analysis of Pd-contaminants in drugs, water, soil, or plants have been reported [176,177]. A tridentate PNO-modified rhodamine-spirolactam ligand for the analysis of Pd-contaminated samples was developed in [176]. Liang et al. have developed fluorescent carbon nanoparticles (CNPs) from citric acid and polyethyleneimine grafted onto mesoporous silica microspheres, which exhibited selective Pd detection with a DL of 0.18 ppm. By using this probe, the Pd ions were adsorbed and detected in soil or drug samples [177].

Ayranci and Ak have developed an iron(III)-sensitive sensor based on a pyrene-substituted 2,5-dithienylpyrrole (TPP) conductive polymer electrochemically deposited on an ITO electrode's surface [178]. The investigation of the electrochemical response of the sensor to different metal ions in aqueous media showed the excellent potentiometric response to Fe(III) ions with a DL of 1.73×10^{-7} M, whereas there was no significant electrochemical signal observed in other metal ion solutions, including Fe(II), Zn(II), Cu(II), Hg(II), and Cd(II). The developed sensor is a promising, disposable, low-cost metal ion sensing platform for in-field testing of aqueous and biological samples. Brodersen et al.

combined PO with DGT to study seagrass-mediated phosphorus and iron solubilization in tropical sediments [179].

The possibility of detecting trace amounts of the extremely toxic Ni(II) ions in soils and other environmental samples by means of a colorimetric sensor based on zwitterionic polypeptide EKEKEKPPPPC (EK)₃-capped gold nanoparticles (AuNPs-(EK)₃), was reported by Parnsubsakul et al. [180]. Due to the presence of alternate carboxylic(−COOH)/amine(−NH₂) groups in its structure, the zwitterionic peptide functioned dually: sensing the metal ions and maintaining the colloidal stability. An addition of Ni²⁺ triggered the aggregation of the AuNPs-(EK)₃ probe and resulted in a visibly observable red-to-purple color change. The developed colorimetric probe was able to detect Ni²⁺ as dilute as 34 nM, and in a linear range of 60–160 nM. The probe was stable in soil, urine, and water samples.

In [181] a miniaturized cable-type electrochemical sensor based on a carbon nanotube immobilized cellulose yarn (CNT-thread) was developed for the detection of Zn(II) in the concentration range 0.1–500 ppm, with high sensitivity (<1 ppm). The two cables, one coated with a polymeric ion receptor (tetrakis(p-aminophenyl) porphyrin) acting as the working electrode, and another prepared with a pristine CNT thread and working as a reference electrode, comprised the final sensor device, which demonstrated good performance when tested by cyclic voltammetry, differential pulse voltammetry, and chronoamperometry; see Figure 7. The sensor was not sensitive to interferences, such as Na⁺, K⁺, Mg²⁺, Cd²⁺, Ca²⁺, Fe²⁺, and Cu²⁺ (low selectivity coefficients in the range 10^{−3}–10^{−5}), and was not influenced by common anions. The possibility of real-time detection of Zn²⁺ in agricultural soil with small deviations (<6%) between the analyte concentrations estimated by the sensor and those estimated by atomic-absorption techniques was noted.

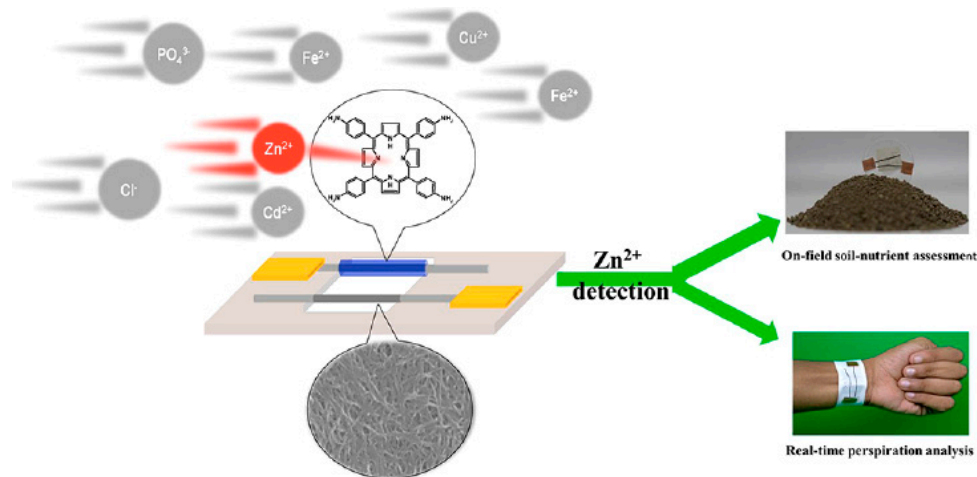


Figure 7. Schematic representation of the cable-type electrochemical sensing device based on CNTs and tetrakis(p-aminophenyl) porphyrin for Zn(II) analysis in soils and sweat. Reprinted with ACS permission from [181].

3.1.5. Multi-Metal (and Multi-Analyte) Sensing

The possibility of simultaneously assessing various soil pollutants with the same sensing device/analytical platform has been investigated previously in several works [182–185]. Thus, in [182] a semi-quantitative method permitting the in-field screening of heavy metal contaminated sites based on the use of disposable screen-printed sensors and differential pulse anodic stripping voltammetry (DPASV) was reported. The possibility of simultaneous determination of Cd(II) and Pd(II) at µg/L levels with RSD < 8% for both analytes (n = 10) in soil and water samples was shown. Application of the sensor to 82 soil samples provided results which well correlated ($R_{Cd}^2 = 0.978$ and $R_{Pb}^2 = 0.973$, respectively) with those of the standard ICP-AES technique. A combination of anodic and cathodic stripping voltammetry on a hanging mercury drop electrode to measure the mobile forms of Zn, Pb, Cd, and Cu in soil samples extracted with ammonium nitrate with a mean RSD of 10% was

reported in [183]. The results were in good agreement with the AAS analysis. Palchetti et al. performed the simultaneous detection of three polluting metals, Pb(II), Cd(II), and Cu(II) with DL of 0.3, 1, and 0.5 $\mu\text{g/L}$, respectively, by employing a miniaturized graphite WE coated with a cellulose-derivative mercury coating and coupled with square wave anodic stripping voltammetry (SWASV) for on-site pollutants analysis [184]. In the work of Silva et al. SWASV on iridium microdisc sensors modified with Hg-microdrops was performed to simultaneously assess lead, cadmium, and copper trace concentrations in extracts from soils collected at different depths (from the surface down to 1 m) [185]. The developed analytical platform demonstrated satisfactory agreement with the standard AAS method; the possibility of measuring polluting metals' concentrations at the 50 ppt level was shown.

Recently, Wang et al. have developed a detection system based on DPASV for transition metal assessment in soils [186]. A disposable screen-printed sensor modified with Nafion polymer and bismuth film, Bi/NA/SP, with ultrasound assisted extraction was used for trace concentrations determination of cadmium and lead content. The DL were 1.6 $\mu\text{g/L}$ and 2.5 $\mu\text{g/L}$ for Cd and Pb, respectively. The feasibility of the developed system for the determination of Cd and Pb in real soil samples collected from Chinese regions with cultivated lands situated near highways or industrial areas was confirmed, with the average recoveries of 97.46% for Cd and 96.68% for Pb.

Mc Eloney, Alves, and Mc Crudden have developed a novel electrochemical technique for the detection of bioavailable cadmium(II) and zinc(II) in soils [187]. Through the sequential deposition of bismuth and gallium thin films on modified carbon screen-printed carbon electrodes (SPEs), the reduced graphene oxide/graphitic carbon nitride (RGO/g-C₃N₄) electrode modification was achieved. The voltammetric analysis of Cd(II) used a bismuth thin film (BiTF) at pH 4.6; Zn(II) was then determined in the same cell, at pH 5.1, using a gallium thin film (GaTF). The LODs and LOQs were determined in the extracted soil matrix as 0.01 and 0.03 mg/kg, respectively, for bioavailable Cd; and 0.01 and 0.04 mg/kg, respectively, for bioavailable Zn. The estimated Cd and Zn levels of numerous soil samples were in a good agreement with standard ICP-OES estimations. The developed approach offers the possibility for rapid on-site portable testing of Cd and Zn in real soil samples, in order to estimate the probability of Cd uptake by crops.

Optical platforms have been also exploited for multi-metal assessment in soils. Hung et al. have previously reported a selective colorimetric method for the detection of aqueous mercuric, silver, and lead ions using label-free gold nanoparticles (Au NPs) and selected alkanethiols that induce a degree of Au NPs aggregation in the presence of the target cation [188]. Upon the aggregation, the ratio of extinction coefficients at 650 to 520 nm (Ex650/520) decreased and was correlated with the molar ratio of the aggregated to the dispersed Au NPs, permitting in this way the selective colorimetric detection of Ag⁺, Hg²⁺, and Pb²⁺, at concentrations as low as nanomolar in river water and Montana soil. The possibility of iron (Fe) and organic carbon (OC) content assessments in soils through non-destructive image analysis with a digital camera was reported in [189]. The indirect measurements of soil OC and Fe were performed by estimating soil colors, which first were interpreted with an RGB color scale and then transformed to variables of other color space models to derive transfer functions for soil OC and Fe contents. In [190], Yokota et al. have reported an optical sensor for photometric detection of six soil nutrients: ammonia nitrogen (NH₄-N), nitrate nitrogen (NO₃-N), available phosphorus (P₂O₅), available iron (Fe), exchangeable manganese (Mn), and exchangeable calcium (CaO). The light emitting diodes (LEDs) of different wavelengths corresponding to the absorption bands of chemical reagents whose colors were developed by reactions with the analyzed soil nutrients, were used as light sources for the analytical platform. The results were in a good agreement with those calculated from absorbances measured by spectrophotometry. An elegant, rapid, and effective digital colorimetric analysis (DCA) procedure for determination of toxic substances (Fe, Cd, Co, Zn, Pb, Ni, Cu, Mn, dyes, nitrites) in waters of various origins, in drilling liquid, in soil, and in vegetables cultivated on this soil was developed and tested in [191]. The specially developed optically transparent polymethacrylate optodes with immobilized

colorimetric reagents were used for analysis. Good correlations were found between the proposed DCA procedure's results and those of traditional solid-phase spectrophotometry (SPS) analysis. The designed DC analyzer is lightweight and small. Additionally, can be widely applied for sanitary quality monitoring of environmental samples.

3.1.6. Metal Detection by Bacterial Sensors (Bioassays) and Bio-Probing

The biological and environmental danger of heavy metals in soil depends to a very large extent on their bioavailability, i.e., on the bioavailable fractions of total contaminant concentration. In order to assess soil microelements' bioavailability, different microorganisms—among them genetically engineered ones—have been employed to provide quantifiable signals of the target chemical(s)' presence in soil. A review on bacterial sensors with high detection sensitivities for several environmentally significant metal targets was reported in [29].

Assessments of bioavailable Cd(II) and Pb(II) in [192], and Cd, Pb, and Zn in [193], were conducted on agricultural smelter-influenced soils (metal content from 1 to 1000 mg/kg) sampled in the Northern France, by employing *Bacillus subtilis* BR151-(pTOO24) and *Staphylococcus aureus* RN4220(pTOO24), whose luminescence is induced in the presence of metal. The possibility of bioassays that signal hazards at the subtoxic level was indicated. The detection of Hg(II) and arsenic (As) performed with soil *Pseudomonas fluorescens* bacteria engineered with reporter gene systems was reported by Petänen group [194]. The good ability of *P. fluorescens* OS8 strains pTPT11 and pTPT31 in mercury and arsenic detection, respectively, in three different soil types (humus, mineral and clay)—with the lowest concentration of Hg measured using pTPT3 1 strain being 0.003 µg/kg, considerably lower than the chemically estimated one (0.05 µg/kg)—is shown in [195]. Brandt et al. have used *Pseudomonas fluorescens* for monitoring bioavailable Cu, total dissolved Cu, and free copper ions' activity in aqueous extracts of soils amended with various amounts of manure [196]. The developed *P. fluorescens* bioassay has permitted assessing the bioavailable Cu species. The measurements performed with the biosensor were backed by analysis of manure and Cu amounts. The *Escherichia coli*-based biosensor used to measure the bioavailability of arsenic (As) in soil—and to assess the impacts of different long-term fertilization regimes containing N, NP, NPK, and M (manure), and NPK + M treatments on the bioavailability of As was reported in [197]. The mercury-inducible promoter P_{merT} and the regulatory gene *merR* were merged with a promoterless reporter gene, *egfp*, to obtain a luminescent *Pseudomonas putida* chromosome whole cell reporter (BMB-ME) for Hg assessment in red soils from China in [198]. The sensor strain showed a detection limit Hg^{2+} of 200 nM, which is comparable to that of the reverse-phase HPLC technique, and no influence of any of the tested transition metal cations appeared with them at nanomolar levels. A modified strain of *Pseudomonas putida* (X4 pczcR3GFP) was reported as a zinc-specific bioprobe in the water extracts of four different soils amended with zinc [199]. The strain was obtained from a promoterless enhanced green fluorescent protein (*egfp*) gene fused with the *czcR3* promoter. A comparison of bioluminescent bacterial sensors, *Escherichia coli* and *Staphylococcus aureus*, and a fungal sensor (eukaryotic; *Saccharomyces cerevisiae*) for Cu and Pb bioavailability assessments was reported in [200]. The sensor cells were tested on 20 urban soils with 14–5323 mg/kg of Pb and 8–12,987 mg/kg of Cu. In [201] some microbial biosensors that were used to monitor the water-soluble biotoxicity of metals upon amendment with ameliorant (activated carbon, bonemeal, bentonite, and calcium polysulphide) were reported. The study compared the effectiveness of ameliorants at immobilizing the metals present in soils; the microbial biosensors were demonstrated to be relevant and rapid screening tools for monitoring the ameliorant dosing associated metal toxicity reduction. Coelho et al. have established the possibility of several bacteria in the same batch having different responses to the concentration ranges of the metals being analyzed [202]. For instance, the responses of two bioreporters, *Escherichia coli* (pCHRGFP1) and *Ochrobactrum tritici* (pCHRGFP2), are within the ranges of 0.5–2 µM and 2–10 µM, respectively, for chromate ions. The toxicity of nano- Co_3O_4 , which can be released in the

soil either through direct disposal of nano-products or from contaminated waste, was investigated in [203] by studying the negative effects on two bioprobe organisms, *Eisenia Andrei* and *Folsomia candidathe*.

3.2. Organic Pollutants in Soils

Soil pollution with organic pollutants of anthropogenic origin, such as petroleum hydrocarbon spills, explosives, plastics and their degradation components, antibiotics, herbicides, pesticides, etc., has become a serious environmental problem.

Assessments of soil pollution are essential to evaluate the bioavailability of contaminated soil. In [204] to evaluate the level of soil contamination with hydrocarbons, the microbial activity was estimated from the quantity of CO₂ emitted by biota respiration. The non-dispersive infrared (NDIR) CO₂ sensor was applied in the study to distinguish among the control and diesel-contaminated soils on the basis of CO₂ content, emitted upon glucose addition. In [205], an electrochemical sensing platform for the quantification of toxic organic pollutant 2-nitroaniline (2-NA) on a bismuth molybdate (Bi₂MoO₆, BMO) functionalized carbon nanofiber (f-CNF)-modified GC electrode was developed and tested on soil and lake water samples. Recoveries in the 97.8–99.4% range display the sensor's potential for efficient detection of the high-risk 2-NA pollutant. A portable potentiometric ISE sensor for direct assays of *p*-aminophenol (PAP), a potentially toxic and mutagenic organic compound used and/or emitted by industrial, pharmaceutical, and agricultural business, was developed and applied for PAP detection in biological samples in [206]. The PVC-based solvent polymeric membrane doped calix-[8]-arene was drop-cast on GCWE. The sensor proved a near-Nernstian slope of 61.9 mV decade⁻¹ within a linear range of 2.99×10^{-5} – 1×10^{-2} M, a LOD of 2.86×10^{-5} M, and rapid response time (1–5 s). The developed method was validated for PAP assays with urine, plasma, water, soil, hair dyes, and marketed paracetamol formulations.

Explosive compounds, such as 2,4,6-trinitrotoluene (TNT), are of great concern for public security and environmental protection, since TNT contamination seriously affects the health of humans, plants, and animals, and the whole ecosystem. The necessity to test TNT content in soils, water supplies, and wastewater is evident not only for environmental reasons, but also for security reasons. Recently, huge attention was paid to the development of TNT-sensitive sensors for soil analysis; most of these devices used optical transduction. Prusti and Chakravarty have developed AIEgen (aggregation-induced emission active fluorogens)-based sensors for the selective and sensitive detection of 2,4,6-trinitrotoluene (TNT) in field soil through fluorescence quenching [207]. The colorimetric sensor based on modified natural wood, first delignified and further functionalized by 3-aminopropyltriethoxysilane (APTES) for visual detection of TNT in water, air, and soil, was reported by Zhang et al. [208]. In the presence of TNT, the wood-based sensor showed a colorimetric transition from light yellow to brown visible to the naked-eye due to the formation of a Meisenheimer complex between APTES and TNT. A smartphone camera was used as the signal detector, and image the RGB components intensities were employed for a qualitative TNT assessment. The developed sensor displayed the linear response in the range of 0.01–5 mM with a DL of 3 μM. A triacetylcellulose (TAC) membrane was used as a fixed carrier for immobilization of the Aliquat336 anion-exchanger in an optochemical sensor for colorimetric determination of trinitrotoluene (TNT) from aqueous samples in [209]. In the presence of TNT, the colorless and transparent membrane becomes a red–orange color with maximal absorption at 530 nm due to the TNT–Aliquat 336 ion pair's formation. The sensor showed a fully reversible linear response in the TNT concentration range 1.0–16.0 mg/L, with a DL of 0.14 mg/L, and good reproducibility and selectivity. It was applied to the determination of TNT in spiked soils from Khuzestan province, Iran, and it showed satisfactory recoveries in the 96–104.4% range. The TNT binding peptides conjugated to fluorescent CdTe/CdS quantum dots (QDs) via thiol groups were employed in a fluorescent TNT sensor developed by Komikawa et al. in [210]. The chemosensor's fluorescence from the QDs was quenched in response to the addition of

TNT, and this response was observed by the naked eye; see Figure 8. The limit of detection of the sensor using fluorescence mode was about 375 nM. The authors have recommended the application of the developed sensing platform for on-site explosive sensing.

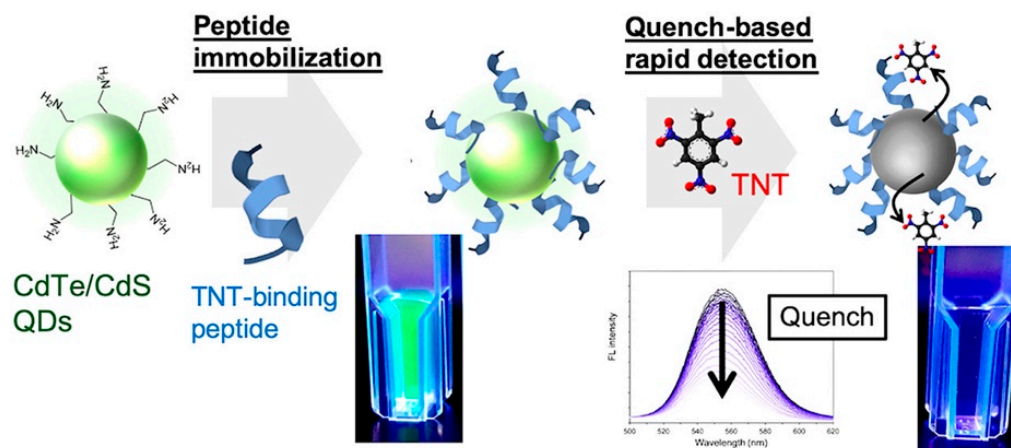


Figure 8. A schematic presentation of TNT-BP-C@QDs preparation and their application for TNT sensing. Reprinted from [210] with ACS permission.

A portable, silicon-based, surface-enhanced Raman scattering (SERS) analytical platform-based silicon wafer chip ($0.5 \text{ cm} \times 0.5 \text{ cm}$) decorated with *o*-aminobenzenethiol (PABT)-modified silver nanoparticles (AgNPs) for signal-on detection of trace amounts of TNT was developed in [211]. The developed sensing chip featured ultrahigh sensitivity to explosives, with a DL for TNT down to $\sim 1 \text{ pM}$ ($\sim 45.4 \text{ fg/cm}^2$) and adaptable reproducibility (relative standard deviation is less than 15%) for the detection of standard solutions of TNT. Coupled with a hand-held Raman spectroscopic device and using 785 nm excitation, the possibility of qualitative analysis of trace TNT even at the 10^{-8} M level from environmental samples, including soils, and the application of a portable device, permitted detection of TNT vapors diffusing from TNT residues ($\sim 10^{-6} \text{ M}$), indicating the utility of the sensor for express monitoring in explosive detection scenarios. A selective colorimetric probe for detection of pentaerythritol tetranitrate (PETN) explosive based on arginine-treated gold nanoparticles (AuNPs) was reported in [212]. Aggregation of AuNPs happened in the presence of PETN, resulting in an AuNP color change from reddish to blue or purple, depending on PETN concentration. A good linear relationship was achieved between the aggregation signal (absorbance ratio of A_{650}/A_{520}) of the probe and the concentration of PETN, with a limit of detection of $0.169 \text{ }\mu\text{mol/L}$. The probe was tested on spiked and non-spiked garden soil samples (0.1 g dispersed in 2.0 mL of acetone). The recovery of 105.9% and RSD below 2% indicate the probe's applicability for PETN testing of soils.

Besides explosives, other organic pollutants, such as phthalates, components of many plastics, hydrazine (actively used in chemical industry), pesticides and herbicides employed in agriculture, and antibiotics, have been intensively analyzed in soils by means of chemical sensors [213–218]. In [214], the optical fiber immunosensor platform for rapid and sensitive detection of phthalate esters (PAEs) was developed. The sensor was constructed by covalent bonding of a coating antigen to the surface of an optical fiber, and the inhibition signal of PAEs to the immune reaction between coating antigen and fluorescent-labeled antibody was detected by photodiode. The sensor was tested in eight PAEs and displayed 100% reactivity to dimethyl phthalate, and broad cross-reactivity to other tested PAEs in the range of 16–72%. The sensor's response was linear on a semilogarithmic scale for the concentration range of $0.01\text{--}100 \text{ }\mu\text{g/L}$. The limits of detection (LODs) of the eight PAEs ranged from 19 to 51 ng/L . The developed method has been successfully applied to the determination of multiple PAEs in greenhouse soils, with RSD from 3.98 to 10.69% and good correlations with the standard GC-MS method's results. Jung et al. have reported an analytical platform for fluorescence assessments of hydrazine in soils based on orthomethoxy-methyl-ether

(o-OMOM) incorporating an electron donor (D)–acceptor (A)-type naphthaldehyde sensing moiety (HyP-1), providing high selectivity and sensitivity [216]. The chemosensor, deposited on a paper strip, or prepared in the form of a spray (sensing moiety solution in DMSO) to be applied to the analyzed sample, showed stable green fluorescence under a commercial hand-held 365 nm UV lamp, and had a fluorescence change to blue upon exposure to hydrazine. The amount of hydrazine-spiked in various soils (sand soil, clay soil, and field soil) was satisfactorily detected with the spray application of HyP-1; see Figure 9.

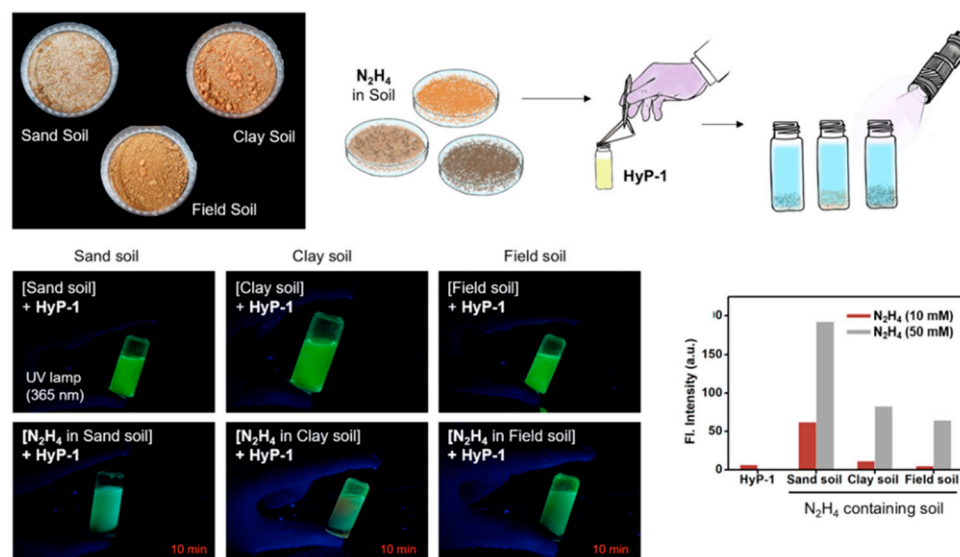


Figure 9. Spray application of HyP-1 for hydrazine assessment in soils. Reprinted from [216] with ACS's permission.

The fluorescent probe, N-N₂H₄, for hydrazine detection in biosamples was prepared by engineering a recognition site of ethyl cyanoacetate with 6-hydroxy-2-naphthaldehyde in [215]. The strong fluorescence emission of the N-N₂H₄ probe was registered at 465 nm upon the hydrazine addition of 0–500 eq; also, the color change of the probe solution treated with N₂H₄ was observed with the naked-eye—from light brown to colorless under ambient light; and the fluorescence was changed from colorless to bright blue under a UV lamp at 365 nm. The probe was tested in living cells, and due to its low toxicity was suggested to be a promising tool for environmental monitoring purposes.

Due to the high consumption and often outright abuse of antibiotics in various industries, from poultry husbandry and food manufacturing to agriculture, the detection of antibiotic pollution in the environment is necessary to avoid animals, plants, and humans being desensitized to these substances. Moreover, the quantification of antibiotics in soils permits one to assess their mobility, bioavailability, and ecotoxicological and health relevance. Reviews on chemical sensors and biosensors for antibiotic detection in food and the environment were previously published by Lakshmi et al. [217] and Sun et al. [218]. In [219] a whole-cell (*Escherichia coli*) fluorescent biosensor for detecting extractable tetracyclines in soils (Alfisol, Mollisol, and Ultisol) using a reporter plasmid (pMTGFP or pMTmCherry) carrying fluorescent protein genes was developed. The developed biosensor had a detection limit for tetracyclines between 5.32 and 10.2 µg/kg soil, and was seven times faster than a typical high-performance liquid chromatography (HPLC) method; and it was shown to be a promising, cost-effective method for measuring extractable concentrations of tetracyclines in a great number of soil samples in large-scale monitoring studies.

3.3. Detection of Herbicides and Pesticides in Soils with (Bio)Chemical Sensors and Bioassays

Herbicides and pesticides are necessary and widely used in agriculture to resist the harmful effects caused by pests, weeds, and diseases that could destroy crops. However, there is growing concern regarding the continuously increasing use of pesticides and herbicides, and their harmful impacts on humans via the food chain.

The pesticides in drinking water should not exceed 0.1 µg/L [9], though there is no well-established limit value for soils. Therefore, the monitoring of these compounds in soils is important. The mobility of herbicides in soil depends on several factors, including the compositions of the organic and inorganic materials, the rates of adsorption and leaching, and degradation rates. Additionally, the synergistic or antagonistic interactions that may occur among herbicides, pesticides, and their metabolites and other additives should be considered. The traditional methods of estimating herbicide and pesticide contents in soils allow the quantification of sorption rates using physicochemical parameters for particular soil types in the laboratory, but they do not accurately represent the natural soil conditions. Hence, the sensory approach to herbicide and pesticide assessments for soils is promising, since it permits online and in-field estimations.

Several studies on electrochemical, optical, mass-sensitive and label-free, enzymatic, bacterial, and immune sensors for herbicide and pesticide detection in agricultural samples have been performed [220–222]. Tang et al. have developed a disposable electrochemical immunosensor for picloram based on a conductive chitosan/gold nanoparticles composite membrane with encapsulated self-synthesized picloram antibodies for competitive immunoreaction in the sample solution, followed by the immobilization of horseradish peroxidase (HRP)-labeled secondary antibodies [220]. The immunosensor was used to detect picloram in the concentration range of 0.005 to 10 µg and the DL of 5 ng/mL. Assessments of amino acid-type P-containing herbicides glyphosate and glufosinate on a double-template, molecularly imprinted, polymer (MIP) nanofilm-modified pencil graphite electrode via DPASV technique in water, soil, and blood serum samples were reported in [221]. The imprinting of both herbicides in MIP provided sensitive and selective analyte detection in linear ranges of 3.98–176.23 ng/L and 0.54–3.96 ng/L, and DLs of 0.35 and 0.19 ng/L, for glyphosate and glufosinate, respectively. Another fully automated immunosensor for glyphosate (*N*-phosphonomethyl), the most frequently used nonselective postemergence herbicide used all around the world, based on the immunocomplex capture assay protocol, was reported by Gonzalez-Martinez et al. [223]. The sensor employed online analyte derivatization with anti-glyphosate serum, glyphosate peroxidase enzyme tracer, and used fluorescent detection. The DL of 0.021 µg/L, an analysis rate of 25 min per assay, autonomy for more than 48 h, and high reusability (>500 analytical cycles.) were achieved. Moreover, the ability to discriminate structurally related molecules with this immunosensor was shown, such as aminomethylphosphonic acid, the main metabolite of glyphosate, and other herbicides, such as glufosinate and glyphosine; its use for water and soil samples gave recoveries lower than 1 µg/L and good correlations with ELISA and standard LC/LC/MS chromatography estimations. In [224], multi-walled carbon nanotubes (MWCNTs), ionic liquid (IL), and copper oxide nanoparticles (CuO) were employed in a hollow fiber (HF)/pencil graphite electrode for glyphosate detection with a DL of 0.22 µg/L. That sensor has shown high selectivity in the presence of metal ions, glufosinate, and other pesticides. The accuracy was further checked by the comparison of results obtained for soil and water samples with those retrieved by the standard chromatographic method. Recently Shrivastava et al. reported the DPV detection of aqueous glyphosate using a Cu-(poly)pyrrole composite electrochemically deposited on activated carbon fiber. The sensor showed a linear response over the 0.02–12 mg/L range, with an LDL of 0.01 mg/L [225]. Application of the sensor for glyphosate assessments of soil and fruit samples with RSD values of 2.41 and 3.87%, respectively, was demonstrated.

A competitive atrazine-selective immunosensor based on a conjugate atrazine-bovine serum albumin immobilized on a nanostructured gold substrate functionalized with polyamidoaminic dendrimers and voltammetry was reported in [222]. A limit of detection

and limit of quantitation of 1.2 and 5 ng/mL, respectively, were obtained; the sensor was used for quantification of trace levels of atrazine in complex matrices: territorial waters, corn-cultivated soils, corn-containing poultry, bovine feeds, and corn flakes for human use. Parathion detection with an amperometric enzyme biosensor based on parathion hydrolyase from *Pseudomonas* sp. Isolated from contaminated soil and immobilized on a carbon electrode was reported in [226]. The LOD of parathion detection was lower than 1 ng/mL. A methyl parathion (MP) sensor based on an MWCNTs-CeO₂-Au nanocomposite and stripping voltammetric detection with an ultra-low detection limit of 3.02×10^{-11} M was developed in [227]. The sensor was applied for MP assessment of water and soils. In [228] an electrochemical, membrane-based, heterogeneous, competitive enzyme-linked immunosorbent assay (ELISA) for isoproturon, a common herbicide, was reported. The sensor worked in a flow injection mode. The DL was estimated as 0.84 ng/mL. Application of the sensor to detection of isoproturon-spiked soil extracts was demonstrated.

Wang et al. have reported a fluorescence biosensor based on a mercury ion-mediated DNA conformational switch and enzyme-assisted cycling amplification for carbamate pesticide detection [229]. The sensor's fluorescence intensity decreased with increasing concentration of the pesticide; the established DL was 3.3 µg/L for the model analyte aldicarb; and practical tests detecting carbamate pesticide residues in fresh ginger and artificial lake water samples were reported. In [230] a method for a fast in-situ pesticide analysis via metabolism/photosynthesis of *Chlamydomonas reinhardtii* algal cells (algae) in tap water inside a microfluidic device with integrated optical pH and oxygen sensors and algal fluorescence was reported. The microfluidic device permitted fast and complementary detection of several pesticides (atrazine, diuron, simazine) dissolved in tap water and is promising for environmental monitoring purposes, including soil analysis. In [231] a one-micrometer-scale, label-free optical sensor based on the surface-enhanced Raman scattering (SERS) principle for detecting sub-PPB levels of highly toxic pesticide alachlor was reported. The developed plasmonic sensor selectively sensed trace amounts of alachlor, down to 0.4 parts-per-billion, and differentiated it from a similar pesticide, demonstrating potential for pesticide assessments of environmental samples.

A non-enzymatic based field-effect transistor (FET) modified with silver-zinc oxide composite and an s-SWCNT decorated film for selective detection of methyl parathion (MP), a restricted use pesticide by EPA, was developed by Kumar et al. in [232]. The electrical response of the Ag-ZnO/s-SWCNTs-FET sensor was due to the MP hydrolysis of Ag-ZnO, resulting in changes in transistor conductance. The device showed a linear response from 1×10^{-16} to 1×10^{-4} M of MP with a DL of 0.27×10^{-16} M in a 0.1 M phosphate buffer solution (PBS). The sensor was tested with MP-spiked soil and rice samples. It showed good recoveries in the range of 97.1–101.54% for the soils. Another non-enzymatic electrochemical sensor was reported for paraoxon-ethyl detection, and was based on a functionalized-MWCNT catalyst, decorated with La³⁺-doped TiO₂ NPs [233]. The GC WE was modified with the developed sensing material and tested in differential pulse voltammetry modes (DPV); see Figure 10. The sensor demonstrated a DL of 0.0019 mM, high selectivity, and good recoveries (95.8–100.6%) with PE spiked environmental samples collected at New Taipei City, Taiwan (water and soil).

Electrochemical detection of trace amounts of amitrole (AMT) herbicide by catalytic oxidation with iron doped tungsten oxide (Fe-WO₃) nanoparticles and a cationic surfactant cetyltrimethylammonium bromide (CTAB)-based carbon paste electrode was recently reported by Ilager et al. [234]. This sensor permitted the voltammetric detection of AMT at nanomolar concentrations (0.84 nM) with a wide linearity range and was effective for AMT detection in water and five soils of different types (red soil, black soil, fertilizer soil, clay soil, and pond soil). It had an RSD lower than 1% and recoveries within 98.2–99.6%. Potentiometric solid-contact ISEs employing a polyaniline, PANI, as the ion-to-electron transducer and based either on molecularly imprinted polymethyl methacrylate (MIP) or on Aaliquat S 336 as a charged carrier, for flucarbazone herbicide anion (belonging to sulfonylurea herbicides group) assessments, were tested by Kamel et al. [235]. The

PANI film was inserted between the ion-sensing membrane and the glassy carbon WE electronic conductor substrate (working electrode) and revealed unique features, such as a high interfacial area, high double-layer capacitance, and enhanced conductivity with high hydrophobicity. The developed ISEs exhibited stable potentiometric responses in the ranges of 10^{-5} – 10^{-2} and 10^{-4} – 10^{-2} M with the detection limits of 5.8×10^{-6} and 8.5×10^{-6} M, for GC/PANI-MIP/FLU—ISE and GC/PANI-Aliquat/FLU—ISE, respectively. The ISEs were tested for the direct measurement of flucarbazon herbicide in soils collected from different agricultural lands and sprayed with flucarbazon. The results were in good agreement with those of the standard liquid chromatographic method (HPLC).

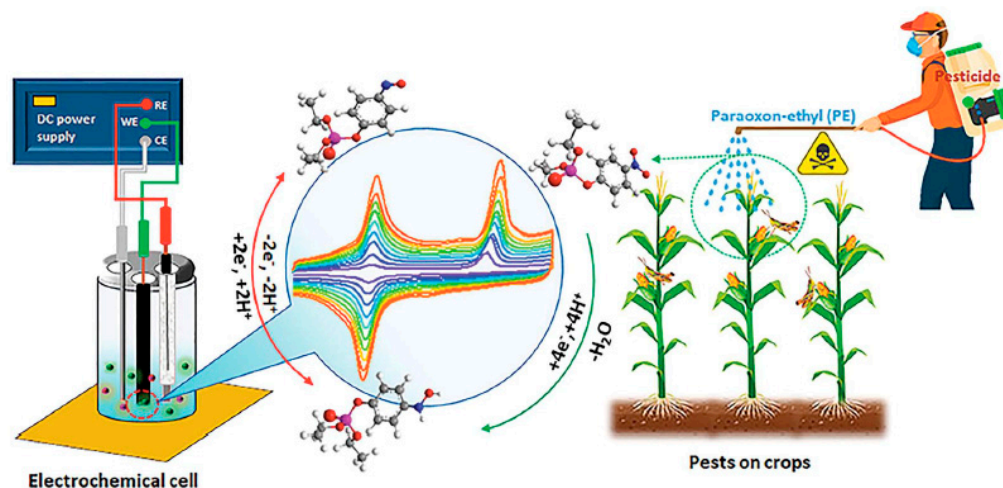


Figure 10. Schematic illustration for the development of novel chemical sensors for pesticide detection. Reproduced from [233] with permission from the Royal Society of Chemistry.

A highly sensitive microcantilever immunosensor for carbofuran insecticide detection in soil and vegetables was developed in [236]. The sensor used monoclonal antibodies to carbofuran as the receptor molecules cross-linked through L-cysteine/glutaraldehyde to the surface of an Au-coated microcantilever. The response of the immunosensor was linear over the range of 1.0×10^{-7} to 1.0×10^{-3} g/L with a detection limit of 0.1 ng/mL, and it was successfully applied to the carbofuran determination of soil and vegetable samples (recoveries in the range of 95.6–104.7%), showing good correlations with the reference technique, ELISA. In [237], Strachan et al. tested cellular and immunological biosensors for common herbicides, such as atrazine, diuron, mecoprop, and paraquat. The immunosensors were based on stabilized recombinant single chain antibodies (stAbs) specific for the four above-mentioned groups of herbicides. Used in combination, the immunosensors could be employed for soil toxicity estimation and quantification of herbicides in aqueous and methanol soil extracts. In [238] a mutant *E. coli* whole-cell biosensor, with a modified ArsR repressor that is highly selective toward trivalent methyl and aromatic arsenicals employed as herbicides and as growth promoters was reported. The biosensor was used for organoarsenical detection in vitro by fluorescence anisotropy assessments of ArsR–DNA interactions.

4. Multisensor Systems for Soil Analysis

Multisensor systems in combination with chemometrics for data treatment are widely applied nowadays for environmental monitoring, and for soil analysis in particular [2]. Chemometric methods are employed either to find correlations between sensor array responses and particular soil properties or parameters, such as pH, SOM, total N, total P, total K, concentrations of certain microelements and pollutants, the oxidation potential of the medium, soil moisture, clay and/or sand content, and color; or to treat simultaneously several parameters for soil discrimination and classification. Depending on the purpose,

such analysis can be qualitative (soil type ranking and classification) or quantitative (determination of certain components' amounts) [9,239].

The mathematical methods employed in the chemometric approach are employed to treat the huge volume of data coming from standard instrumental and laboratory methods of soil analysis, and from chemical sensors or multisensory systems. The chemometric techniques most often applied for soil analysis are principal component analysis (PCA), cluster and hierarchical cluster analysis (CA, HCA), support vector machine (SVM), and various regression methods—partial least squares (PLS), multiple linear regression (MLR), principal component regression (PCR), artificial neural networks (ANN), etc.; see Figure 11. Detailed descriptions of common pattern recognition protocols employed in multivariate analysis can be found in the literature—for instance, in [9,240,241].

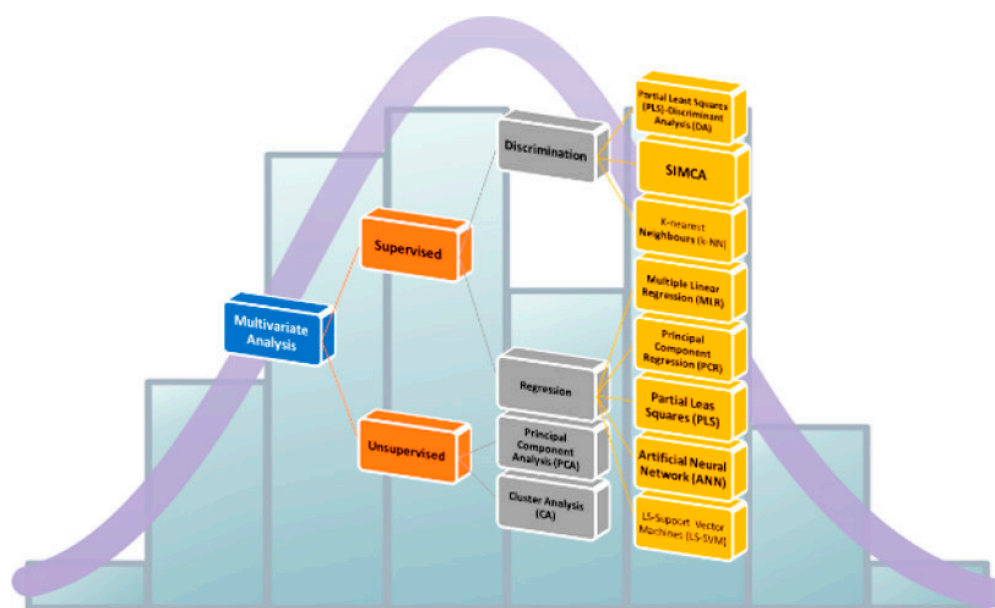


Figure 11. Methods of chemometric analysis commonly employed for environmental monitoring and soil analysis. Reprinted with ACS permission from [9].

In our previous review [2] the utility of the multisensor approach was described regarding soil discrimination and classification [242], and simultaneous assessments of several parameters and nutrients in soils [243,244] and composts [245]; along with the possibility of “on-the-go” soil mapping through pH and the direct measurement of other parameters (SDM) [52], or agitated soil measurements (ASM) [53] with ion-selective electrodes, and ion sensitive field effect transistors [246].

Determination of transition and heavy metal cations, such as Pb^{2+} , Cd^{2+} , Cu^{2+} , and Zn^{2+} , in soils by PVC potentiometric sensor array at the mg/kg level was reported in [247]. A portable trace metal analyzer based on anodic stripping voltammetry (ASV) for the detection of copper ions in acetic acid soil extracts in the laboratory and in-field was developed in [248]. The ability to estimate the labile soil fertility through the assessment of the mobile forms of soil humic substances, and the possibility to distinguish different soil types through SOM analysis by sensory systems based on poly(o-ethoxyaniline) (POEA) conducting polymer [249] or an array of metallic potentiometric sensors [250], were also reported.

The recent publications confirm the continuous interest and growing progress in the application of chemical sensor arrays for soil analysis. For example, an electronic tongue sensing device based on chemically modified 3D-printed interdigitated electrodes (IDEs) and impedance spectroscopy has been employed for the recognition of 16 samples of sandy and clayey soils enriched with different concentrations of nitrogen (N), phosphorus (P), and potassium (K), macronutrients [251]. The e-tongue consisted of one bare and three IDEs functionalized with poly(diallyl-dimethyl-ammonium chloride) solution/copper

phthalocyanine-3,4',4'',4'''-tetrasulfonic acid tetrasodium salt (PDDA/CuTsPc), PDDA/montmorillonite clay (MMt-K), and PDDA/poly(3,4-ethylenedioxythiophene)-poly(styrene sulfonate) (PEDOT:PSS) layer-by-layer films. The e-tongue output data were analyzed by principal component analysis (PCA) without any pre-treatment. All the tested soil samples were easily distinguished from one another. For both types of soils, the first principal component on the PCA score plots, PC1, was directly related to soil fertility, being especially sensitive to total N and K contents. The obtained results indicate the utility of the developed e-tongue system for precision agriculture aims—for instance, the locally monitoring of plant nutrients within agricultural fields.

Sophocleous et al. have developed a low-cost, versatile, stand-alone soil quality monitoring system [252,253]. The system is based on a screen-printed sensor array, equipped with a power module, a control-communications module, and a sensor interface module. The sensor array entails a potentiometric pH sensor consisting of a solid-state, silver/silver chloride (Ag/AgCl) reference electrode; a pH-sensitive ion-selective electrode based on ruthenium(II) oxide with almost Nernstian sensitivity (slope of 55 mV/pH), operating in a pH range of 2–12; an amperometric, dissolved oxygen (DO₂) sensor based on a potassium nitrate (KNO₃) gel and a PVC oxygen permeable membrane; a four-point conductivity sensor based on a Pt electrode and a dipole–dipole configuration; and a wide range platinum resistance thermometer. The system is battery-powered and can recharge via a solar panel or a power supply. It could be useful in precision agriculture for direct soil quality monitoring.

In their recent work [254], Khaydukova et al. have developed a potentiometric multi-sensor system, composed of 26 sensors (11 sensors with anion sensitivity, 10 sensors with cation selectivity, and 5 redox-sensitive sensors) for a “one shot” simultaneous evaluation of the nitrogen (N), phosphorous (P), and potassium (K) contents in soil water extracts. They tested twenty soil samples collected in various geographical locations over West Bengal, India. An application of the partial least squares regression (PLS) method has shown good correlations of the responses of the potentiometric electronic tongue with the NPK amounts (responsible for soil fertility), along with estimations of the pH and conductivity of the soil samples, with correlation coefficients from 0.69 to 0.96. The quantification of N was possible with an RMSE of 50 mg/kg in the range of 60–426 mg/kg. The proposed approach permits one to perform fast measurements (limited to some minutes), it does not require any additional chemical reagents, and it has potential for in-field soil analysis. Another multisensor system for measurement of soil macronutrients (NPK, available in ionic forms: K⁺, NO₃⁻, and H₂PO₄⁻) using a MEMS-based lab-on-a-chip platform was reported by Patkar, Ashwin, and Rao [255]. The piezoresistive silicon microcantilevers coated with a polymer matrix containing tris-dodecylmethylammonium nitrate, TDMANO₃, and commercial nitrate ionophore VI for nitrate; 18-crown-6 ether for potassium; and tributyltin chloride for phosphate detection, were embedded in the system. The pilot studies for the on-site soil testing have been carried out.

A voltammetric microelectrode sensor array using disposable screen-printed electrodes modified with bismuth, gold nanoparticles, and conductive polymers for the in-situ determination of toxic heavy metals in samples of water and soil was reported by Kurup et al. [256]. Using machine learning techniques, decision trees were developed to identify heavy metals' presence based on peak potential. The ability to sense Zn(II), Cd(II), Pb(II), As(III), and Hg(II) at the limits of detection specified by the US EPA for drinking water was shown.

In modern sensoristics, the simultaneous integration of sensor, processor, and actuator is employed in neuromorphic systems—the artificial sensing systems of next generation, which are applied in neuro-robotics and neuro-prosthetics to emulate the functions of human organs, but also can be applied in different fields of human activity. Thus, recently, Bao, Seol, and Kim presented a 3D integrated neuromorphic sensing system including an ion-selective sensor, an electrical oscillator, and a synaptic transistor, which mimic sensory receptors, neurons, and synapses in biological systems, respectively, for the detection of

low concentrations of soil nutrients in smart farms [257]. As a feasibility study, the amount of K^+ ions in fertilized soil was estimated, but the potential applications of the developed 3D neuromorphic system can be extended for other sensing functions by alternating with diverse sensory receptors for online nutrient monitoring in smart agriculture applications.

Recently, our research group has demonstrated the possibility of using arrays of optodes with PVC-based solvent polymeric membranes for improved assessments of Mg^{2+} and Cd^{2+} concentrations in fertilizers [117] and in soils [158]. Thus, through the inclusion of various ion-exchanger/ionophore ratios inside the optode sensing membranes, a series of novel, all-solid-state cross-sensitive sensors based on phenyl-substituted diaza-18-crown-6 8-hydroxyquinoline (DCHQ-Ph) was investigated in [117]. Combined together in the sensor array, the five cross-sensitive DCHQ-Ph-doped optodes performed better than when being used separately, and allowed a reduction in the RSD of magnesium determination in room plant fertilizers (down to 3.7% in comparison to the 5.5% for single optodes) and achieving an LDL of 4.6×10^{-7} mol/L. Similarly, in [158] two N_2S_2 pyridinophane-based fluorescent ligands were employed to form a cross-sensitive optical sensor array, which allowed quantitative determination of Cd^{2+} in aqueous extracts from three soil samples with different anthropogenic influences: from beside a low-cost-flights runway (Ciampino G.B. Pastine Airport, Rome), from a university garden (Faculty of Science, "Tor Vergata" University, Rome), and from a dump site (Castello di Cisterna, Naples). The PLS1 regression model was trained to relate the luminescent response of the optodes array and the Cd^{2+} ion content in calibration solutions of known concentrations. The correlation coefficients, R^2 , were 0.993 and 0.983 for calibration and validation steps, and the root mean squared error of validation, RMSEV, was 0.225 in $-\log [Cd^{2+}]$ units; see Figure 12. The model was fitted with 3PCs, representing 99.3% and 98.1% of the total explained variance at calibration and validation steps, respectively. A detection limit of 1.8×10^{-7} mol/L for Cd^{2+} ion was estimated by the 3s method. The amounts of Cd^{2+} in soils found with the optode sensor array were in good agreement with the Cd^{2+} contents estimated with the standard AAS method. The recoveries were in a narrow range from 98.5% to 100.5%, and the mean RSD was 0.96%.

Finally, a useful methodological guideline (from an electronics and system architecture point of view) for the integration of ISFET sensors into precision agriculture and digital agriculture applications is presented in the paper of Taylor et al. [258]. This methodology aims to establish a clear procedure when designing electronic systems based on ISFET sensors that allow the direct or indirect evaluation of nutrient status and pH in agricultural soils. The suggested approaches for sensor selection, calibration, and subsequent integration into the final analytical system, along with system electronics and integration architecture, can help researchers, engineers, and designers to conclude on the feasibility implementing ISFET sensors within their systems.

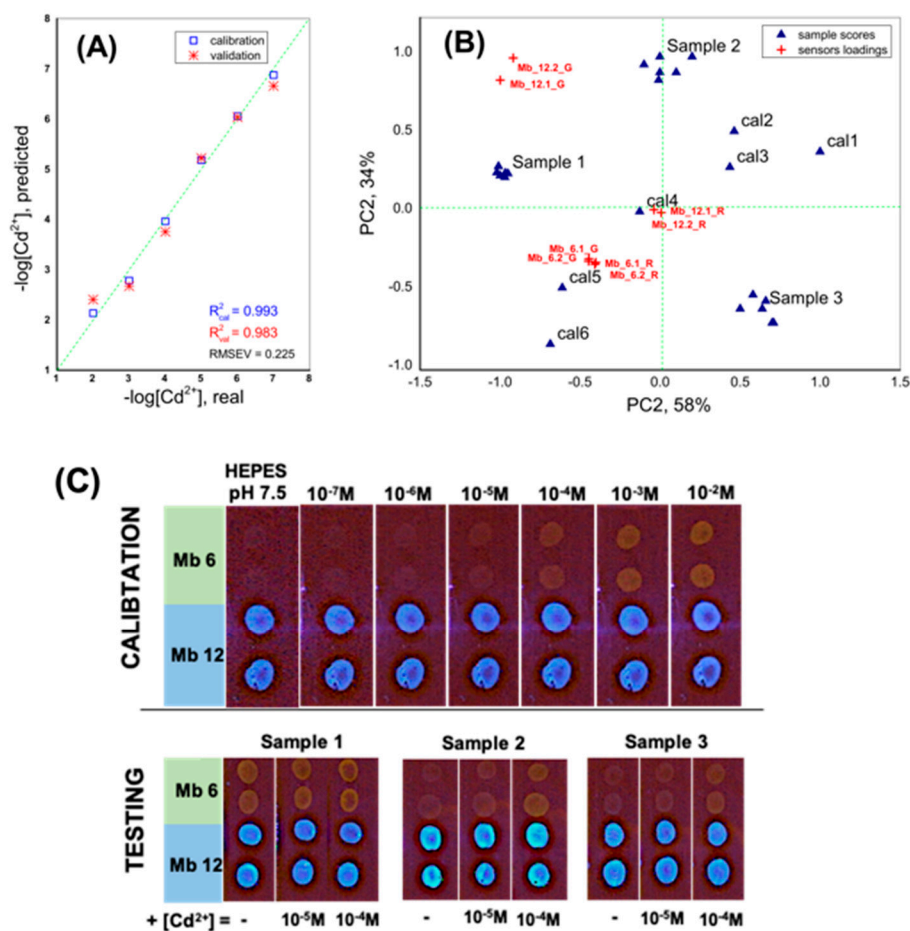


Figure 12. (A) PLS1 calibration curve employed for Cd^{2+} assessment in soils via an optical sensor array based on N_2S_2 pyridinophan-based fluorescent ligands. (B) PCA scores and loadings plot, and (C) photograms of the of the fluorescent sensor array's response in Cd^{2+} calibration solutions in the concentration range from 1.0×10^{-7} to 1.0×10^{-2} mol/L and in the analyzed aqueous extracts of soil samples. Reproduced from [158] with permission from the Centre National de la Recherche Scientifique (CNRS) and the Royal Society of Chemistry.

5. Multicomponent Soil Analysis with Gas Sensor Arrays

Gas sensors and sensor arrays with different types of signal transmission (mass-sensitive, electrical, electro-chemical or optical) are promising candidates in the development of analytical systems for the real-time and continuous monitoring of important trace gases (CO_2 , SO_2 , NH_3 , VOCs, etc.) in the natural environment, including soils [9,41,259]. Both commercially available and in-house developed gas sensor systems have been reported for the monitoring of soil contamination with aromatic volatile organic contaminants (VOC) [260–262], and for soil organic matter (SOM) determination through the detection of VOCs in gases emitted by soil [48]. For instance, the Figaro-type e-nose was employed by Yang et al. to assess contents of benzene, toluene, ethyl benzene, xylene, and their mixtures in the exhaust gas from a soil vapor extraction (SVE) process [260]. A diamond-based chemical sensor for benzene and toluene analysis and petroleum pollution of soil was reported by [261]. A QMBs-based sensor array modified with six different metalloporphyrins, hydrophilic polyethylene-imine, and hydrophobic polymethylphenylsiloxane films and coupled with SPME-GC/MS was reported to analyze clay loam forest soil artificially contaminated with phenanthrene [262]. The electronic nose system based on MQ gas sensors for simultaneous assessment of multiple soil gasses (namely, MQ-4, MQ-8, and MQ-135 gas sensors, commonly used to detect CH_4 , H_2 , and CO_2 in air quality monitoring) referred

to as SENose (short for soil electric nose), was reported by Pineda and Pérez in [263]; see Figure 13.

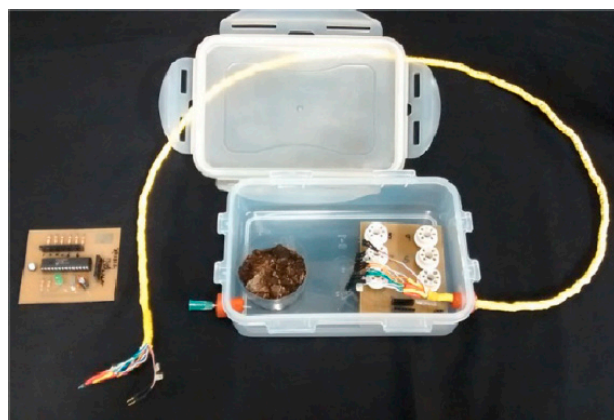


Figure 13. An image of SENose during the soil respiration test. Reported with permission from [263].

The SENose was tested in soil samples from Colombia and Ecuador, to study gas emission patterns in D(+) glucose induced soil respiration tests, and to analyze the respiration of soil with reduced microbial activity (initially autoclaved and further contaminated with diesel oil as the C source). The results demonstrated good discriminating power of SENose when detecting changes in respiration in soil samples in a short period of time, allowing one to track periods of intense soil microbial activity. Adequate organic C sources tracking in soils with SENose may also assist in the identification of specific metabolic groups of microorganisms.

In [264], Badura et al. have demonstrated the possibility of identifying BTEX-group compounds (i.e., benzene, toluene, ethylbenzene, and xylenes) in contaminated soils using a near real-time monitoring system based on two sensing arrays, each composed of 17 semiconductor Taguchi Gas Sensors (Figaro Engineering Inc., Arlington Heights, IL, USA) and a pattern recognition technique. High classification ratios were obtained for both gas sensor arrays (array I: 88–94%; array II: 94–96% of properly classified samples). Moreover, the best identification result with classification rates reaching 97.1–100% was achieved when two sub-arrays' outputs were treated together. Monitoring soil's variability and the need for selective soil irrigation, through evaluating the water content of the soil or the water requirements of the cultivated plants (tomatoes and maize crops) with in-situ portable multisensor eNose systems based on metal oxide (MOX) gas sensors, were demonstrated by Fabbri et al. in [265]. Two different eNoses, each composed of four MOX gas sensors (based on tin oxide doped with Pd (2%), Au (2%), or PdAl, ZnO, and WO₃; or STN, a solid solution of SnO₂, TiO₂, and Nb₂O₅) and heated at temperatures from 350 to 500 °C for analysis), were used to monitor VOCs gaseous emissions from the soil–plant–atmosphere system of two intensive crops: tomatoes—to detect marker compounds such as ethylene, ozone, and ethanol; and in maize, to detect isoprene, methanol, ethanol, and acetaldehyde/ozone. Data collected from eNoses were processed and compared with Meteosat information and the log of farming operations. The system's utility was shown both from a technological point of view, by providing irrigation advice regarding the time of intervention and the volumes to be used; and from a biological point of view, to help investigate the correlations between morphological changes in plants and their water stress. In a similar investigation, a fertigation system based on MOX gas sensors was developed to manage the frequency and typology of the irrigation and fertigation processes, controlled by a cloud software platform implementing a decision-making algorithm based on the information provided by the weather service and a wireless sensor network (WSN) installed in the field [266]. The system was equipped with an ultra-low-power MOX gas sensor (model CCS811) to detect the total VOCs and equivalent CO₂ (eCO₂) concentrations; a digital temperature and humidity sensor (model BMP280); and a micro-electro-mechanical system (MEMS) MOX gas

sensor (model MiCS-5914). Its utility for calibrating irrigation and fertigation operations as a function of crop typology, growth phase, soil parameters, and environmental parameters was demonstrated. Recently, the application of wireless sensor networks in agriculture for surveillance and monitoring the environment, for instance, to detect the presence of crops diseases, temperature, the moisture content of soil, soil pH, soil nutrients, etc., has become a quite common practice. Examples of WSNs' development and applications in canopy areas are reviewed in [267], and insights and suggestions on WSN design for plantation applications are provided.

6. Conclusions

Updates on applications of chemical sensors, biosensors, and bioassays for soil analysis reported over the last two decades have constituted the present review. Chemical sensors are of great interest for many high-impact social and economic fields. The rising levels of pollution due to expanding economies, along with the ongoing tightening of air, water, and land quality standards, have supported the high demand for chemical sensors (Mordor Intelligence, GLOBAL CHEMICAL SENSOR MARKET, 2021–2026). In fact, the sensor market over the last decade has been experiencing a constant increment, with a nearly five percent increase per year. In 2020 it was valued at USD 21.39 billion, and is expected to reach a value of USD 32.96 billion by 2026, with growth of 7.51%.

The latest trends in chemical sensors' applications for soil analysis underpin the great potential of these devices, due to their simplicity, low costs, and sufficient selectivity, allowing rapid, nondestructive, and user-friendly assessments of soil vulnerability and quality parameters, such as contents of main soil nutrients and pollutants, soil mobile fertility, microelement contents and bioavailability, moisture, salinity, and pH.

Advances in novel sensing materials, applications of familiar electronic devices for signal recognition and transmission, and the use of integrated sensing platforms, have resulted in effective sensor technology development for soil analysis. Sensors are widely applied nowadays for soil quality assessments requested for precision agriculture purposes, and they are extremely important for proper soil management and land maintenance, attesting in this way to be effective and promising replacements to the standard wet chemistry procedures and instrumental methods of soil analysis. Further progress on sensor network integration, assisted by wireless signal transmitters for remote sensing, will enable even more the effective transfer of sensors from the laboratory to the field and online applications. In this way, sensor technology will significantly impact the sustainability of agriculture, reduce negative anthropological impacts, and improve soil quality—and consequently, human wellbeing. Additionally, the use of chemical sensor arrays in combination with chemometric techniques for data analysis provides the ability to assess several soil parameters simultaneously, and opens new horizons for sensory applications not only for soil classification and soil quality assessments, but also for quantitative analyses, and overall estimations of anthropogenic impacts on soil conditions.

Author Contributions: Conceptualization, L.L., M.N., N.K.; methodology, N.K., L.L. and M.N.; investigation, M.N., L.L. and N.K.; resources, R.P.; data curation, M.N., L.L.; writing—original draft preparation, L.L. and M.N.; writing—review and editing, R.P., L.L., M.N.; supervision, L.L. and R.P.; funding acquisition, R.P., M.N. All authors have read and agreed to the published version of the manuscript.

Funding: This research received no external funding.

Conflicts of Interest: The authors declare no conflict of interest.

References

1. Doran, J.W.; Zeiss, M.R. Soil health and sustainability: Managing the biotic component of soil quality. *Appl. Soil Ecol.* **2000**, *15*, 3. [CrossRef]
2. Lvova, L.; Nadporozhskaya, M. Chemical sensors for soil analysis: Principles and applications. In *New Pesticides and Soil Sensors*; Grumezescu, A.M., Ed.; Series Nanotechnology in the Agri-Food Industry; Elsevier: Amsterdam, The Netherlands, 2017; Volume 10, pp. 637–678. [CrossRef]
3. Targulian, V.O.; Goryachkin, S.V. (Eds.) *Soil Memory: Soil as a Memory of Biosphere-Geosphere-Anthroposphere Interaction*; Institute of Geography, Russian Academy of Sciences: Moscow, Russia, 2008. (In Russian)
4. Schoenholtz, S.H.; Miegroet, H.V.; Burger, J.A. A review of chemical and physical properties as indicators of forest soil quality: Challenges and opportunities. *For. Ecol. Manag.* **2000**, *138*, 335. [CrossRef]
5. Soil Atlas of Europe, European Soil Bureau Network European Commission, 2005, 128p. Office for Official Publications of the European Communities, L-2995 Luxembourg ©European Communities, 2005/Catalogue Number LB-37-01-744-EN-C ISBN 92-894-8120-XEUR 21676. Available online: <https://esdac.jrc.ec.europa.eu/content/soil-atlas-europe> (accessed on 15 January 2022).
6. Doran, J.W.; Parkin, T.B. *Quantitative Indicators of Soil Quality: A Minimum Data Set*; Doran, J.W., Jones, A.J., Eds.; Methods for Assessing Soil Quality; Soil Science Society of America: Madison, Wisconsin, USA, 1996; pp. 25–37.
7. Fraters, D. *Generalized Soil Map of Europe: Aggregation of the FAO-Unesco Soil Units Based on the Characteristics Determining the Vulnerability to Soil Degradation Processes*; RIVM, Report 71240300; RIVM: Biltoven, The Netherlands, 1994.
8. Bouwer, E.J.; Crowe, P.B. Biological processes in drinking water treatment. *J. Am. Water Works Assoc.* **1988**, *80*, 82. [CrossRef]
9. Chapman, J.; Truong, V.K.; Elbourne, A.; Gangadoo, S.; Cheeseman, S.; Rajapaksha, P.; Latham, K.; Crawford, R.J.; Cozzolino, D. Combining chemometrics and sensors: Toward new applications in monitoring and environmental analysis. *Chem. Rev.* **2020**, *120*, 6048. [CrossRef] [PubMed]
10. Bünemann, E.K.; Bongiorno, G.; Bai, Z.; Creamer, R.E.; De Deyn, G.; de Goede, R.; Flesskens, L.; Geissen, V.; Kuyper, T.W.; Mäder, P.; et al. Soil quality—A critical review. *Soil Biol. Biochem.* **2018**, *120*, 105. [CrossRef]
11. Marios, S.; Georgiou, J. Precision agriculture: Challenges in sensors and electronics for real-time soil and plant monitoring. In Proceedings of the 2017 IEEE Biomedical Circuits and Systems Conference, BioCAS 2017 Proc., Turin, Italy, 19–21 October 2017; p. 135591.
12. Hulanichi, A.; Geab, S.; Ingman, F. Chemical sensors definitions and classification. *Pure. Appl. Chem.* **1991**, *63*, 1247. [CrossRef]
13. Göpel, W.; Hesse, J.; Zemel, J.N. *Sensors: A Comprehensive Survey*; VCH: New York, NY, USA, 1989; Volume 4.
14. Liu, C.C. Electrochemical Sensors. In *The Biomedical Engineering Handbook*, 2nd ed.; Bronzino, J.D., Ed.; CRC Press LLC: Boca Raton, FL, USA, 2000.
15. Bakker, E.; Bühlmann, P.; Pretsch, E. Carrier-Based Ion-Selective Electrodes and Bulk Optodes. 1. General Characteristics. *Chem. Rev.* **1997**, *97*, 3083. [CrossRef]
16. Bühlmann, P.; Pretsch, E.; Bakker, E. Carrier-Based Ion-Selective Electrodes and Bulk Optodes. 2. Ionophores for Potentiometric and Optical Sensors. *Chem. Rev.* **1998**, *98*, 1593. [CrossRef]
17. Ali, M.A.; Dong, L.; Dhau, J.; Khosla, A.; Kaushik, A. Perspective—Electrochemical Sensors for Soil Quality Assessment. *J. Electrochem. Soc.* **2020**, *167*, 037550. [CrossRef]
18. McDonagh, C.; Burke, C.S.; MacCraith, B.D. Optical chemical sensors. *Chem. Rev.* **2008**, *108*, 400. [CrossRef]
19. You, L.; Zha, D.J.; Anslyn, E.V. Recent advances in supramolecular analytical chemistry using optical sensing. *Chem. Rev.* **2015**, *115*, 7840. [CrossRef] [PubMed]
20. Fukuhara, G. Analytical supramolecular chemistry: Colorimetric and fluorimetric chemosensors. *J. Photochem. Photobiol. C Photochem. Rev.* **2020**, *42*, 100340. [CrossRef]
21. Holland, K.H.; Lamb, D.W.; Schepers, J.S. Radiometry of Proximal Active Optical Sensors (AOS) for Agricultural Sensing. *IEEE J. Sel. Top. Appl. Earth Obs. Remote Sens.* **2012**, *8*, 1793. [CrossRef]
22. Li, C.; Ding, S.; Yang, L.; Zhu, Q.; Chen, M.; Tsang, D.C.W.; Cai, G.; Feng, C.; Wang, Y.; Zhang, C. Planar optode: A two-dimensional imaging technique for studying spatial-temporal dynamics of solutes in sediment and soil. *Earth Sci. Rev.* **2019**, *197*, 102916. [CrossRef]
23. Borisov, S.M.; Wolfbeis, O.S. Optical biosensors. *Chem. Rev.* **2008**, *108*, 423. [CrossRef]
24. Ebralidze, I.I.; Laschuk, N.O.; Poisson, J.; Zenkina, O.V. Colorimetric sensors and sensor arrays. In *Micro and Nano Technologies, Nanomaterials Design for Sensing Applications*; Zenkina, O.V., Ed.; Elsevier: Amsterdam, The Netherlands, 2019; pp. 1–39, ISBN 9780128145050.
25. Ma, Y.; Li, Y.; Ma, K.; Wang, Z. Optical colorimetric sensor arrays for chemical and biological analysis. *Sci. China Chem.* **2018**, *61*, 643. [CrossRef]
26. Sauerbrey, G. Verwendung von Schwingquarzen zur Wägung dünner Schichten und zur Mikrowägung. *Z. Phys.* **1959**, *155*, 206. [CrossRef]
27. Kuchmenko, T.A.; Lvova, L.B. A Perspective on recent advances in piezoelectric chemical sensors for environmental monitoring and foodstuffs analysis. *Chemosensors* **2019**, *7*, 39. [CrossRef]
28. Rogers, K.R. Recent advances in biosensor techniques for environmental monitoring. *Anal. Chim. Acta* **2006**, *568*, 222. [CrossRef]
29. Magrisso, S.; Erel, Y.; Belkin, S. Microbial reporters of metal bioavailability. *Microb. Biotechnol.* **2008**, *1*, 320. [CrossRef]

30. FAO. *Guidelines for Soil Profile Description*; Food and Agriculture Organization of the United Nations, Soil Resources, Management and Conservation Service, Land and Water Development Division: Rome, Italy, 1990; 70p.
31. Starr, M.R. (Ed.) *Report Soil Expert Panel Meeting*; Helsinki, Finland, 1990; 66p.
32. ISO 18400-104:2018; Soil Quality—Amplifying—Part 104: Strategies. ISO: Geneva, Switzerland, 2018. Available online: <https://www.iso.org/obp/ui/#iso:std:iso:18400:-104:ed-1:v1:en>(accessed on 15 January 2022).
33. Lozet, J.; Mathieu, K. *Explanatory Dictionary of Soil Science*; Mir: Moscow, Russia, 1998; 398p. (In Russian)
34. Gaffney, J.S.; Marley, N.A.; Clark, S.B. *Humic and Fulvic Acids and Organic Colloidal Materials in the Environment*; Humic and Fulvic Acids ACS Symposium Series; American Chemical Society: Washington, DC, USA, 1996.
35. Bitutsky, N.P. *Mineral Nutrition of Plants*; St. Petersburg University Press: St. Petersburg, Russia, 2014; 540p.
36. Troeh, F.R.; Thompson, L.M. *Soils and Soil Fertility*, 6th ed.; Wiley: Hoboken, NJ, USA, 2005.
37. Kashyap, B.; Kumar, R. Sensing methodologies in agriculture for soil Moisture and nutrient monitoring. *IEEE Access* **2021**, *9*, 14095. [[CrossRef](#)]
38. Sinfield, J.V.; Fagerman, D.; Colic, O. Evaluation of sensing technologies for on-the-go detection of macro-nutrients in cultivated soils. *Comput. Electron. Agric.* **2010**, *70*, 1–18. [[CrossRef](#)]
39. Lobsey, C.R.; Viscarra Rossel, R.A.; McBratney, A.B. Proximal soil nutrient sensing using electrochemical sensors. In *Proximal Soil Sensing*; Viscarra Rossel, R.A., McBratney, A.B., Minasny, B., Eds.; Springer: Berlin/Heidelberg, Germany, 2010; p. 77.
40. Kim, D.-Y.; Kadam, A.; Shinde, S.; Saratale, R.G.; Patra, J.; Ghodake, G. Recent developments in nanotechnology transforming the agricultural sector: A transition replete with opportunities. *J. Sci. Food Agric.* **2018**, *98*, 849. [[CrossRef](#)] [[PubMed](#)]
41. Li, T.; Wu, Y.; Huang, J.; Zhang, S. Gas sensors based on membrane diffusion for environmental monitoring. *Sens. Act. B* **2017**, *243*, 566. [[CrossRef](#)]
42. Alexandrova, L.N. *Soil Organic Matter and the Processes of Its Transformation*; Nauka: Leningrad, Russia, 1980; 288p. (In Russian)
43. Orlov, D.S.; Sadovnikova, L.K.; Sukhanova, N.I. *Soil Chemistry*; Higher School: Moscow, Russia, 2005; 558p. (In Russian)
44. Piccolo, A. The Supramolecular structure of humic substances. *Soil Sci.* **2001**, *166*, 810. [[CrossRef](#)]
45. Fedotov, G.N.; Shoba, S.A. On the nature of humic substances. *Eurasian Soil Sci.* **2015**, *48*, 1292. [[CrossRef](#)]
46. Hayesa, M.H.B.; Swift, R.S. Vindication of humic substances as a key component of organic matter in soil and water. *Adv. Agron.* **2020**, *163*, 1–37.
47. Plata, M.R.; Hernando, J.; Zougagh, M.; Contento, A.M.; Villasenor, M.J.; Sanchez-Rojas, J.L.; Rios, A. Characterization and analytical validation of a microcantilever-based sensor for the determination of total carbonate in soil samples. *Sens. Act. B* **2008**, *134*, 245. [[CrossRef](#)]
48. Zhu, L.; Jia, H.; Chen, Y.; Wang, Q.; Li, M.; Huang, D.; Bai, Y. A Novel method for soil organic matter determination by using an artificial olfactory system. *Sensors* **2019**, *19*, 3417. [[CrossRef](#)]
49. Delwiche, C.C. The Nitrogen cycle. *Sci. Am.* **1970**, *223*, 136. [[CrossRef](#)]
50. Artigas, J.; Jimenez, C.; Lemos, S.G.; Nogueira, A.R.A.; Torre-Neto, A.; Alonso, J. Development of a screen-printed thick-film nitrate sensor based on a graphite-epoxy composite for agricultural applications. *Sens. Act. B* **2003**, *88*, 337. [[CrossRef](#)]
51. Yagodina, O.V.; Nikolskaya, E.B.; Shor, N.B. Gas-gap sensors for the determination of nitrogen oxides and nitrites. *Anal. Chim. Acta.* **2000**, *409*, 143. [[CrossRef](#)]
52. Adamchuk, V.I.; Lund, E.D.; Sethuramasamyraja, B.; Morgan, M.T.; Dobermann, A.; Marx, D.B. Direct measurement of soil chemical properties on-the-go using ion-selective electrodes. *Comput. Electron. Agric.* **2005**, *48*, 272. [[CrossRef](#)]
53. Sethuramasamyraja, B.; Adamchuk, V.I.; Dobermann, A.; Marx, D.B.; Jones, D.D.; Meyer, G.E. Agitated soil measurement method for integrated on-the-go mapping of soil pH, potassium and nitrate contents. *Comput. Electron. Agric.* **2008**, *60*, 212. [[CrossRef](#)]
54. Birrell, S.J.; Hummel, J.W. Real-time multi-ISFET/FIA soil analysis system with automatic sample extraction. *Comput. Electron. Agric.* **2001**, *32*, 45. [[CrossRef](#)]
55. Price, R.R.; Hummel, J.W.; Birrell, S.J.; Ahmad, I.S. Rapid nitrate analysis of soil cores using ISFETs. *Trans. ASAE* **2003**, *46*, 601. [[CrossRef](#)]
56. Gieling, T.H.; van Straten, G.; Janssen, H.J.J.; Wouters, H. ISE and Chemfet sensors in greenhouse cultivation. *Sens. Act. B.* **2005**, *105*, 74. [[CrossRef](#)]
57. Yenil, N.; Yemis, F. Nitrite in nature: Determination with polymeric materials. *Pak. J. Anal. Environ. Chem.* **2018**, *19*, 104. [[CrossRef](#)]
58. Jiang, H.; Yu, W.; Waimin, J.F.; Glassmaker, N.; Raghunathan, N.; Jiang, X.; Ziaie, B.; Rahimi, R. Inkjet-printed Solid-state Potentiometric Nitrate Ion Selective Electrodes for Agricultural Application. In Proceedings of the 2019 IEEE Sensors, Montreal, QC, Canada, 27–30 October 2019; p. 8956650.
59. Piök, R.M.; Piech, B. Paczosa-Bator, TTF-TCNQ solid contact layer in all-solid-state ion-selective electrodes for potassium or nitrate determination. *J. Electrochem. Soc.* **2018**, *165*, B60. [[CrossRef](#)]
60. Garland, N.T.; McLamore, E.S.; Cavallaro, N.D.; Mendivelso-Perez, D.; Smith, E.A.; Jing, D.; Claussen, J.C. Flexible laser-induced graphene for nitrogen sensing in soil. *ACS Appl. Mater. Interfaces* **2018**, *10*, 39124. [[CrossRef](#)] [[PubMed](#)]
61. Chen, M.; Zhang, M.; Wang, X.; Yang, Q.; Wang, M.; Liu, G.; Yao, L. An all-solid-state nitrate ion-selective electrode with nanohybrids composite films for in-situ soil nutrient monitoring. *Sensors* **2020**, *20*, 2270. [[CrossRef](#)]
62. Ali, M.A.; Wang, X.; Chen, Y.; Jiao, Y.; Mahal, N.K.; Moru, S.; Castellano, M.J.; Schnable, J.C.; Schnable, P.S.; Dong, L. Continuous monitoring of soil nitrate using a miniature sensor with poly(3-octyl-thiophene) and molybdenum disulphide nanocomposite. *ACS Appl. Mater. Interfaces* **2019**, *11*, 29195. [[CrossRef](#)]

63. Ali, M.A.; Jiang, H.; Mahal, N.K.; Weber, R.J.; Kumar, R.; Castellano, M.J.; Dong, L. Microfluidic impedimetric sensor for soil nitrate detection using graphene oxide and conductive nanofibers enabled sensing interface. *Sens. Act. B* **2017**, *239*, 1289. [[CrossRef](#)]
64. Minami, T.; Sasaki, Y.; Minamiki, T.; Wakida, S.-I.; Kurita, R.; Niwa, O.; Tokito, S. Selective nitrate detection by an enzymatic sensor based on an extended-gate type organic field-effect transistor. *Biosens. Bioelectron.* **2016**, *81*, 87. [[CrossRef](#)]
65. Massah, J.; Vakilian, K.A. An intelligent portable biosensor for fast and accurate nitrate determination using cyclic voltammetry. *Biosyst. Eng.* **2019**, *177*, 49. [[CrossRef](#)]
66. Vakilian, K.A.; Massah, J. A portable nitrate biosensing device using electrochemistry and spectroscopy. *IEEE Sens. J.* **2018**, *18*, 3080. [[CrossRef](#)]
67. Choosang, J.; Numnuam, A.; Thavarungkul, P.; Kanatharana, P.; Radu, T.; Ullah, S.; Radu, A. Simultaneous detection of ammonium and nitrate in environmental samples using on ion-selective electrode and comparison with portable colorimetric assays. *Sensors* **2018**, *18*, 3555. [[CrossRef](#)] [[PubMed](#)]
68. Bagheri, H.; Hajian, A.; Rezaei, M.; Shirzadmehr, A. Composite of Cu metal nanoparticles-multiwall carbon nanotubes-reduced graphene oxide as a novel and high performance platform of the electrochemical sensor for simultaneous determination of nitrite and nitrate. *J. Hazard. Mater.* **2017**, *324*, 762. [[CrossRef](#)] [[PubMed](#)]
69. Guerrero, A.; De Neve, S.; Mouazen, A.M. Current sensor technologies for in situ and on-line measurement of soil nitrogen for variable rate fertilization: A review. *Adv. Agron.* **2021**, *168*, 1–38.
70. Da Silveira Petrucci, J.F.; Wilk, A.; Cardoso, A.A.; Mizaikoff, B. A Hyphenated Preconcentrator-Infrared-Hollow-Waveguide Sensor System for N₂O Sensing. *Sci. Rep.* **2018**, *8*, 5909. [[CrossRef](#)] [[PubMed](#)]
71. Merl, T.; Koren, K. Visualizing NH₃ emission and the local O₂ and pH microenvironment of soil upon manure application using optical sensors. *Environ. Int.* **2020**, *144*, 106080. [[CrossRef](#)]
72. Li, T.; Zhou, M.; Qiu, Y.; Huang, J.; Wu, Y.; Zhang, S.; Zhao, H. Membrane-based conductivity probe for real-time in-situ monitoring rice field ammonia volatilization. *Sens. Act. B* **2019**, *286*, 62. [[CrossRef](#)]
73. Kim, H.; Sudduth, K.A.; Hummel, J.W. Soil macronutrient sensing for precision agriculture. *J. Environ. Monit.* **2009**, *11*, 1810. [[CrossRef](#)] [[PubMed](#)]
74. Lemos, S.G.; Menezes, E.A.; Chaves, F.S.; Nogueira, A.R.A.; Torre-Neto, A.; Parra, A.; Alonso, J. In situ soil phosphorus monitoring probe compared with conventional extraction procedures. *Comm. Soil Sci. Plant Analysis.* **2009**, *40*, 1282. [[CrossRef](#)]
75. Abbas, M.N.; Radwan, A.L.A.; Nooredeen, N.M.; El-Ghaffar, M.A.A. Selective phosphate sensing using copper monoamino-phthalocyanine functionalized acrylate polymer-based solid-state electrode for FIA of environmental waters. *J. Solid State Electrochem.* **2016**, *20*, 1599. [[CrossRef](#)]
76. Barhoumi, L.; Baraket, A.; Nooredeen, N.M.; Ali, M.B.; Abbas, M.N.; Bausells, J.; Errachid, A. Silicon nitride capacitive chemical sensor for phosphate ion detection based on copper phthalocyanine-acrylate polymer. *Electroanalysis* **2017**, *29*, 1586. [[CrossRef](#)]
77. Ebuele, V.O.; Congrave, D.G.; Gwenin, C.D.; Fitzsimmons-Thoss, V. Development of a cobalt electrode for the determination of phosphate in soil extracts and comparison with standard methods. *Anal. Lett.* **2018**, *51*, 834. [[CrossRef](#)]
78. Xu, K.; Kitazumi, Y.; Kano, K.; Shirai, O. Phosphate ion sensor using a cobalt phosphate coated cobalt electrode. *Electrochim. Acta* **2018**, *282*, 242. [[CrossRef](#)]
79. Zou, Z.; Han, J.; Jang, A.; Bishop, P.L.; Ahn, C.H. A disposable on-chip phosphate sensor with planar cobalt microelectrodes on polymer substrate. *Biosens. Bioelectron.* **2007**, *22*, 1902. [[CrossRef](#)]
80. Arvas, M.B.; Gorduk, O.; Gencten, M.; Sahin, Y. Preparation of a novel electrochemical sensor for phosphate detection based on a molybdenum blue modified poly(vinyl chloride) coated pencil graphite electrode. *Anal. Methods* **2019**, *11*, 3874. [[CrossRef](#)]
81. Cinti, S.; Talarico, D.; Palleschi, G.; Moscone, D.; Arduini, F. Novel reagentless paper-based screen-printed electrochemical sensor to detect phosphate. *Anal. Chim. Acta* **2016**, *919*, 78. [[CrossRef](#)]
82. Bhat, K.S.; Nakate, U.T.; Yoo, J.-Y.; Wang, Y.; Mahmoudi, T.; Hahn, Y.-B. Nozzle-jet-printed silver/graphene composite-based field effect transistor sensor for phosphate ion detection. *ACS Omega* **2019**, *4*, 8373. [[CrossRef](#)] [[PubMed](#)]
83. Sedaghat, S.; Jeong, S.; Zareei, A.; Peana, S.; Glassmaker, N.; Rahimi, R. Development of a nickel oxide/oxyhydroxide-modified printed carbon electrode as an all solid-state sensor for potentiometric phosphate detection. *NJC* **2019**, *43*, 18619. [[CrossRef](#)]
84. Borse, V.; Jain, P.; Sadawana, M.; Srivastava, R. Turn-on fluorescence assay for inorganic phosphate sensing. *Sens. Act. B Chem.* **2016**, *225*, 340. [[CrossRef](#)]
85. Ahmad, R.; Ahn, M.-S.; Hahn, Y.-B. ZnO nanorods array based field effect transistor biosensor for phosphate detection. *J. Colloid Interface Sci.* **2017**, *498*, 292. [[CrossRef](#)]
86. Gilbert, L.; Jenkins, A.T.A.; Browning, S.; Hart, J.P. Development of an amperometric, screen-printed, single-enzyme phosphate ion biosensor and its application to the analysis of biomedical and environmental samples. *Sens. Act. B* **2011**, *160*, 1322. [[CrossRef](#)]
87. Kopiec, G.G.; Starzec, K.; Kochana, J.; Kinnunen-Skidmore, T.P.; Schuhmann, W.; Campbell, W.H.; Ruff, A.; Plumeré, N. Bioelectrocatalytic and electrochemical cascade for phosphate sensing with up to 6 electrons per analyte molecule. *Biosens. Bioelectron.* **2018**, *117*, 501. [[CrossRef](#)]
88. Storer, C.; Coldrick, Z.; Tate, D.; Donoghue, J.; Grieve, B. Towards phosphate detection in hydroponics using molecularly imprinted polymer sensors. *Sensors* **2018**, *18*, 531. [[CrossRef](#)] [[PubMed](#)]
89. Bogrekci, I.; Lee, W.S. Spectral Soil Signatures and sensing Phosphorus. *Biosyst. Eng.* **2005**, *92*, 527. [[CrossRef](#)]

90. Sarwar, M.; Lechner, J.; Naja, G.M.; Li, C.-Z. Smart-phone, paper based fluorescent sensor for ultra-low inorganic phosphate detection in environmental samples. *Microsyst. Nanoeng.* **2019**, *5*, 56. [CrossRef] [PubMed]
91. Potassium for Crop Production. Available online: <https://extension.umn.edu/phosphorus-andpotassium/potassium-crop-production> (accessed on 4 August 2020).
92. Ciesla, J.; Ryzak, M.; Bieganski, A.; Tkaczyk, P.; Walczak, R.T. Use of ion-selective electrodes for determination of content of potassium in Egner-Rhiem soil extracts. *Res. Agric. Eng.* **2007**, *53*, 29. [CrossRef]
93. Lemos, S.G.; Nogueira, A.R.; Torre-Neto, A.; Parra, A.; Artigas, J.; Alonso, J. In-Soil Potassium Sensor System. *J. Agric. Food Chem.* **2004**, *52*, 5810. [CrossRef]
94. Kim, H.J.; Hummel, J.W.; Sudduth, K.A.; Motavalli, P.P. Simultaneous analysis of soil macronutrients using ion-selective electrodes. *Soil Sci. Soc. Am. J.* **2007**, *71*, 1867. [CrossRef]
95. Kim, H.J.; Sudduth, K.A.; Hummel, J.W.; Drummond, S.T. Validation testing of a soil macronutrient sensing system. *Trans. ASABE* **2013**, *56*, 23. [CrossRef]
96. Yoon, J.H.; Park, H.J.; Park, S.H.; Lee, K.G.; Choi, B.G. Electrochemical characterization of reduced graphene oxide as an ion-to-electron transducer and application of screen-printed all-solid-state potassium ion sensors. *Carbon Lett.* **2020**, *30*, 73. [CrossRef]
97. Rosenberg, R.; Bono, M.S.; Braganza, S.; Vaishnav, C.; Karnik, R.; Hart, A.J. In-field determination of soil ion content using a handheld device and screen-printed solid-state ion-selective electrodes. *PLoS ONE* **2018**, *13*, e0203862. [CrossRef]
98. Yu, K.; He, N.; Kumar, N.; Wang, N.; Bobacka, J.; Ivaska, A. Electrosynthesized polypyrrole/zeolite composites as solid contact in potassium ion-selective electrode. *Electrochim. Acta* **2017**, *228*, 66. [CrossRef]
99. Fakih, I.; Centeno, A.; Zurutuza, A.; Ghaddab, B.; Siaj, M.; Szkopek, T. High resolution potassium sensing with large-area graphene field-effect transistors. *Sens. Act. B* **2019**, *291*, 8. [CrossRef]
100. Naderi, M.; Hosseini, M.; Ganjali, M.R. Naked-eye detection of potassium ions in a novel gold nanoparticle aggregation-based aptasensor. *Spectrochim. Acta A* **2018**, *195*, 75. [CrossRef] [PubMed]
101. Ning, J.; Lin, X.; Su, F.; Sun, A.; Liu, H.; Luo, J.; Wang, L.; Tian, Y. Development of a molecular K⁺ probe for colorimetric/fluorescent/photoacoustic detection of K⁺. *Anal. Bioanal. Chem.* **2020**, *412*, 6947. [CrossRef] [PubMed]
102. Buss, W.; Shepherd, J.G.; Heal, K.V.; Mašek, O. Spatial and temporal microscale pH change at the soil-biochar interface. *Geoderma* **2018**, *331*, 5. [CrossRef]
103. Stagenborg, S.A.; Carignano, M.; Haag, L. Predicting soil pH and buffer pH in situ with a real-time sensor. *Agron. J.* **2007**, *99*, 85. [CrossRef]
104. Silva, F.C.S.; Molin, J.P. Real time soil sensing for determination of tropical soils pH. In *Precision Agriculture '13*; Wageningen Academic Publishers: Wageningen, The Netherlands, 2013; p. 41.
105. Schirrmann, M.; Gebbers, R.; Kramer, E.; Seidel, J. Soil pH mapping with an on-the-go sensor. *Sensors* **2011**, *11*, 573. [CrossRef] [PubMed]
106. Korostynska, O.; Arshak, K.; Gill, E.; Arshak, A. Review on state-of-the-art in polymer based pH sensors. *Sensors* **2007**, *7*, 3027. [CrossRef] [PubMed]
107. Bratov, A.; Abramova, N.; Munoz, J.; Dominguez, C.; Alegret, S.; Bartroli, J. Photocurable Polymer Matrices for Potassium-Sensitive Ion-Selective Electrode Membranes. *Anal. Chem.* **1995**, *67*, 3589. [CrossRef]
108. Lemos, S.G.; Nogueira, A.R.A.; Torre-Neto, A.; Parra, A.; Alonso, J. Soil calcium and pH monitoring sensor system. *J. Agric. Food Chem.* **2007**, *55*, 4658. [CrossRef] [PubMed]
109. Motellier, S.; Noir, M.H.; Pitsch, H.; Durdault, B. pH determination of clay interstitial water using a fiber-optic sensor. *Sens. Act. B* **1995**, *29*, 345. [CrossRef]
110. Hoefer, C.; Santner, J.; Borisov, S.M.; Wenzel, W.W.; Puschenreiter, M. Integrating chemical imaging of cationic trace metal solutes and pH into a single hydrogel layer. *Anal. Chem. Acta* **2017**, *950*, 88. [CrossRef]
111. Patil, S.; Ghadi, H.; Ramgir, N.; Adhikari, A.; Rao, V.R. Monitoring soil pH variation using Polyaniline/SU-8 composite film based conductometric microsensor. *Sens. Act. B* **2019**, *286*, 583. [CrossRef]
112. Chang, Y.H.; Iyama, Y.; Tadenuma, K.; Kawaguchi, S.; Takarada, T.; Falina, S.; Syamsul, M.; Kawarada, H. Over 59 mV/pH sensitivity with fluorocarbon thin film via fluorine termination for pH sensing using boron-doped diamond solution-gate field-effect transistors. *PSSA* **2020**, *218*, 2000278. [CrossRef]
113. Wilczek, A.; Szyplowska, A.; Skierucha, W.; Ciesla, J.; Pichler, V.; Janik, G. Determination of soil pore water salinity using an FDR sensor working at various frequencies up to 500 MHz. *Sensors* **2012**, *12*, 10890. [CrossRef]
114. Visconti, F.; Martínez, D.; Molina, M.J.; Ingelmo, J.F. A combined equation to estimate the soil pore-water electrical conductivity: Calibration with the WET and 5TE sensors. *Soil Res.* **2014**, *52*, 419. [CrossRef]
115. Aljoumani, B.; Sanchez-Espigares, J.A.; Wessolek, G. Estimating pore water electrical conductivity of sandy soil from time domain reflectometry records using a time-varying dynamic linear model. *Sensors* **2018**, *18*, 4403. [CrossRef] [PubMed]
116. Artigas, J.; Beltran, A.; Jiménez, C.; Bartroli, J.; Alonso, J. Development of a photopolymerisable membrane for calcium ion sensors. *Appl. Soil Drain. Waters. Anal. Chim. Acta.* **2001**, *426*, 3. [CrossRef]
117. Lvova, L.; Guanais Goncalves, C.; Prodi, L.; Sgarzi, M.; Zaccheroni, N.; Lombardo, M.; Legin, A.; Di Natale, C.; Paolesse, R. Systematic approach in Mg²⁺ ions analysis with a combination of tailored fluorophore design. *Anal. Chim. Acta* **2017**, *988*, 96. [CrossRef] [PubMed]

118. Tulliani, J.M.; Inserra, B.; Ziegler, D. Carbon-Based Materials for Humidity Sensing: A Short Review. *Micromachines* **2019**, *10*, 232. [[CrossRef](#)] [[PubMed](#)]
119. Wang, X.; Liu, F.; Han, X. Influence of soil physical and chemical properties on performance of soil profile moisture sensor. *Trans. Chin. Soc. Agric. Machin.* **2012**, *43*, 97.
120. Da Costa, E.F.; de Oliveira, N.E.; Morais, F.J.O.; Carvalhaes-Dias, P.; Duarte, L.F.C.; Cabot, A.; Dias, J.A.S. A self-powered and autonomous fringing field capacitive sensor integrated into a micro sprinkler spinner to measure soil water content. *Sensors* **2017**, *17*, 575. [[CrossRef](#)] [[PubMed](#)]
121. Kalita, H.; Palaparthi, V.S.; Baghini, M.S.; Aslam, M. Electrochemical synthesis of graphene quantum dots from graphene oxide at room temperature and its soil moisture sensing properties. *Carbon* **2020**, *165*, 9. [[CrossRef](#)]
122. Patil, S.; Ramgir, N.; Mukherji, S.; Rao, V.R. PVA modified ZnO nanowire based microsensors platform for relative humidity and soil moisture measurement. *Sens. Act. B* **2017**, *253*, 1071. [[CrossRef](#)]
123. Sophocleous, M.; Atkinson, J.K.; Smethurst, J.A.; Espindola-Garcia, G.; Ingenito, A. The use of novel thick-film sensors in the estimation of soil structural changes through the correlation of soil electrical conductivity and soil water content. *Sens. Act. A* **2020**, *301*, 111773. [[CrossRef](#)]
124. Rivera, D.; Granda, S.; Arumí, J.L.; Sandoval, M.; Billib, M. A methodology to identify representative configurations of sensors for monitoring soil moisture. *Environ. Monitor. Assessm.* **2012**, *184*, 6563. [[CrossRef](#)]
125. Neumann, P.P.; Bartholmai, M.; Lazik, D. Leak detection with linear soil gas sensors under field conditions—First experiences running a new measurement technique. *Proc. IEEE Sens. J.* **2017**, 7808658.
126. Lazik, D.; Ebert, S.; Leuthold, M.; Hagenau, J.; Geistlinger, H. Membrane based measurement technology for in situ monitoring of gases in soil. *Sensors* **2009**, *9*, 756. [[CrossRef](#)] [[PubMed](#)]
127. Strömberg, N.; Hulth, S. Assessing an imaging ammonium sensor using time correlated pixel-by-pixel calibration. *Anal. Chim. Acta* **2005**, *550*, 61. [[CrossRef](#)]
128. Delin, S.; Strömberg, N. Imaging-optode measurements of ammonium distribution in soil after different manure amendments. *Eur. J. Soil Sci.* **2011**, *62*, 295. [[CrossRef](#)]
129. Christel, W.; Zhu, K.; Hofer, C.; Kreuzeder, A.; Santner, J.; Bruun, S.; Magid, J.; Jensen, L.S. Spatiotemporal dynamics of phosphorus release, oxygen consumption and greenhouse gas emissions after localized soil amendment with organic fertilizers. *Sci. Total Environ.* **2016**, *119*, 554–555.
130. Van Nguyen, Q.; Jensen, L.S.; Bol, R.; Wu, D.; Triolo, J.M.; Vazifehkhoran, A.H.; Bruun, S. Biogas digester hydraulic retention time affects oxygen consumption patterns and greenhouse gas emissions after application of digestate to soil. *J. Environ. Qual.* **2017**, *46*, 1114. [[CrossRef](#)]
131. Rabus, D.; Friedt, J.-M.; Arapan, L.; Lamare, S.; Baqué, M.; Audouin, G.; Chérioux, F. Subsurface H₂S Detection by a surface acoustic wave passive wireless sensor Interrogated with a ground penetrating radar. *ACS Sens.* **2020**, *5*, 1075. [[CrossRef](#)] [[PubMed](#)]
132. Ur Rahim, H.; Qaswar, M.; Uddin, M.; Giannini, C.; Herrera, M.L.; Rea, G. Nano-Enable Materials Promoting Sustainability and Resilience in Modern Agriculture. *Nanomaterials* **2021**, *11*, 2068. [[CrossRef](#)] [[PubMed](#)]
133. Ganie, A.S.; Bano, S.; Khan, N.; Sultana, S.; Rehman, Z.; Rahman, M.M.; Sabir, S.; Coulon, F.; Khan, M.Z. Nanoremediation technologies for sustainable remediation of contaminated environments: Recent advances and challenges. *Chemosphere* **2021**, *275*, 130065. [[CrossRef](#)]
134. Tajik, S.; Beitollahi, H.; Nejad, F.G.; Dourandish, Z.; Khalilzadeh, M.A.; Jang, H.W.; Venditti, R.A.; Varma, R.S.; Shokouhimehr, M. Recent developments in polymer nanocomposite-based electrochemical sensors for detecting environmental pollutants. *Ind. Eng. Chem. Res.* **2021**, *60*, 1112. [[CrossRef](#)]
135. Kong, X.; Ho, S.C.M.; Song, G.; Cai, C.S. Scour monitoring system using Fiber Bragg Grating sensors and water-swellaable polymers. *J. Bridge Eng.* **2017**, *22*, 04017029. [[CrossRef](#)]
136. Bhaskar, S.; Pradeep Kumar, M.; Avinash, M.N.; Harshini, S.B. Real time farmer assistive flower harvesting agricultural robot. *I2CT* **2021**, *2021*, 9417817.
137. Briffa, J.; Sinagra, E.; Blundell, R. Heavy metal pollution in the environment and their toxicological effects on humans. *Heliyon* **2020**, *6*, e04691. [[CrossRef](#)] [[PubMed](#)]
138. *Guidelines for Drinking-Water Quality*, 4th ed.; World Health Organization: Geneva, Switzerland, 2017. Available online: <https://www.who.int/publications/i/item/9789241549950> (accessed on 15 January 2022).
139. Kumar, M.; Puri, A. A review of permissible limits of drinking water. *Indian J. Occup. Environ. Med.* **2012**, *16*, 40. [[PubMed](#)]
140. Md Noh, M.F.; Tothill, I.E. Development and characterisation of disposable gold electrodes, and their use for lead(II) analysis. *Anal. Bioanal. Chem.* **2006**, *386*, 2095.
141. Abbaspour, A.; Mirahmadi, E.; Khalafi-nejad, A.; Babamohammadi, S. A highly selective and sensitive disposable carbon composite PVC-based membrane for determination of lead ion in environmental samples. *J. Haz. Mater.* **2010**, *174*, 656. [[CrossRef](#)]
142. McGraw, C.M.; Radu, T.; Radu, A.; Diamond, D. Evaluation of liquid- and solid-contact. Pb²⁺-selective polymer-membrane electrodes for soil analysis. *Electroanalysis* **2008**, *20*, 340. [[CrossRef](#)]
143. Wilson, D.; de los Ángeles Arada, M.; Alegret, S.; del Valle, M. Lead(II) ion selective electrodes with PVC membranes based on two bis-thioureas as ionophores: 1,3-bis(N-benzoylthioureido) benzene and 1,3-bis(N-furoylthioureido)benzene. *J. Haz. Mater.* **2010**, *181*, 140. [[CrossRef](#)]

144. Chen, Y.-T.; Hseih, C.-Y.; Sarangadharan, I.; Sukesan, R.; Lee, G.-Y.; Chyi, J.-I.; Wang, Y.-L. Beyond the limit of ideal nernst sensitivity: Ultra-high sensitivity of heavy metal ion detection with ion-selective high electron mobility transistors. *ECS J. Solid State Sci. Technol.* **2018**, *7*, Q176. [[CrossRef](#)]
145. Sakhraoui, H.E.E.Y.; Madani, A.; Nessark, B.; Mazouz, Z.; Attia, G.; Fourati, N.; Zerrouki, C.; Maouche, N.; Othmane, A.; Yaakoubi, N.; et al. Design of L-cysteine and acrylic acid imprinted polypyrrole sensors for picomolar detection of lead ions in simple and real media. *IEEE Sensors* **2020**, *20*, 4147. [[CrossRef](#)]
146. Dali, M.; Zinoubi, K.; Chrouda, A.; Abderrahmane, S.; Cherrad, S.; Jaffrezic-Renault, N. A biosensor based on fungal soil biomass for electrochemical detection of lead (II) and cadmium (II) by differential pulse anodic stripping voltammetry. *J. Electroanal. Chem.* **2018**, *813*, 9. [[CrossRef](#)]
147. Liu, C.-W.; Huang, C.-C.; Chang, H.-T. Highly selective DNA-based sensor for lead(II) and mercury(II) ions. *Anal. Chem.* **2009**, *81*, 2383. [[CrossRef](#)] [[PubMed](#)]
148. Li, C.L.; Liu, K.T.; Lin, Y.W.; Chang, H.T. Fluorescence detection of lead(II) ions through their induced catalytic activity of DNAzymes. *Anal. Chem.* **2010**, *83*, 225. [[CrossRef](#)] [[PubMed](#)]
149. Lin, Y.W.; Liu, C.W.; Chang, H.T. Fluorescence detection of mercury (II) and lead (II) ions using aptamer/reporter conjugates. *Talanta* **2011**, *84*, 324. [[CrossRef](#)]
150. Xiao, Y.; Rowe, A.A.; Plaxco, K.W. Electrochemical detection of parts-per-billion lead via an electrode-bound DNAzyme assembly. *J. Am. Chem. Soc.* **2007**, *129*, 262. [[CrossRef](#)] [[PubMed](#)]
151. Liang, G.; Man, Y.; Li, A.; Jin, X.; Liu, X.; Pan, L. DNAzyme-based biosensor for detection of lead ion: A review. *Microchem. J.* **2017**, *131*, 145. [[CrossRef](#)]
152. Dolati, S.; Ramezani, M.; Abnous, K.; Taghdisi, S.M. Recent nucleic acid based biosensors for Pb²⁺ detection. *Sens. Act. B* **2017**, *246*, 864. [[CrossRef](#)]
153. Khoshbin, Z.; Housaindokht, M.R.; Verdian, A.; Bozorgmehr, M.R. Simultaneous detection and determination of mercury (II) and lead (II) ions through the achievement of novel functional nucleic acid-based biosensors. *Biosens. Bioelectron.* **2018**, *116*, 130. [[CrossRef](#)]
154. Singh, H.; Bamrah, A.; Bhardwaj, S.K.; Deep, A.; Khatri, M.; Kim, K.-H.; Bhardwaj, N. Nanomaterial-based fluorescent sensors for the detection of lead. *J. Hazard. Mater.* **2021**, *407*, 124379. [[CrossRef](#)] [[PubMed](#)]
155. Md Noh, M.F.; Kadara, R.O.; Tothill, I.E. Development of cysteine-modified screen-printed electrode for the chronopotentiometric stripping analysis of cadmium(II) in wastewater and soil extracts. *Anal. Bioanal. Chem.* **2005**, *382*, 1175.
156. Radovanović, M.; Vasiljević, D.; Krstić, D.; Antić, I.; Korzhyk, O.; Stojanović, G.; Škrbić, B.D. Flexible sensors platform for determination of cadmium concentration in soil samples. *Comput. Electron. Agric.* **2019**, *166*, 105001. [[CrossRef](#)]
157. Das, T.R.; Sharma, P.K. Sensitive and selective electrochemical detection of Cd²⁺ by using bimetal oxide decorated Graphene oxide (Bi₂O₃/Fe₂O₃@GO) electrode. *Microchem. J.* **2019**, *147*, 1203. [[CrossRef](#)]
158. Garau, A.; Lvova, L.; Macedi, E.; Ambrosi, G.; Aragoni, M.C.; Arca, M.; Caltagirone, C.; Coles, S.J.; Formica, M.; Fusi, V.; et al. N₂S₂ Pyridinophane-based fluorescent chemosensors for selective optical detection of Cd²⁺ in soils. *NJC* **2020**, *44*, 20834. [[CrossRef](#)]
159. Linder, M.C.; Hazegh-Azam, M. Copper biochemistry and molecular biology. *Am. J. Clin. Nutr.* **1996**, *63*, 797s. [[PubMed](#)]
160. Elmizadeh, H.; Soleimani, M.; Faridbod, F.; Bardajee, G.R. Ligand-Capped CdTe quantum dots as a fluorescent nanosensor for detection of copper ions in environmental water sample. *J. Fluoresc.* **2017**, *27*, 2323. [[CrossRef](#)]
161. Huang, X.; Xia, P.; Liu, B.; Huang, H. An azamacrocyclic functionalized GaAs (100) optical sensor for copper ion (II) detection in phosphate buffered saline solution. *Sens. Act. B* **2018**, *257*, 853. [[CrossRef](#)]
162. Chen, D.; Chen, P.; Zong, L.; Sun, Y.; Liu, G.; Yu, X.; Qin, J. Colorimetric and fluorescent probes for real-time naked eye sensing of copper ion in solution and on paper substrate. *R. Soc. Open Sci.* **2018**, *4*, 171161.
163. Rahman, F.U.; Yu, S.B.; Khalil, S.K.; Wu, Y.P.; Koppireddi, S.; Li, Z.T.; Wang, H.; Zhang, D.W. Chromone and benzyldithiocarbamate based probe: A highly selective and sensitive platform for colorimetric sensing of Cu²⁺, single crystal of the complex and DFT calculations. *Sens. Act. B* **2018**, *263*, 594. [[CrossRef](#)]
164. Sengupta, P.; Ganguly, A.; Bose, A. A phenolic acid based colourimetric 'naked-eye' chemosensor for the rapid detection of Cu(II) ions. *Spectrochim. Acta A* **2018**, *198*, 204. [[CrossRef](#)]
165. Kim, S.Y.; Lee, S.Y.; Jung, J.M.; Kim, M.S.; Kim, C. Selective detection of Cu²⁺ and S²⁻ by a colorimetric chemosensor: Experimental and theoretical calculations. *Inorg. Chim. Acta* **2018**, *471*, 709. [[CrossRef](#)]
166. Chandra, S.; Dhawangale, A.; Mukherji, S. Hand-held optical sensor using denatured antibody coated electro-active polymer for ultra-trace detection of copper in blood serum and environmental samples. *Biosens. Bioelectron.* **2018**, *110*, 38. [[CrossRef](#)] [[PubMed](#)]
167. Sutariya, P.G.; Soni, H.; Gandhi, S.A.; Pandya, A. Novel tritopic calix[4]arene CHEF-PET fluorescence paper based probe for La³⁺, Cu²⁺, and Br⁻: Its computational investigation and application to real samples. *J. Luminesc.* **2019**, *212*, 17. [[CrossRef](#)]
168. Zhang, G.; Zhang, H.; Zhang, J.; Ding, W.; Xu, J.; Wen, Y. Highly selective fluorescent sensor based on electrosynthesized oligo(1-pyreneboronic acid) enables ultra-trace analysis of Cu²⁺ in environment and agro-product samples. *Sens. Act. B* **2017**, *253*, 224. [[CrossRef](#)]
169. Lvova, L.; Acciari, E.; Mandoj, F.; Pomarico, G.; Paolesse, R. Fast optical sensing of metals: A case study of Cu²⁺ assessment in soils. *ECS J. Solid State Sci. Technol.* **2020**, *9*, 061004. [[CrossRef](#)]

170. Kopylovich, M.N.; Mahmudov, K.T.; Pombeiro, A.J.L. Poly(vinyl) chloride membrane copper-selective electrode based on 1-phenyl-2-(2-hydroxyphenylhydrazo)butane-1,3-dione. *J. Haz. Mater.* **2011**, *186*, 1154. [[CrossRef](#)] [[PubMed](#)]
171. Singh, A.K.; Sahani, M.K.; Bandi, K.R.; Jain, A.K. Electroanalytical studies on Cu (II) ion-selective sensor of coated pyrolytic graphite electrodes based on N₂S₂O₂ and N₂S₂O₃ heterocyclic benzothiazol ligands. *Mater. Sci. Eng. C* **2014**, *41*, 206. [[CrossRef](#)]
172. Bandi, K.R.; Singh, A.K.; Upadhyay, A. Electroanalytical and naked eye determination of Cu²⁺ ion in various environmental samples using 5-amino-1,3,4-thiadiazole-2-thiol based Schiff bases. *Mater. Sci. Eng. C* **2014**, *34*, 149. [[CrossRef](#)]
173. Ekrami, E.; Pouresmaeli, M.; Shariati, P.; Mahmoudifard, M. A review on designing biosensors for the detection of trace metals. *Appl. Geochem.* **2021**, *127*, 104902. [[CrossRef](#)]
174. Wu, X.; Huang, Q.; Mao, Y.; Wang, X.; Wang, Y.; Hu, Q.; Wang, H.; Wang, X. Sensors for determination of uranium: A review. *Tr. Anal. Chem.* **2019**, *118*, 89. [[CrossRef](#)]
175. Van der Horst, C.; Silwana, B.; Iwuoha, E.; Somerset, V. Bismuth–silver bimetallic nanosensor application for the voltammetric analysis of dust and soil samples. *J. Electroanal. Chem.* **2015**, *752*, 1–11. [[CrossRef](#)]
176. Li, H.; Fan, J.; Hu, M.; Cheng, G.; Zhou, D.; Wu, T.; Song, F.; Sun, S.; Duan, C.; Peng, X. Highly sensitive and fast-responsive fluorescent chemosensor for palladium: Reversible sensing and visible recovery. *Chem. Eur. J.* **2012**, *18*, 12242. [[CrossRef](#)]
177. Liang, G.G.; Cai, Q.; Zhu, W.; Xu, Y.; Qian, X. A highly selective heterogeneous fluorescent sensor for palladium ions. *Anal. Methods* **2015**, *7*, 4877. [[CrossRef](#)]
178. Ayrançi, R.; Ak, M. An Electrochemical sensor platform for sensitive detection of iron (III) ions based on pyrene-substituted poly(2,5-dithienylpyrrole). *J. Electrochem. Soc.* **2019**, *166*, B291. [[CrossRef](#)]
179. Brodersen, K.E.; Koren, K.; Moßhammer, M.; Ralph, P.J.; Kuhl, M.; Santner, J. Seagrass-mediated phosphorus and iron solubilization in tropical sediments. *Environ. Sci. Technol.* **2017**, *51*, 14155. [[CrossRef](#)]
180. Parnsubsakul, A.; Oaew, S.; Surareungchai, W. Zwitterionic peptide-capped gold nanoparticles for colorimetric detection of Ni. *Nanoscale* **2018**, *10*, 5466. [[CrossRef](#)]
181. Mondal, S.; Subramaniam, C. Point-of-care. cable-type electrochemical Zn²⁺ sensor with ultrahigh sensitivity and wide detection range for soil and sweat analysis. *ACS Sustain. Chem. Eng.* **2019**, *7*, 14569. [[CrossRef](#)]
182. Cooper, J.; Bolbot, J.A.; Saini, S.; Setford, S.J. Electrochemical method for the rapid on site screening of cadmium and lead in soil and water samples. *Water Air Soil Pollut.* **2007**, *179*, 183. [[CrossRef](#)]
183. Nedeltcheva, T.; Atanassova, M.; Dimitrov, J.; Stanislavova, L. Determination of mobile form contents of Zn, Cd, Pb and Cu in soil extracts by combined stripping voltammetry. *Anal. Chim. Acta.* **2005**, *528*, 143. [[CrossRef](#)]
184. Palchetti, I.; Laschi, S.; Mascini, M. Miniaturised stripping-based carbon modified sensor for in field analysis of heavy metals. *Anal. Chim. Acta* **2005**, *530*, 61. [[CrossRef](#)]
185. Silva, P.R.M.; El Khakani, M.A.; Chaker, M.; Dufresne, A.; Courchesne, F. Simultaneous determination of Cd, Pb and Cu metal trace concentrations in water certified samples and soil extracts by means of Hg-electroplated –Ir microelectrode array based sensors. *Sens. Act. B.* **2001**, *76*, 250. [[CrossRef](#)]
186. Wang, Z.; Sun, X.; Li, C.; He, X.; Liu, G. On-site detection of heavy metals in agriculture land by a disposable sensor based virtual instrument, *Comput. Electron. Agric.* **2016**, *123*, 176. [[CrossRef](#)]
187. Mc Eleney, C.; Alves, S.; Mc Crudden, D. Novel determination of Cd and Zn in soil extract by sequential application of bismuth and gallium thin films at a modified screen-printed carbon electrode. *Anal. Chim. Acta* **2020**, *1137*, 94. [[CrossRef](#)]
188. Hung, Y.-L.; Hsiung, T.-M.; Chen, Y.-Y.; Huang, Y.-F.; Huang, C.-C. Colorimetric detection of heavy metal ions using label-free gold nanoparticles and alkanethiols. *J. Phys. Chem. C* **2010**, *114*, 16329. [[CrossRef](#)]
189. Viscarra Rossel, R.A.; Fouad, Y.; Walter, C. Using a digital camera to measure soil organic carbon and iron contents. *Biosyst. Eng.* **2008**, *100*, 149. [[CrossRef](#)]
190. Yokota, M.; Okada, T.; Yamaguchi, I. An optical sensor for analysis of soil nutrients by using LED light sources. *Meas. Sci. Technol.* **2007**, *18*, 2197. [[CrossRef](#)]
191. Muravyov, S.V.; Gavrilenko, N.A.; Saranchina, N.V.; Baranov, P.F. Polymethacrylate sensors for rapid digital colorimetric analysis of toxicants in natural and anthropogenic objects. *IEEE Sens. J.* **2019**, *19*, 4765. [[CrossRef](#)]
192. Ivask, A.; Francois, M.; Kahru, A.; Dubourguier, H.-C.; Virta, M.; Douay, F. Recombinant luminescent bacterial sensors for the measurement of bioavailability of cadmium and lead in soils polluted by metal smelters. *Chemosphere* **2004**, *55*, 147. [[CrossRef](#)]
193. Kahru, A.; Ivask, A.; Kasemets, K.; Pollumaa, L.; Kurvet, I.; Francois, M.; Dubourguier, H.-C. Biotests and biosensors in ecotoxicological risk assessment of field soils polluted with zinc, lead, and cadmium, *Environ. Toxicol. Chem.* **2005**, *24*, 2973. [[CrossRef](#)]
194. Petänen, T.; Virta, M.; Karp, M.; Romantschuk, M. Construction and use of broad host range mercury and arsenite sensor plasmids in the soil bacterium *Pseudomonas fluorescens* OS8. *Microbial Ecol.* **2001**, *41*, 360. [[CrossRef](#)]
195. Petänen, T.; Romantschuk, M. Use of bioluminescent bacterial sensors as an alternative method for measuring heavy metals in soil extracts. *Anal. Chim. Acta.* **2002**, *456*, 55. [[CrossRef](#)]
196. Brandt, K.K.; Holm, P.E.; Nybroe, O. Evidence for bioavailable copper-dissolved organic matter complexes and transiently increased copper bioavailability in manure-amended soils as determined by bioluminescent bacterial biosensors. *Environ. Sci. Technol.* **2008**, *42*, 3102. [[CrossRef](#)] [[PubMed](#)]

197. Hou, Q.-H.; Ma, A.-Z.; Lv, D.; Bai, Z.-H.; Zhuang, X.-L.; Zhuang, G.-Q. The impacts of different long-term fertilization regimes on the bioavailability of arsenic in soil: Integrating chemical approach with *Escherichia coli* arsRp::luc-based biosensor. *Appl. Microbiol. Biotechnol.* **2014**, *98*, 6137. [[CrossRef](#)]
198. Wei, H.; Cheng, H.; Mao, T.; Zhong, W.-H.; Lin, X.-G. A chromosomally based luminescent bioassay for mercury detection in red soil of China. *Appl. Microbiol. Biotechnol.* **2010**, *87*, 981. [[CrossRef](#)]
199. Liu, P.; Huang, Q.; Chen, W. Construction and application of a zinc-specific biosensor for assessing the immobilization and bioavailability of zinc in different soils. *Environ. Pollut.* **2012**, *164*, 66. [[CrossRef](#)]
200. Peltola, P.; Ivask, A.; Aström, M.; Virta, M. Lead and Cu in contaminated urban soils: Extraction with chemical reagents and bioluminescent bacteria and yeast. *Sci. Total Environ.* **2005**, *350*, 194. [[CrossRef](#)] [[PubMed](#)]
201. Maletić, S.P.; Watson, M.A.; Dehlawi, S.; Diplock, E.E.; Mardlin, D.; Paton, G.I. Deployment of microbial biosensors to assess the performance of ameliorants in metal-contaminated soils. *Water Air Soil Pollut.* **2015**, *226*, 85. [[CrossRef](#)]
202. Coelho, C.; Branco, R.; Natal-da-Luz, T.; Sousa, J.P.; Morais, P.V. Evaluation of bacterial biosensors to determine chromate bioavailability and to assess ecotoxicity of soils. *Chemosphere* **2015**, *128*, 62. [[CrossRef](#)] [[PubMed](#)]
203. Bouguerra, S.; Gavina, A.; Rasteiro, M.D.G.; Rocha-Santos, T.; Ksibi, M.; Pereira, R. Derivation of terrestrial predicted no-effect concentration (Pnec) for cobalt oxide nanomaterial. In *Recent Advances in Environmental Science from the Euro-Mediterranean and Surrounding Regions*; Kallel, A., Ksibi, M., Ben Dhia, H., Khélifi, N., Eds.; EMCEI 2017, Advances in Science, Technology & Innovation (IEREK Interdisciplinary Series for Sustainable Development); Springer: Cham, Switzerland, 2018; pp. 405–407.
204. Kaur, J.; Adamchuk, V.I.; Whalen, J.K.; Ismail, A.A. Development of an NDIR CO₂ sensor-based system for assessing soil toxicity using substrate-induced respiration. *Sensors* **2015**, *15*, 4734. [[CrossRef](#)] [[PubMed](#)]
205. Krishnapandi, A.; Muthukutty, B.; Chen, S.-M.; Arul, K.T.; Shiuan, H.J.; Selvaganapathy, M. Bismuth molybdate incorporated functionalized carbon nanofiber as an electrocatalytic tool for the pinpoint detection of organic pollutant in life samples. *Ecotoxicol. Environ. Saf.* **2021**, *209*, 111828. [[CrossRef](#)]
206. Saad, A.S.; Edrees, F.H.; Elsaady, M.T.; Amin, N.H.; Abdelwahab, N.S. Experimentally designed sensor for direct determination of the environmentally hazardous compound and occupational exposure biomarker (p-aminophenol) in different sampling matrices. *J. Electrochem. Soc.* **2020**, *167*, 147504. [[CrossRef](#)]
207. Prusti, B.; Chakravarty, M. An electron-rich small AIEgen as a solid platform for the selective and ultrasensitive on-site visual detection of TNT in the solid. solution and vapor states. *Analyst* **2020**, *145*, 1687. [[CrossRef](#)]
208. Zhang, Y.; Cai, Y.; Dong, F.; Bian, L.; Li, H.; Wang, J.; Du, J.; Qi, X.; He, Y. Chemically modified mesoporous wood: A versatile sensor for visual colorimetric detection of trinitrotoluene in water, air, and soil by smartphone camera. *Anal. Bioanal. Chem.* **2019**, *411*, 8063. [[CrossRef](#)]
209. Shafiee, M.; Larki, A.; Faal, A.Y. Fabrication of an optochemical sensor based on triacetylcellulose polymer for colorimetric determination of trinitrotoluene. *Propellants Explos. Pyrotech.* **2020**, *45*, 438.
210. Komikawa, T.; Tanaka, M.; Tamang, A.; Evans, S.D.; Critchley, K.; Okochi, M. Peptide-Functionalized Quantum Dots for Rapid Label-Free Sensing of 2,4,6-Trinitrotoluene. *Bioconjugate Chem.* **2020**, *31*, 1400. [[CrossRef](#)] [[PubMed](#)]
211. Chen, N.; Ding, P.; Shi, Y.; Jin, T.; Su, Y.; Wang, H.; He, Y. Portable and reliable surface-enhanced raman scattering silicon chip for signal-on detection of trace trinitrotoluene explosive in real systems. *Anal. Chem.* **2017**, *89*, 5072. [[CrossRef](#)] [[PubMed](#)]
212. Taefi, Z.; Ghasemi, F.; Hormozi-Nezhad, M.R. Selective colorimetric detection of pentaerythritol tetranitrate (PETN) using arginine-mediated aggregation of gold nanoparticles. *Spectrochim. Acta A* **2020**, *228*, 117803. [[CrossRef](#)]
213. Zhang, X.-Y.; Yang, Y.-S.; Wang, W.; Jiao, Q.-C.; Zhu, H.-L. Fluorescent sensors for the detection of hydrazine in environmental and biological systems: Recent advances and future prospects. *Coord. Chem. Rev.* **2020**, *417*, 213367. [[CrossRef](#)]
214. Tang, M.; Wu, Y.; Deng, D.; Wei, J.; Zhang, J.; Yang, D.; Li, G. Development of an optical fiber immunosensor for the rapid and sensitive detection of phthalate esters. *Sens. Act. B* **2018**, *258*, 304. [[CrossRef](#)]
215. Li, Z.; Ren, M.; Wang, L.; Lin, W. An ethyl cyanoacetate based turn-on fluorescent probe for hydrazine and its bio-imaging and environmental applications. *Anal. Methods* **2018**, *10*, 4016. [[CrossRef](#)]
216. Jung, Y.; Ju, I.G.; Choe, Y.H.; Kim, Y.; Park, S.; Hyun, Y.-M.; Oh, M.S.; Kim, D. Hydrazine exposé: The next-generation fluorescent probe. *ACS Sens.* **2019**, *4*, 441. [[CrossRef](#)]
217. Lakshmi, P.R.; Nanjan, P.; Kannan, S.; Shanmugaraju, S. Recent advances in luminescent metal–organic frameworks (LMOFs) based fluorescent sensors for antibiotics. *Coord. Chem. Rev.* **2021**, *435*, 213793. [[CrossRef](#)]
218. Sun, Y.; Zhao, J.; Liang, L. Recent development of antibiotic detection in food and environment: The combination of sensors and nanomaterials. *Microchim. Acta* **2021**, *188*, 21. [[CrossRef](#)]
219. Ma, Z.; Liu, J.; Li, H.; Zhang, W.; Williams, M.A.; Gao, Y.Z.; Gudda, F.O.; Lu, C.; Yang, B.; Waigi, M.G. A fast and easily parallelizable biosensor method for measuring extractable tetracyclines in soils. *Environ. Sci. Technol.* **2020**, *54*, 758. [[CrossRef](#)] [[PubMed](#)]
220. Tang, L.; Zeng, G.M.; Shen, G.L.; Li, Y.P.; Hang, Y.Z.; Huang, D.L. Rapid detection of picloram in agricultural field samples using a disposable immunomembrane-based electrochemical sensor. *Environ. Sci. Technol.* **2008**, *43*, 1207. [[CrossRef](#)] [[PubMed](#)]
221. Prasad, B.B.; Jauhari, D.; Tiwari, M.P. Doubly imprinted polymer nanofilm-modified electrochemical sensor for ultra-trace simultaneous analysis of glyphosate and glufosinate. *Biosens. Bioelectron.* **2014**, *59*, 81. [[CrossRef](#)] [[PubMed](#)]

222. Gianetto, M.; Umiltà, E.; Careri, M. New competitive dendrimer-based and highly selective immunosensor for determination of atrazine in environmental, feed and food samples: The importance of antibody selectivity for discrimination among related triazinic metabolites. *Anal. Chim. Acta.* **2014**, *806*, 197. [[CrossRef](#)]
223. Gonzalez-Martinez, M.A.; Brun, E.M.; Puchades, R.; Maquieira, A.; Ramsey, K.; Rubio, F. Glyphosate Immunosensor. Application for Water and Soil Analysis. *Anal. Chem.* **2005**, *77*, 4219. [[CrossRef](#)]
224. Gholivand, M.B.; Akbari, A.; Norouzi, L. Development of a novel hollow fiber-pencil graphite modified electrochemical sensor for the ultra-trace analysis of glyphosate. *Sens. Act. B* **2018**, *272*, 415. [[CrossRef](#)]
225. Shrivastava, S.; Kumar, A.; Verma, N.; Chen, B.-Y.; Chang, C.-T. Voltammetric detection of aqueous glyphosate on a copper and poly(pyrrole)-electromodified activated carbon fiber. *Electroanalysis* **2021**, *33*, 916. [[CrossRef](#)]
226. Sacks, V.; Eshkenazi, I.; Neufeld, N.; Dosoretz, K.; Rishpon, J. Immobilized parathion hydrolase: An amperometric sensor for parathion. *Anal. Chem.* **2000**, *72*, 2055. [[CrossRef](#)] [[PubMed](#)]
227. Dong, J.; Wang, X.; Qiao, F.; Liu, P.; Ai, S. Highly sensitive electrochemical stripping analysis of methyl parathion at MWCNTs–CeO₂–Au nanocomposite modified electrode. *Sens. Acta B* **2013**, *186*, 774. [[CrossRef](#)]
228. Baskeyfield, D.E.H.; Davis, F.; Magan, N.; Tothill, I.E. A membrane-based immunosensor for the analysis of the herbicide isoproturon. *Anal. Chim. Acta* **2011**, *699*, 223. [[CrossRef](#)] [[PubMed](#)]
229. Wang, X.; Hou, T.; Dong, S.; Liu, X.; Li, F. Fluorescence biosensing strategy based on mercury ion-mediated DNA conformational switch and nicking enzyme-assisted cycling amplification for highly sensitive detection of carbamate pesticide. *Biosens. Bioelectron.* **2016**, *77*, 644. [[CrossRef](#)] [[PubMed](#)]
230. Tahirbegi, I.B.; Ehgartner, J.; Sulzer, P.; Zieger, S.; Kasjanow, A.; Paradiso, M.; Strobl, M.; Bouwes, D.; Mayr, T. Fast pesticide detection inside microfluidic device with integrated optical pH, oxygen sensors and algal fluorescence. *Biosens. Bioelectron.* **2017**, *88*, 188. [[CrossRef](#)]
231. Segal, E.; Haleva, E.; Salomon, A. Ultrasensitive plasmonic sensor for detecting sub-ppb levels of alachlor. *ACS Appl. Nano Mater.* **2019**, *2*, 1285. [[CrossRef](#)]
232. Kumar, T.H.V.; Raman Pillai, S.K.; Chan-Park, M.B.; Sundramoorthy, A.K. Highly selective detection of an organophosphorus pesticide, methyl parathion, using Ag–ZnO–SWCNT based field-effect transistors. *J. Mater. Chem. C* **2020**, *8*, 8864. [[CrossRef](#)]
233. Nehru, R.; Chen, S.-M. A La³⁺-doped TiO₂ nanoparticle decorated functionalized-MWCNT catalyst: Novel electrochemical non-enzymatic sensing of paraoxon-ethyl. *Nanoscale Adv.* **2020**, *2*, 3033. [[CrossRef](#)]
234. Ilager, D.; Seo, H.; Shetti, N.P.; Kalanur, S.S. CTAB modified Fe–WO₃ as an electrochemical detector of amitrole by catalytic oxidation. *J. Environ. Chem. Eng.* **2020**, *8*, 104580. [[CrossRef](#)]
235. Kamel, A.H.; Amr, A.E.-G.E.; Abdalla, N.S.; El-Naggar, M.; Al-Omar, M.A.; Alkahtani, H.M.; Sayed, A.Y.A. Novel solid-state potentiometric sensors using Polyaniline (PANI) as a solid-contact transducer for flucarbazone herbicide assessment. *Polymers* **2019**, *11*, 1796. [[CrossRef](#)] [[PubMed](#)]
236. Dai, Y.; Wang, T.; Hu, X.; Liu, S.; Zhang, M.; Wang, C. Highly sensitive microcantilever-based immunosensor for the detection of carbofuran in soil and vegetable samples. *Food Chem.* **2017**, *229*, 432. [[CrossRef](#)]
237. Strachan, G.; Capel, S.; Maciel, H.; Porter, A.J.R.; Paton, G.I. Application of cellular and immunological biosensor techniques to assess herbicide toxicity in soils. *Eur. J. Soil Sci.* **2002**, *53*, 37. [[CrossRef](#)]
238. Chen, J.; Sun, S.; Li, C.-Z.; Zhu, Y.-G.; Rosen, B.P. Biosensor for organoarsenical herbicides and growth promoters. *Environ. Sci. Technol.* **2014**, *48*, 1141. [[CrossRef](#)]
239. *Multisensor Systems for Chemical Analysis—Materials and Sensors*; Lvova, L.; Kirsanov, D.; Legin, A.; Di Natale, C. (Eds.) Pan Stanford Publishing: Singapore, 2014; pp. 69–138, ISBN 9789814411158.
240. Esbensen, K. *Multivariate Data Analysis in Practice*, 5th ed.; Camo Press: Trondheim, Norway, 2004; 590p.
241. Śliwińska, M.; Wisniewska, P.; Dymerski, T.; Namiesnik, J.; Wardencki, W. Food Analysis Using Artificial Senses. *J. Agric. Food Chem.* **2014**, *62*, 1423. [[CrossRef](#)]
242. Mimendia, A.; Gutierrez, J.M.; Alcaniz, J.P.; del Valle, M. Discrimination of soils and assessment of soil fertility using information from an Ion Selective Electrodes array and Artificial Neural Networks. *Clean Soil Air Water.* **2014**, *42*, 1808. [[CrossRef](#)]
243. McGrath, D.; Skotnikov, A. Automated work-station for soil analysis. *Comm. Soil Sci. Plant Anal.* **1996**, *27*, 1795. [[CrossRef](#)]
244. Gutierrez, M.; Alegret, S.; Caceres, R.; Casadesus, J.; Marfa, O.; del Valle, M. Nutrient solution monitoring in greenhouse cultivation employing a potentiometric electronic tongue. *J. Agric. Food Chem.* **2008**, *56*, 1810. [[CrossRef](#)]
245. Chikae, M.; Kerman, K.; Nagatani, N.; Takamura, Y.; Tamiya, E. An electrochemical on-field sensor system for the detection of compost maturity. *Anal. Chim. Acta.* **2007**, *581*, 364. [[CrossRef](#)] [[PubMed](#)]
246. Artigas, J.; Beltran, A.; Jimenez, C.; Baldi, A.; Mas, R.; Dominguez, C.; Alonso, J. Application of ion sensitive field effect transistor based sensors to soil analysis. *Comp. Electron. Agric.* **2001**, *31*, 281. [[CrossRef](#)]
247. Wilson, D.; Gutierrez, J.M.; Alegret, S.; del Valle, M. Simultaneous Determination of Zn(II), Cu(II), Cd(II) and Pb(II) in Soil Samples Employing an Array of Potentiometric Sensors and an Artificial Neural Network Model. *Electroanalysis* **2012**, *24*, 2249. [[CrossRef](#)]
248. Beni, V.; Ogurtsov, V.I.; Bakunin, N.V.; Arrigan, D.W.M.; Hill, M. Development of a portable electroanalytical system for the stripping voltammetry of metals: Determination of copper in acetic acid soil extracts. *Anal. Chim. Acta* **2005**, *552*, 190. [[CrossRef](#)]
249. Venancio, E.C.; Consolin Filho, N.; Constantino, C.J.L.; Martin-Neto, L.; Mattoso, L.H.C. Studies on the interaction between humic substances and conducting polymers for sensor application. *J. Braz. Chem. Soc.* **2005**, *16*, 24. [[CrossRef](#)]

250. Lvova, L.; D'Amico, A.; Pede, A.; Di Natale, C.; Paolesse, R. Metallic Sensors in Multisensory Analysis. In *Multisensor Systems for Chemical Analysis—Materials and Sensors*; Lvova, L., Kirsanov, D., Legin, A., Di Natale, C., Eds.; Pan Stanford Publishing: Singapore, 2014; pp. 69–138, ISBN 9789814411158. [[CrossRef](#)]
251. Da Silva, T.A.; Braunger, M.L.; Neris Coutinho, M.A.; Rios do Amaral, L.; Rodrigues, V.; Riul, A., Jr. 3D-Printed graphene electrodes applied in an impedimetric electronic tongue for soil analysis. *Chemosensors* **2019**, *7*, 50. [[CrossRef](#)]
252. Sophocleous, M.; Karkotis, A.; Georgiou, J. A versatile, stand-alone system for a screen-printed, soil-sensing array for Precision Agriculture. *IEEE J. Emerg. Sel. Top. Circuits Syst.* **2021**, *11*, 449–457. [[CrossRef](#)]
253. Sophocleous, M.; Karkotis, A.; Georgiou, J. A versatile, stand-alone system for a screen-printed, soil-sensing array for Precision Agriculture. In Proceedings of the 2020 IEEE Sensors, Rotterdam, The Netherlands, 25–28 October 2020; p. 9278890.
254. Khaydukova, M.; Kirsanov, D.; Sarkar, S.; Mukherjee, S.; Ashina, J.; Bhattacharyya, N.; Chanda, S.; Bandyopadhyay, R.; Legin, A. One shot evaluation of NPK in soils by “electronic tongue”. *Comput. Electron. Agric.* **2021**, *186*, 106208. [[CrossRef](#)]
255. Patkar, R.S.; Ashwin, M.; Rao, V.R. Piezoresistive microcantilever based lab-on-a-chip system for detection of macronutrients in the soil. *Solid-State Electron.* **2017**, *138*, 94. [[CrossRef](#)]
256. Kurup, P.; Sullivan, C.; Hannagan, R.; Yu, S.; Azimi, H.; Robertson, S.; Ryan, D.; Nagarajan, R.; Ponrathnam, T.; Howe, G. A Review of Technologies for Characterization of Heavy Metal Contaminants. *Indian Geotech J.* **2017**, *47*, 421–436. [[CrossRef](#)]
257. Bao, C.; Seol, S.K.; Kim, W.S. A 3D integrated neuromorphic chemical sensing system. *Sens. Act. B* **2021**, *332*, 129527. [[CrossRef](#)]
258. Taylor, G.A.; Parra, C.; Carrillo, H.; Mouazen, A. A decision framework reference for ISFET sensor-based electronic systems design for agriculture industry applications. In Proceedings of the 2020 IEEE 17th India Council International Conference, INDICON 2020, New Delhi, India, 10–13 December 2020; p. 9342231.
259. Rock, F.; Barsan, N.; Weimar, U. Electronic Nose: Current Status and Future Trends. *Chem. Rev.* **2008**, *108*, 705. [[CrossRef](#)]
260. Yang, J.-W.; Cho, H.-J.; Lee, S.-H.; Lee, J.-Y. Characterization of SnO₂ ceramic gas sensor for exhaust gas monitoring of SVE process. *Environ. Monit. Assessm.* **2004**, *92*, 153. [[CrossRef](#)]
261. Gurbuz, Y.; Kang, W.P.; Davidson, J.L.; Kerns, D.V. Diamond microelectronic gas sensor for detection of benzene and toluene. *Sens. Act. B.* **2004**, *99*, 207. [[CrossRef](#)]
262. De Cesare, F.; Pantalei, S.; Zampetti, E.; Macagnano, A. Electronic nose and SPME techniques to monitor phenanthrene biodegradation in soil. *Sens. Act. B.* **2008**, *131*, 63. [[CrossRef](#)]
263. Pineda, D.M.; Pérez, J.C. SENose: An under U\$50 electronic nose for the monitoring of soil gas emissions. *Comput. Electron. Agric.* **2017**, *133*, 15. [[CrossRef](#)]
264. Badura, M.; Szczurek, A.; Banaszkiwicz, K. BTEX compounds identification by means of gas sensors array. *E3S Web Conf.* **2018**, *44*, 00007. [[CrossRef](#)]
265. Fabbri, B.; Valt, M.; Parretta, C.; Gherardi, S.; Gaiardo, A.; Malagù, C.; Mantovani, F.; Strati, V.; Guidi, V. Correlation of gaseous emissions to water stress in tomato and maize crops: From field to laboratory and back. *Sens. Act. B.* **2020**, *303*, 127227. [[CrossRef](#)]
266. Visconti, P.; de Fazio, R.; Velázquez, R.; Del-Valle-soto, C.; Giannoccaro, N.I. Development of sensors-based agri-food traceability system remotely managed by a software platform for optimized farm management. *Sensors* **2020**, *20*, 3632. [[CrossRef](#)]
267. Khairunniza-Bejo, S.; Ramli, N.; Muharam, F.M. Wireless sensor network (WSN) applications in plantation canopy areas: A review. *Asian J. Sci. Res.* **2018**, *11*, 151. [[CrossRef](#)]